The fatter the better:
Selecting microalgae cells for outdoor lipid production

Iago Dominguez Teles

Thesis committee

Promotor
Prof. Dr R. H. Wijffels
Professor of Bioprocess Engineering
Wageningen University

Co-promotors

Dr M. J. Barbosa
Associate Professor, Bioprocess Engineering
Wageningen University and Research

Dr D. M. M. Kleinegris
Senior Researcher, Wageningen Food and Biobased Research
Wageningen University and Research

Other members
Dr J. van den Oost, Wageningen University
Dr F.B. dos Santos, University of Amsterdam, the Netherlands
Dr O. Kruse, Bielefeld University, Germany
Dr J. A. Olivares, Los Alamos National Laboratory, USA

This research was conducted under the auspices of the Graduate School VLAG (Advanced studies in Food Technology, Agrobiotechnology, Nutrition and Health Sciences).

The fatter the better:
Selecting microalgae cells for outdoor lipid production

Iago Dominguez Teles

Thesis
submitted in fulfilment of the requirements for the degree of doctor
at Wageningen University
by the authority of the Rector Magnificus
Prof. Dr A.P.J. Mol
in the presence of the
Thesis Committee appointed by the Academic Board
to be defended in public
on Friday 28 October 2016
at 4 p.m. in the Aula.

I. D. Teles
The fatter the better: Selecting microalgae cells for outdoor lipid production
164 pages.

PhD thesis, Wageningen University, Wageningen, NL (2016)
With references, with summary in English, Dutch, Portuguese and Spanish

ISBN 978-94-6257-882-1
DOI: 10.18174/387306

A mi padre, por la libertad
À minha mãe, pela força
À minha avó Yolanda, pela calma, pelo jeito e pelas ostras

“Kitsch causes two tears to flow in quick succession. The first tear says: How nice to see children running on the grass!
The second tear says: How nice to be moved, together with all mankind, by children running on the grass!
It is the second tear that makes kitsch kitsch.
The brotherhood of man on earth will be possible only on a base of kitsch.”

Milan Kundera, The Unbearable Lightness of Being

Contents

Introduction and thesis outline

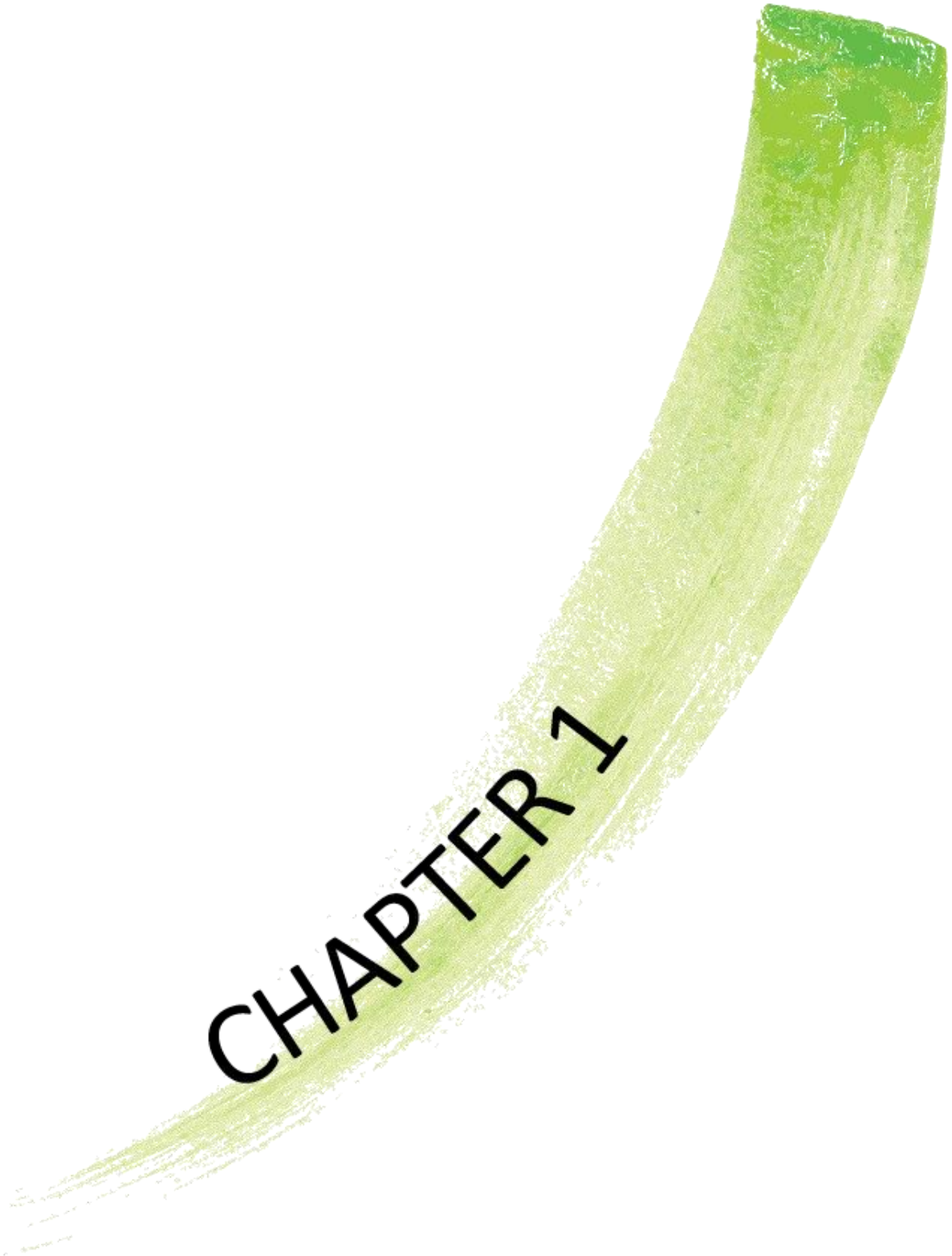

Introduction

Microalgae are photosynthetic microorganisms that have been gathering attention in the last decades due to their potential to replace commodities, such as food, feed, chemicals and fuels [1]. Microalgae have a versatile metabolism, which can be exploited to produce different products (proteins, lipids and carbohydrates) [2]. Economic analyses, however, show that production costs of microalgal biomass are ranging from 5 to 6€ per kg of dry biomass [3], which clearly requires further reduction, especially when aiming at low-value market products (e.g. biofuels). Despite extensive research in the last decades, microalgae are still not feasible for the commodities market [4]. They are, however, economically feasible for higher valued markets (such as omega-3 fatty-acids, food supplements and "new foods"), and also as feed for aquaculture [5–7].

Further effort should, hence, be focused on cost reduction. Cost reduction can be achieved by 2 ways: [1] decrease capital and operational costs of production/processing systems and [2] increase microalgae productivity (thus increasing the yields on light for phototrophic systems). The yields can either be increased via process optimization to improve the light usage by the cells [8] or via developing new strains with superior performance [9]. Developing strains with superior performance can be achieved with multiple approaches: selection of better strains [10], adaptive laboratory evolution [11], random mutagenesis [12] and genetic manipulation [13] , or combination(s) of these [9,14].

In the present thesis we focused on cell selection to take advantage of the natural biological variability of species to select cells on desired characteristics [9], hence borrowing the concept from plant breeding. Two approaches present potential to explore the natural variability of microalgae without resourcing to genetic engineering: (1) adaptive laboratory evolution (ALE) and (2) cell sorting. (1) The ALE approach consists in exposing a population of cells to a continuous and specific selection factor to select for competent cells that can survive to the next generation [13]. (2) Cell sorting consists in actively selecting cells with a specific phenotype in a given cell population. It gives the possibility to select cells that have a phenotype of interest and to use these sorted cells to establish new cell populations. The selected phenotype, if stable, can be exploited to improve the performance of the strains, similar to the approach used to improve plant crops. The best technology to do so with microalgae is fluorescence assisted cell sorting (FACS), which allows fast screening and selection of cells [15].

In this thesis we applied both approaches to select new cell populations with increased productivities for industrial application. We hypothesized that repeated N-starvation could be used as a selection factor using both ALE and FACS to select new populations of cells with increased lipid productivities. Previous works have shown the potential of ALE to develop new strains of *Chlorella vulgaris* with increased biomass productivity (using LED with different wavelengths [11]), of *Dunaliella salina* with increased carotenoids content (using blue and red LEDs [16]), of *Chlorella* sp. with increased CO_2 uptake and growth rate [17], and of *Chlamydomonas reinhardtii* (starchless mutant) with almost double growth rate under constant light [18]. Altogether, these findings highlight the potential of some microalgae strains to be modified using ALE in a relatively short cycle experiments (from 45 to 100 days).

FACS can, differently from ALE, be used to select specific cells among the population, allowing even single cell sorting [19,20]. A few research groups have recently applied FACS to microalgae with different approaches and outcomes, mainly focusing on selecting lipid-rich cells after random mutagenesis, hence introducing an source of genetic variation [9,14,21,22]. Nevertheless, some of the cells selected for high-lipid content have shown a reduction in growth [21,23], highlighting the need to assess the performance of the sorted populations after sorting. Furthermore, none of these articles have compared the performance of sorted populations under simulated industrial conditions and neither described testing after a longer period of storage. We developed an approach to fill the gaps from the above mentioned researches and to estimate the production potential of microalgae strains.

The viability of sorted cells is an important factor when aiming at re-growing cells after selection, hence we first developed a method to detect and sort viable lipid-rich cells of *Chlorococcum littorale* [15]. Our results showed that we can distinguish the top lipid producer cells from the rest of the population, and that we can keep the cells viability after staining and sorting [15]. After assuring cell viability the most important factor when selecting cells is to define the sorting criteria (what we did at chapters 4 and 5). We have shown that the relative lipid content (lipid/cell, i.e. lipid fluorescence/autofluorescence) was successful in selecting cells with the same growth rates as the original under N-replete conditions, but that produced more TAGs when exposed to N-starvation in comparison with the original population (chapter 5). Most of the previously published research has been done under laboratory scale and in small volumes, many times with no mention to biomass or lipid productivities. We, instead, have worked with reactors (0.4 to 1.9 liters) and under simulated outdoors conditions to report biomass and lipid productivities, hence evaluating the industrial potential of the developed cell population. Finally, to assess the performance of selected cells right after sorting might include a variation in the experiments (the post-sorting acclimation and growth) [22–24]. Hence, we indicate that it is necessary to compare the performance between original and sorted populations after both have been similarly acclimated (Chapter 5). All things considered, we presented an approach designed to fill the gaps from previous research to allow evaluation of the industrial potential of microalgae strains with improved industrial potential.

Thesis outline

This thesis aimed to select cells of *Chlorococcum littorale* with improved phenotypes, assuming that these cells could establish new populations with increased industrial performance. At **Chapter 2** we wanted to know what happened during time to biomass and lipid productivities of *Chlorococcum littorale* repeatedly subjected to N-starvation. Hence, we also discussed the implications of using repeated N-starvation for ALE experiments. **Chapter 3** introduces an approach to detect and to select microalgae cells with increased lipid content. Here we optimized a method to rapidly screen and sort lipid rich cells of *C. littorale* using FACS. The method was designed to maintain cellular viability so the cells could be used to produce new inoculum. In **chapter 4** we evaluated a question that emerged while deciding which criteria to use for sorting lipid-rich cells: does cellular size affects lipid productivity of *C. littorale*? We hypothesized that cells with different diameters have different division rates, which could affect lipid productivity. Therefore, we assessed the influence of cell diameter, as a sorting parameter, on both biomass and lipid productivity of *Chlorococcum littorale*. In **chapter 5** we present a strategy to sort cells of *C. littorale* with increased TAG productivity using the method developed at chapter 3. Our strategy consisted of sorting cells with a high lipid/cell content after a period of N-starvation. The sorted populations were used to start another round of N-starvation followed again by sorting, which was done in 5 subsequent rounds. Both the original and the sorted population with the highest lipid productivity (namely, S5) were compared under simulated Dutch summer conditions to confirm our results and to evaluate the industrial potential of S5. In **chapter 6** we extrapolated our results (indoor and outdoor) to other climate conditions. We first validated, for *C. littorale*, a previously developed model that describes the carbon partitioning of microalgae under N-starvation (i.e. which components are photosynthetically produced by the cells in the absence of nitrogen). Next, we ran simulations changing the light conditions to four different locations worldwide (Wageningen, Oslo, Rio de Janeiro and Cádiz) to estimate both biomass and TAG productivities. **Chapter 7** presents the general discussion of the thesis, with a discussion on how can we improve the productivity of microalgae systems by selecting cells with increased industrial potential.

Repeated N-starvation doesn't affect lipid productivity of *Chlorococcum littorale*

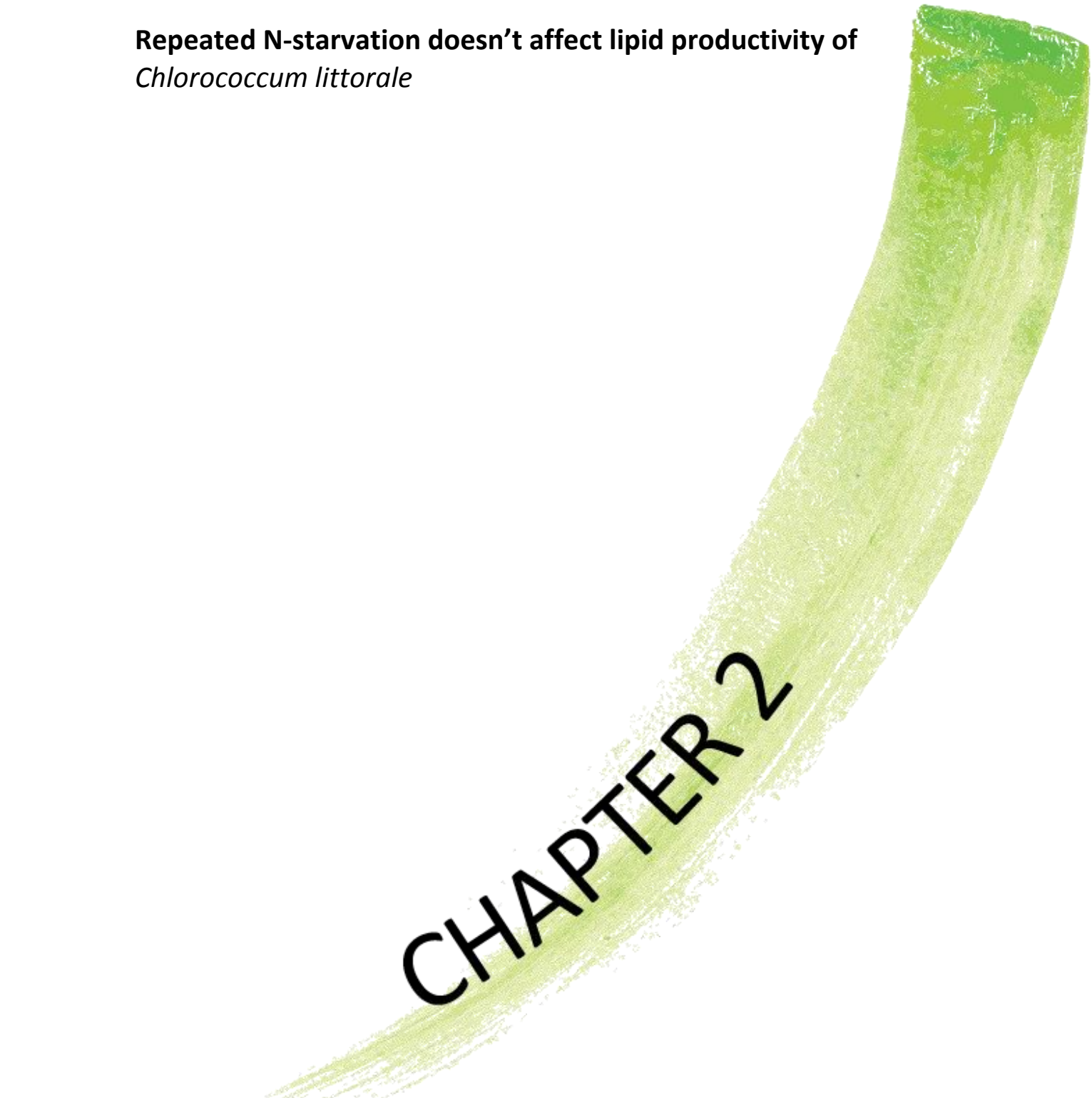

This chapter has been published as: Cabanelas, Iago Teles Dominguez; Kleinegris, Dorinde MM; Wijffels, René H; Barbosa, Maria J. 2016. Repeated N-starvation doesn't affect lipid productivity of *Chlorococcum littorale*. Bioresource Technology 219, 576–582.

Highlights:

- *C. littorale* biomass productivity was stable under repeated N-starvation (147 days)
- *C. littorale* showed fast recovery of PSII after long repeated N-starvation
- Repeated N-starvation cycles reduced biomass productivity, but not lipid content
- Repeated short N-starvation cycles led to similar lipid productivities as batch N-starved

ABSTRACT:

In the present work we wanted to know what happens during time to biomass and lipid productivities of *Chlorococcum littorale* repeatedly subjected to N-starvation. Experiments were done using repeated cycles of batch-wise N run-out (after 3 days $N_{=0}$). Two different cycles were used: 8 cycles of repeated short-starvation (7 days of $N_{=0}$) over a total period of 72 days and 5 cycles of repeated long-starvation (13 days of $N_{=0}$) over a total period of 75 days. Batches (using fresh inocula) were done separately as control. Shorter and longer periods of starvation showed no differences in biomass productivities and PSII quantum yield evolution. The repeated short-starvation-batches showed the same lipid productivities as the control short-starvation batches. Most importantly, the biomass lipid content was the same between control and repeated-batches. Altogether, the results point to *C. littorale* as a resilient and stable strain, with potential to be used under semi continuous cultivation.

Key-words: microalgae; repeated-batch; *Chlorococcum littorale*; nitrogen-starvation; adaptive laboratory evolution (ALE)

2.1. Introduction

Microalgae-based technology has the potential to supply new sustainable products due to its versatility (biomass can be simultaneously refined into multiple products) and sustainability (e.g., CO_2 neutral and no arable land required) [5,25,26]. Microalgae products have various applications ranging from commodities (e.g., oils and carbohydrates for chemicals and fuels) to fine chemicals (e.g., rare fatty-acids and pigments) [3,6]. Although microalgae products are a reality in the high-value market of fine chemicals, the current productivities and consequent high production costs do not allow them to be at present, a competitive feedstock for the low-market value of biofuels, for example [27,28,1]. Microalgal lipids are one of the most versatile among microalgal products with uses ranging from commodities to food supplements and animal feed [29,30]

There are two main approaches to increase microalgal lipid volumetric productivity: process optimization and strain improvement. Process optimization is used to maximize the production of a certain compound using already available strains [31]. Strain improvement is used to select cells that display an increased baseline production of a certain compound, which can be achieved via breeding and artificial selection [13,16,32] and/or mutagenesis [12,14,21]. A combination of process optimization and strain improvement could significantly increase productivity and reduce production costs.

Batch cultivation is the most commonly used strategy for microalgal lipid production [8,29,33,34]. The traditional approach for microalgae lipid production works in 2 steps: microalgae biomass is produced in one system (growth phase) and then transferred to a second system where lipid production is induced by nitrogen starvation (”stress” phase), usually via dilution in N-free medium [21,35]. Instead of always producing a new inoculum to start a new batch for lipid production by N-starvation, it has been suggested that a repeated batch process using part of the produced lipid-rich biomass as inoculum could yield higher lipid productivities [36]. This would remove the need for systems allocated for biomass production (growth phase), which consume production time and area that otherwise could be allocated to actual lipid production processes. However, the repeated batch approach could also lead to reduced productivity, due to a higher risk of operational crashes and contaminations. Furthermore, exposure to identical conditions can also lead to changes/mutations in the original strain, a feature that can be exploited to develop new strains with improved phenotypes [13].

Interestingly, repeated batch can also be used in laboratory evolution experiments, in which a cell population is subjected to a repeated environmental pressure to push for changes leading to a new, improved strain [13]. Although such approach has been extensively used with *E. coli* and *S. cerevisiae*, only recent results have shown the potential with microalgae [11,16,18].

In the present work we wanted to know what happens during time to biomass and lipid productivities of *Chlorococcum littorale* repeatedly subjected to N-starvation. *Chlorococcum littorale* was selected for the current work based on its high photosynthetic activity under N-starvation and high TAG content [37,38]. Current microalgal lipid production relies on cycles of N-starvation repeated batches, which makes the above question relevant for lipid production by

microalgae. Our work focusses on comparing two process – batch (reference strategy) and repeated-batch – to evaluate two aspects of the same question: 1] are the biomass and lipid productivities in the repeated-batch different from the control batch? and 2] does repeated-batch result in stable biomass and lipid productivities through time? We discuss, at last, the implications of our results to ALE experiments.

2.2. Materials and methods

2.2.1. Microorganism and culture conditions

Chlorococcum littorale (NBRC 102761) was purchased from the culture collection of NIES, Japan. This strains has been described by [39,40]. Artificial seawater medium was used to prepare inoculum and to perform experiments in reactors. Medium composition (g l^{-1}): NaCl 24.55; $MgSO_4.7H_2O$ 6.60; $MgCl_2.6H_2O$ 5.60; $CaCl_2.2H_2O$ 1.50; $NaNO_3$ 1.70; HEPES 11.92; $NaHCO_3$ 0.84; EDTA-Fe (III) 4.28; K_2HPO_4 0.13; KH_2PO_4 0.04; trace elements in mg l^{-1}: $Na_2EDTA.2H_2O$ 0.19; $ZnSO_4.7H_2O$ 0.022; $CoCl.6H_2O$ 0.01; $MnCl_2.2H_2O$ 0.148; $Na_2MoO_4.2H_2O$ 0.06; $CuSO_4.5H_2O$ 0.01). The inoculum was grown in 0.2 l borosilicate Erlenmeyer flasks under controlled conditions (orbital-shaker-incubator, INFORS HT, Switzerland): mixing at 120 rpm, light intensity 150 µmol m^{-2} s^{-1}, temperature at 25 C and CO_2 supply of 2% over air flow in the headspace.

N-starvation experiments were carried out in flat panel reactors as described by [41]. The working volume of the reactors was 380 ml with a light path of 14 mm. Operation was performed at continuous illumination (incident light 410 µmol m^{-2} s^{-1}) using LED lamps with a warm white light spectrum (Bridgelux, BXRA W1200). The pH was kept constant at 7.0 by pulse-wise CO_2 addition to the airflow.

Nitrogen starvation was achieved via nitrogen run-out, i.e., cells were allowed to consume all available nitrogen (which happened after 48h in the current experiments). The nitrogen content in the medium (N-NO_3 mg l^{-1}) was measured daily using the Sulphanilamide N-1-naphthyl method (APHA 4500-NO3-F) with an automatic analyser (SEAL AQ2).

2.2.2. Repeated N-starvation experiments

The repeated N-starvation experiments consisted of repeated cycles of batch-wise N run-out, i.e., at the end of each batch the reactor was diluted to the initial biomass concentration (OD750 of 0.5) with fresh, sterile nitrogen replete medium. The experiments followed the scheme presented in Figure 2.1. Two different cycle durations were used: 8 cycles of repeated short-starvation (RSS, 6 days of N-starvation; grey points in Figure 2.1**Figure**, 72 days in total) followed by 5 cycles of repeated long-starvation (RLS, 12 days of N-starvation; dark points in Figure 2.1, 75 days in total). The first 8 cycles were subsequent cycles of short-starvation and from the ninth cycle onward it was decided to increase the cycle duration to long-starvation to evaluate the effect of a longer period of starvation on *C. littorale*. All cycles had the first 2 days of cultivation as the growth phase (arrow, Figure 2.2), after which all nitrogen was taken up by the cells. The starvation-phase was considered to start on the second day.

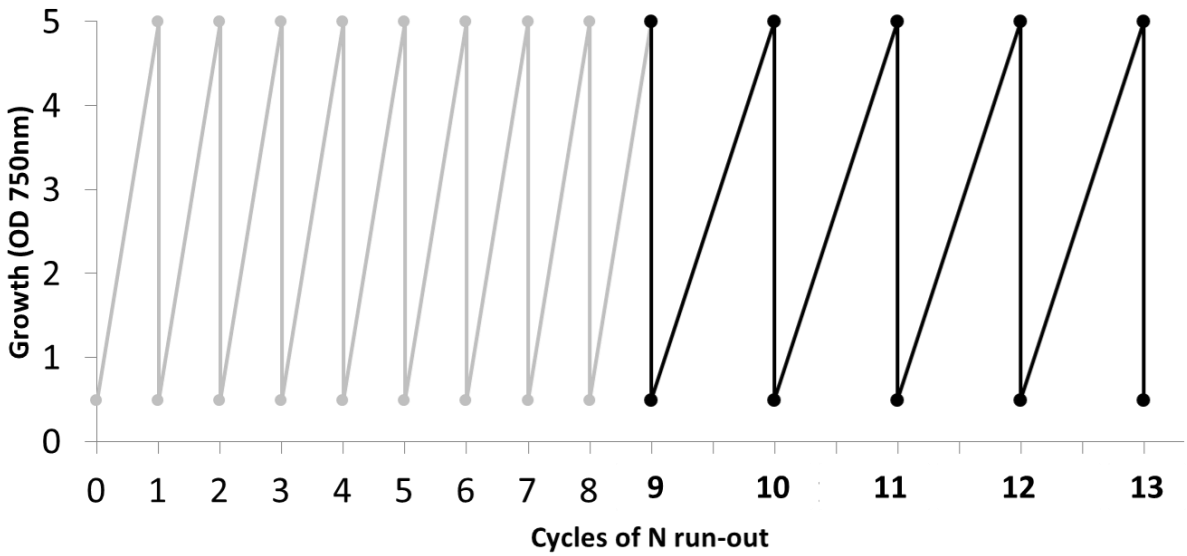

Figure 2.1: Repeated N-starvation experiments. Each cycle represents one batch-wise N run-out cultivation composed of 2 phases: a growth or recovery phase (day 0 to day 2) and a N-starvation phase (from the day 2 onward). At the end of a cycle, biomass concentration was diluted to 0.5 (OD 750) and used as inoculum for the subsequent run. The grey points represent the repeated short-starvation period (RSS, 7 days of N-starvation, 9 cultivation days) and the dark points represent the repeated long-starvation period (13 days of N-starvation, 15 cultivation days).

The cultivations from repeated N-starvation were compared with control experiments: 3 independent batches always starting with fresh inoculum made from plate to flask, all grown under the same conditions as previously stated. Each experiment was used to be compared with both Short-starvation and Long-starvation experiments. Hence, samples were taken on the 9th day of cultivation of each cycle to be compared with control short-starvation (CSS) and samples were also taken on the 15th day of cultivation to be compared with Long starvation-experiment (CLS).

2.2.3. Fatty-acids (FA) and triglycerides (TAG) analyses

Samples of biomass were harvested at the above mentioned time points. Biomass samples were centrifuged at 2500 x g for 5 minutes, washed twice with MilliQ® water and stored at -18 °C (supernatant was discarded). Subsequently, biomass samples were freeze-dried for 24 h. Triacylglycerides (TAG) and total fatty-acid (FA) extraction and quantification were done with the capillary column gas chromatographic method, as described by [41]. Chemicals were acquired from Sigma Aldrich and C15:0 (pentadecanoic acid, also from Sigma Aldrich) was used as internal standard for quantification.

2.2.4. Calculations

Biomass productivity (P_x, g L^{-1} d^{-1}) was calculated using Equation 1,

$$Px = \frac{(Cxt2 - Cxt0)}{(t2 - t0)} \qquad \text{Equation 1}$$

where the biomass concentration (C_x, g L^{-1}) of the reactor at the beginning (t_0, in days) and at the end of the growth phase (t_2, in days) were used.

Growth rate (μ) was calculated using Equation 2,

$$\mu = \frac{Ln(Cxt2 - Cxt0)}{(t2 - t0)} \quad \text{Equation 2}$$

where the natural logarithmic (Ln) of biomass concentration (C_x, g L^{-1}) of the reactor at the beginning (t_0) and at the end of the growth phase (t_2) were used.

The decrease rate of the photosystem II (PSII) quantum yield (QY_r) was calculated using Equation 3,

$$QYr = \frac{Ln(QYtf - QYt3)}{(tf - t3)} \quad \text{Equation 3}$$

where the natural logarithmic (Ln) of PSII quantum yield at two different points were used: the final day of starvation (t_f, which was t_9 and t_{15} for short and long starvation periods, respectively) and the beginning of the nitrogen run-out (t_2).

Total fatty-acids productivity (P_{FA}, g L^{-1} d^{-1}) was calculated using Equation 4,

$$PFA = \frac{(CFAtf * Cxtf)}{(tf - t3)} \quad \text{Equation 4}$$

where C_{FA} is the fatty-acid content in biomass (g g^{-1}) at the end of the starvation phase (t_f, which was t_9 and t_{15} for short and long starvation periods, respectively) and C_x is the biomass concentration (g L^{-1}) also at the end of the starvation phase. The total time of starvation (t, in days) is represented by the interval between the end (t_f) and the beginning (t_2) of the starvation phase.

Triacylglycerides productivity (P_{TAG}, g L^{-1} d^{-1}) was calculated using Equation 4, with the difference that the fatty-acid biomass content (C_{FA}) was replaced by the triacylglycerides biomass content (C_{TAG}, g g^{-1}). Both FA and TAG were analysed to evaluate the effect of the starvation on the productivity of both reserve lipids (TAG) and polar lipids (considered as the difference between FA and TAG).

2.2.5. Data analysis

Null hypothesis significance testing (NHST) was used to compare the results between and among samples. On-way analysis of variance (ANOVA) was used to assess statistical significance within groups. Subsequently, to compare groups between and among each other, the one-step multiple comparison test of Tukey was used as a post-hoc test. In all cases the assumptions of the statistical testes were checked: normality was assessed with the Kolmorogov-Smirnov test and homoscedasticity among tested groups was assessed with Levene's Test. For both assumptions and hypothesis, the probability of type I error (α) was set at 0.05. All analyses were carried out with the software SPSS v.22.

2.3. Results and Discussion

2.3.1. Biomass and lipid productivity under repeated N-starvation

The repeated N-starvation experiment was a continuous series of repeated batches that was divided into two phases: 8 cycles of short-starvation (RSS, 7 days of starvation) and 5 cycles of long-starvation (RLS, 13 days of starvation) (Figure 2.1). The results obtained for each period were averaged and are presented in Figure 2.2 and Table 2.1. No statistical differences were observed when comparing the growth rates (μ) and biomass productivities of RSS and RLS between and among each other (Table 2.1). This result shows two things: 1] the constant biomass productivity throughout repeated batches and that 2] doubling the starvation time showed no effect on subsequent biomass productivity in the next cycle.

The average growth rate from the repeated starvation periods (RSS and RLS) were also compared with the average growth rates of the controls (three independent batches). There was no difference in growth rate (μ) among all experiments (between 0.56-0.72 d^{-1}, Table 2.1). Similar growth rates show that *C. littorale* has a good capability of producing new functional biomass after N resupply, and was not affected by the repeated cycles of N-starvation. Comparable results were obtained with *Chlorella pyrenoidosa* using different intervals of harvesting followed by nitrogen resupply [42].

Biomass productivity (Px), however, was statistically higher in the control batch experiments when compared with the repeated starvation cycles (1.52 g L^{-1} against 1.1 [RSS] and 1.0 g L^{-1} [RLS],Table 2.1). This result can be explained from the repeated N-starvation, since N is essential to produce new functional biomass [21,43,44]. In repeated batches the biomass used to start a new cultivation has a lower nitrogen content in comparison with the biomass used to start a culture in the control batch. Thus, under the same conditions and equal nitrogen concentrations in the fresh medium, an inoculum with lower intracellular nitrogen content will reach lower values of biomass in comparison with the traditional batch, while retaining the same growth rate [44,45].

Table 2.1: Growth parameters and productivities of *Chlorococcum littorale* under repeated N-starvation and control N-starvation experiments. For both cases both short and long starvation periods are presented. Different letters mean statistical significance (ANOVA, $p<0.05$). Growth rate and biomass productivities were calculated between day 0-2. All other parameters were calculated using the N-starvation period (day 2 to the end of the cultivation. All productivities are presented in mg L^{-1} d^{-1} while the rates are per day (d^{-1}).

		Repeated N-starvation		Control N-starvation	
		Short (RSS)	**Long (RLS)**	**Short (CSS)**	**Long (CLS)**
PARAMETERS					
growth rate	**μ**	0.56±0.12 [a]	0.60±0.14 [a]	0.72±0.12 [a]	0.72±0.12 [a]
Biomass productivity	**P_X**	1.10±0.26 [a]	1.02±0.16 [a]	1.52±0.19 [b]	1.52±0.19 [b]
FA productivity	**P_{FA}**	0.28±0.02 [a]	0.15±0.02 [b]	0.33±0.03 [a]	0.22±0.01 [c]
TAG productivity	**P_{TAG}**	0.21±0.03 [a]	0.12±0.02 [b]	0.24±0.05 [a]	0.18±0.01 [a]
QY decrease rate	**Qy_r**	-0.21±0.07 [a]	-0.07±0.01 [b]	-0.19±0.01 [a]	-0.09±0.01 [b]
Growth phase	**d**	2	2	2	2
N-starvation phase	**d**	7	13	7	13
Total Cultivation time per cycle	**d**	9	15	9	15
Number of cycles		8	5	3	3

Other researchers have evaluated the effect of repeated-batch (with N run-out) on the biomass productivities of other species. *Chromochloris zofingiensis* showed a reduction from 0.75 to 0.66 g L^{-1} d^{-1} in biomass productivity when comparing the repeated-batch with the control batch, respectively [46]. Another related work [47] evaluated the effect of different cycles duration on *Nannochloropsis sp*. under repeated batch in a lab-scale flat panel photobioreactor. In the work of Benvenuti et al. [47], short repeated batches (1 day), showed an increase in biomass productivity from 0.68 (reference batch) to 0.94 g L^{-1} d^{-1}, while longer repeated batches (2 and 3 days), showed a reduction from 0.68 to 0.57 and 0.43 g L^{-1} d^{-1}, respectively. Comparing results from different research is limited due to intrinsic variables (used species and experimental design). The analyses of our results and the above mentioned data, however, indicate that the nitrogen concentration and the duration of the starvation cycle play a major role when aiming at repeated-batch microalgae cultivation.

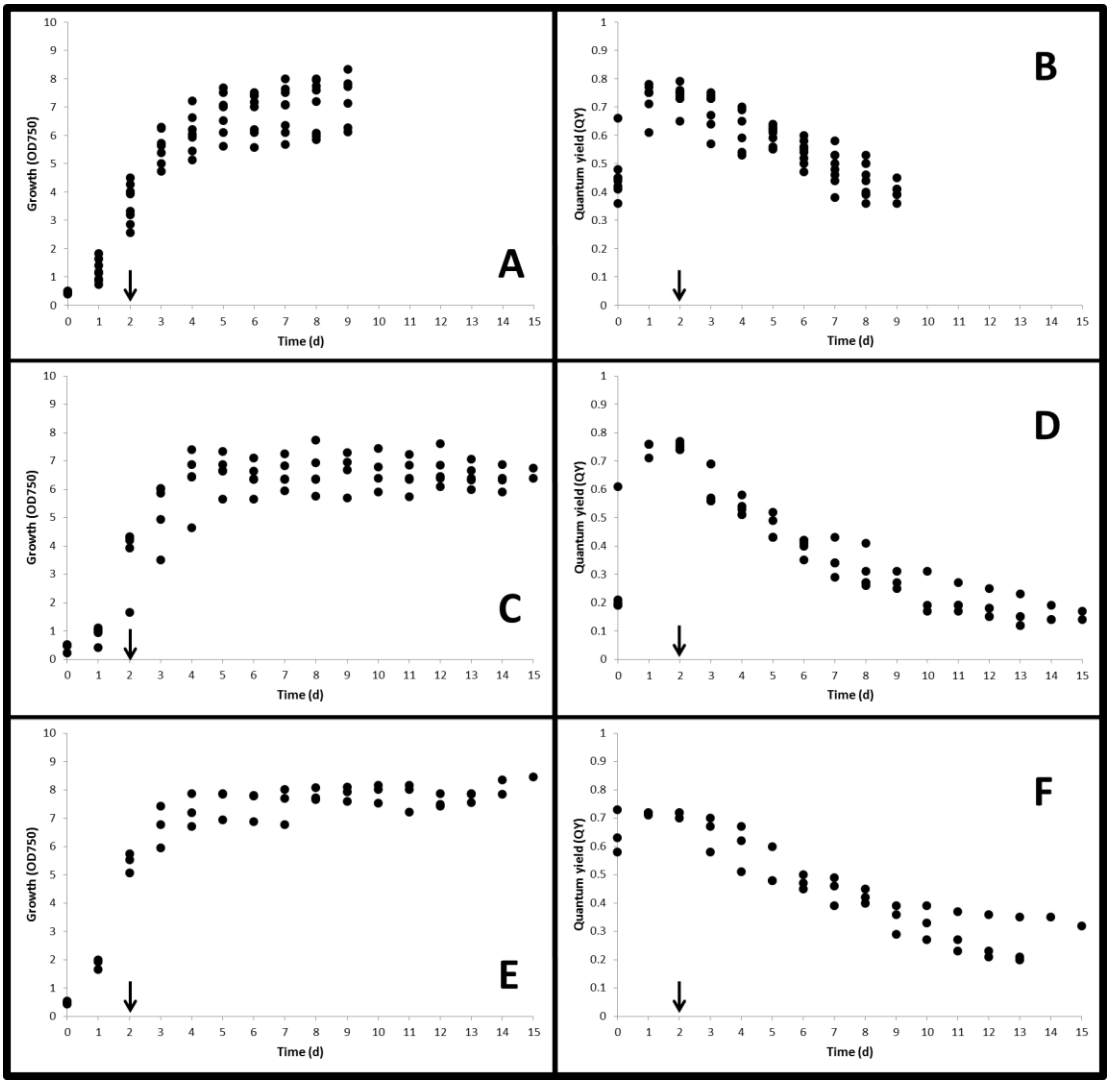

Figure 2.1: Biomass production over time for repeated short-starvation (RSS, A), repeated long-starvation (RLS, C) and the control long-starvation (CLS, E). Time-evolution of the quantum yield of photosystem II (QY) for repeated short-starvation (RSS, B), repeated long-starvation (RLS, D) and the control long-starvation (CLS, F). The control short-starvation (CSS) is considered from day 0 to day 9 of Figures E and F. Arrows mark the beginning of the N-starvation period, which was the same for all experiments. Figures A and B represent the overlapped curves of 8 independent experiments (total 72 days), figures C and D represent 5 overlapped experiments (total 75 days) and figures E and F of 3 experiments (total 45 days).

Additional to the growth rates and biomass productivities, the QY of PSII was also followed daily during the repeated cycles and control (Table 2.1; Figure 2.2). The QYr was used to estimate the reduction rate in the PSII activity during N-starvation [35,37]. No statistical difference was found between batches with the same starvation period, but batches with longer starvation periods showed higher QYr (both, RSS and CSS; and RLS and CLS, Table 2.1). Our results show that the QYr is dependent on the duration of N-starvation and was not affected by the repeated starvation cycles. The QY values at the end of the stress period Figure 2.2) were approximately 0.4 for the RSS and approximately 0.2 for the LRS, but those values returned to the same values

of non-starved biomass (between 0.7 and 0.8) within 24 h of nitrogen re-supply. This finding indicates a quick recovery of photosynthetic capacity after N-resupply for *C. littorale*.

As it can be observed in Figure 2.3, no statistical differences (ANOVA, $p>0.05$) can be observed in the FA and TAG biomass content when comparing all four cycles among each other (the complete composition of both total fatty-acids and TAG's can be found in the supplementary materials). As it can be seen, most lipids of *C. littorale* are synthesized within the first 6 days of starvation. After doubling the starvation period only 5% more lipids are synthesized (Figure 2.3 and Table 2.1). Additionally to a stable lipid content, the saturation degree of both FA and TAG showed no differences when comparing all four cycles among each other starvation (Figure 2.3A). In line with these previous findings, the biomass lipid content (both FA and TAG) shows that repeated N-starvation cycles over a period of 147 days did not affect the lipid metabolism of *Chlorococcum littorale*.

Lipid productivities (both FA and TAG) were stable throughout the repeated-starvation experiments with the same duration (both short and long starvation periods). The highest lipid productivities, however, were obtained for the short periods of starvation (ANOVA $p<0.05$, Table 2.1). This result is explained by the response of microalgae when exposed to N-starvation: an increase in biomass lipid content is observed within the first hours/days after starvation starts [35]. Lipid productivity (both FA and TAG) was the same between short repeated-starvation and short control starvation (RSS: 0.28 and CSS: 0.33 g L^{-1} d^{-1}, ANOVA $p>0.05$, Table 2.1). Different results were obtained when comparing the experiments with long starvation periods: in this case the RLS showed statistically lower values of lipid productivity when compared with the CLS (0.15 against 0.22 g L^{-1} d^{-1}, respectively). Since lipid content was the same in both RLS and CLS, the smaller lipid productivity of RLS is explained by the lower biomass productivities obtained (a reduction from 1.5 [CLS] to 1.0 g [RLS] L^{-1} d^{-1}). These results show that the repeated N-starvation didn't impair lipid production and that for shorter periods of starvation *Chlorococcum littorale* showed the same lipid productivities as batch cultivations.

Altogether, our results show that repeated-batch is a suitable approach to produce *Chlorococcum littorale* for two reasons: 1] Under repeated N-starvation (short starvation cycles) TAG productivity was the same as the control-batch; and 2] Under repeated N-starvation (short and long cycles) both biomass and lipid productivities were stable throughout time.

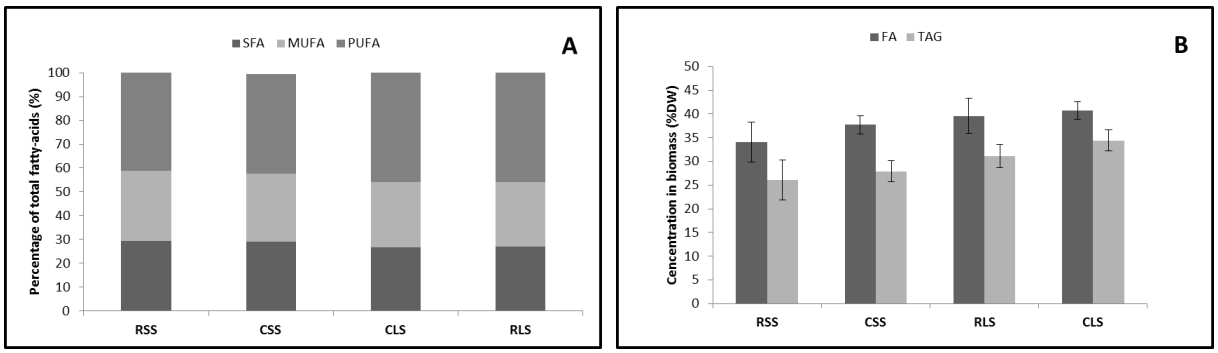

Figure 2.2: Saturation degree of all 4 sets of experiments (A), the distribution shows the percentage (of total fatty acids) as saturated (SFA), monounsaturated (MUFA) en polyunsaturated (PUFA). (B) shows the final accumulated fatty-acids and TAGs for all 4 sets of experiments (shown as % dry weight). Acronyms are: RSS: repeated short-starvation; CSS: control short starvation; RLS: repeated long-starvation; CLS: control long starvation.

2.3.2. Implications for adaptive laboratory evolution (ALE) experiments

Repeated batch operation is also used in experiments that aim at inducing changes in a population of microorganisms by repeatedly exposing them to stress factors (e.g. nutrient deprivation, competition for resources and abiotic factors like light and temperature). This approach is known as adaptive laboratory evolution (ALE), and the principle is that continuously diluting a microorganism culture under specific stress factors will cause random selection of cells [13]. The expected goal is to have final populations that are more fit to the selective environment than the wildtype starting population. Previous work [11] showed an increase of 30% in biomass productivity of *Chlorella vulgaris* after 15 cycles (thus 45 days) of repeated batch (always with N) under red-LED lamps (6604nm instead of 680nm). Similarly, increased yield of β-carotenes was achieved with *Dunaliella salina* combining red and blue LED lamps under ALE experiments after 16 cycles (80 days) of repeated-batch (with N) [16]. An ALE approach using CO_2 concentrations between 2-30% generated cell lines of *Chlorella sp*. with improved growth rate and chlorophyll contents after 31 cycles (97 days) under a CO_2 concentration at 10 % [17]. Finally, improved growth (17-48% in comparison with Wt) was found in starch-less mutants of *Chlamydomonas reinhardtii* after 28 cycles of 3-day growth under constant light [18]. Altogether, these previous works highlight the potential of some microalgae strains to be modified using adaptive laboratory evolution in a relatively short cycle of experiments, comparable to the duration of our experiments.

The possibility of improving microalgae performance in our experimental set-up was a secondary aspect of our research question. Although not a primary expectation from our work, the review above mentioned highlights the possibility to achieve cell lines of microalgae after relatively short periods of evolution (approximately 90 days). Another question is to access how stable are these differences shown by other authors, i.e. are these differences due to physiological adaptations or permanent mutations? Such question was not addressed the reviewed works above mentioned. The review of ALE experiments show that the most common response of microalgae to repeated stress is an increase in growth rate, which would increase the lipid productivity if the lipid metabolism is not affected [11,13,17,18]. In addition, the response to repeated stress (light, nutrients and temperature) is highly strain-dependent [13,18]. With that in

mind, one should pay attention to which abiotic/biotic variables can most potentially affect one's working strain.

Chlorococcum littorale showed a sharp and stable recovery in photosynthetic activity (QY) and nitrogen uptake rate immediately after N-resupply. At the same time the growth rates were maintained and lipid productivity of shortly starved biomass when compared with the control batch. Combined, these factors indicate a strain that can handle nitrogen environmental stress very well. In our experiments light was kept constant (400 µmols m^2 s^{-1}, in a reactor with 1.4 cm depth), while other reports have shown positive growth under 2000 µmols m^2 s^{-1} (1 cm flat panel reactor, 18 g L^{-1} cell density)[38]. Since our experiments were aimed at studying the effect of nitrogen starvation, the light used was kept constant at 400 µmols m^2 s^{-1}. If aiming at inducing improved growth in *C. littorale* performance, one could consider ALE experiments under high light conditions or under sharp changes in light intensity, to introduce intensive selective pressure. Another option would be to use temperature as a selection pressure, since in the current experiments temperature was kept constant (at 25˚ C) throughout the experiments. Previous work shown that *C. littorale* can grow from 16 to 32 degrees Celsius, with optimum around 28 [48], showing that temperature might be a stress factor to induce the development of thermotolerant cell lines.

The stable performance of *C. littorale* shown in this work, indicates that this strain has a natural capability to handle fluctuations in the nutrient supply regime, which could indicate a possible strain to be used under fluctuating climate conditions. The resilience of *C. littorale* to repeated nitrogen starvation makes it suitable for repeated-batch cultivations and potentially unsuitable for inducing changes via ALE using N-starvation as a stress factor.

2.4. Conclusions

Shorter and longer periods of N-starvation didn't affect PSII quantum yield evolution and biomass productivity of *C. littorale*. Repeated short-starvation batches could be used as an operational strategy since it didn't affect lipid productivity. Longer periods of starvation, however, had lower lipid productivities when compared with the equivalent control. Most importantly, the biomass lipid content was the same between control and repeated batches, highlighting that the lipid metabolism was not impaired. Altogether, *C. littorale* is a resilient and stable strain, that can be cultivated in a semi continuous mode for both biomass and lipid production.

2.5. Supplementary materials

Table S2.6.1: Fatty-acid (FA) and triacylglycerol's (TAG) composition and concentration of *C. littorale* under all four experimental groups: RSS: repeated short-starvation; CSS: control short starvation; RLS: repeated long-starvation; CLS: control long starvation.

	RSS			CSS				RLS			CLS		
FA	**Average**		**SD**	**Average**		**SD**		**Average**		**SD**	**Average**		**SD**
C12	0.03%	±	0.0%	0.03%	±	0.0%		0.10%	±	0.0%	0.03%	±	0.0%
C14	0.21%	±	0.1%	0.27%	±	0.1%		0.24%	±	0.0%	0.23%	±	0.1%
C16	7.30%	±	2.3%	8.20%	±	0.0%		6.52%	±	1.1%	8.27%	±	0.6%
C16:1	1.00%	±	0.2%	1.05%	±	0.0%		0.72%	±	0.2%	1.00%	±	0.2%
C16:2	0.56%	±	0.2%	0.48%	±	0.0%		0.45%	±	0.1%	0.41%	±	0.1%
C16:3	0.77%	±	0.7%	0.60%	±	0.1%		1.51%	±	0.1%	0.70%	±	0.1%
C16:4	3.18%	±	0.9%	4.08%	±	1.2%		3.38%	±	0.7%	4.45%	±	0.2%
C18	1.17%	±	0.3%	1.12%	±	0.0%		2.61%	±	0.2%	1.06%	±	0.2%
C18:1	7.87%	±	2.1%	8.86%	±	0.1%		6.93%	±	1.3%	8.91%	±	1.3%
C18:2	2.52%	±	0.4%	2.45%	±	0.2%		3.41%	±	0.3%	2.45%	±	0.2%
C18:3	5.53%	±	2.0%	7.22%	±	1.1%		8.04%	±	1.4%	8.19%	±	0.5%
TOTAL	**30.14%**	**±**	**7.2%**	**34.36%**	**±**	**2.8%**		**35.71%**	**±**	**5.5%**	**35.69%**	**±**	**3.5%**
TAG													
C12	0.03%	±	0.0%	0.05%	±	0.0%		0.21%	±	0.0%	0.02%	±	0.0%
C14	0.13%	±	0.0%	0.25%	±	0.1%		0.18%	±	0.0%	0.18%	±	0.0%
C16	5.82%	±	1.6%	3.58%	±	0.1%		7.67%	±	0.9%	7.97%	±	0.6%
C16:1	0.90%	±	0.2%	0.79%	±	0.7%		0.97%	±	0.2%	0.85%	±	0.1%
C16:2	0.45%	±	0.1%	0.50%	±	0.3%		0.39%	±	0.2%	0.34%	±	0.0%
C16:3	0.78%	±	0.9%	0.28%	±	0.2%		0.63%	±	0.1%	0.62%	±	0.0%
C16:4	2.67%	±	0.8%	1.87%	±	0.1%		4.53%	±	0.5%	4.42%	±	0.2%
C18	1.01%	±	0.3%	0.71%	±	0.2%		0.95%	±	0.3%	0.93%	±	0.1%
C18:1	6.70%	±	1.8%	7.29%	±	0.4%		8.39%	±	1.1%	8.03%	±	0.9%
C18:2	2.34%	±	0.2%	1.91%	±	1.3%		2.37%	±	0.4%	2.32%	±	0.2%
C18:3	4.27%	±	1.5%	6.12%	±	0.3%		7.53%	±	0.5%	7.96%	±	0.5%
TOTAL	**25.11%**	**±**	**7.5%**	**23.36%**	**±**	**3.7%**		**33.8%**	**±**	**4.2%**	**33.6%**	**±**	**2.5%**

Rapid method to screen and sort lipid accumulating microalgae

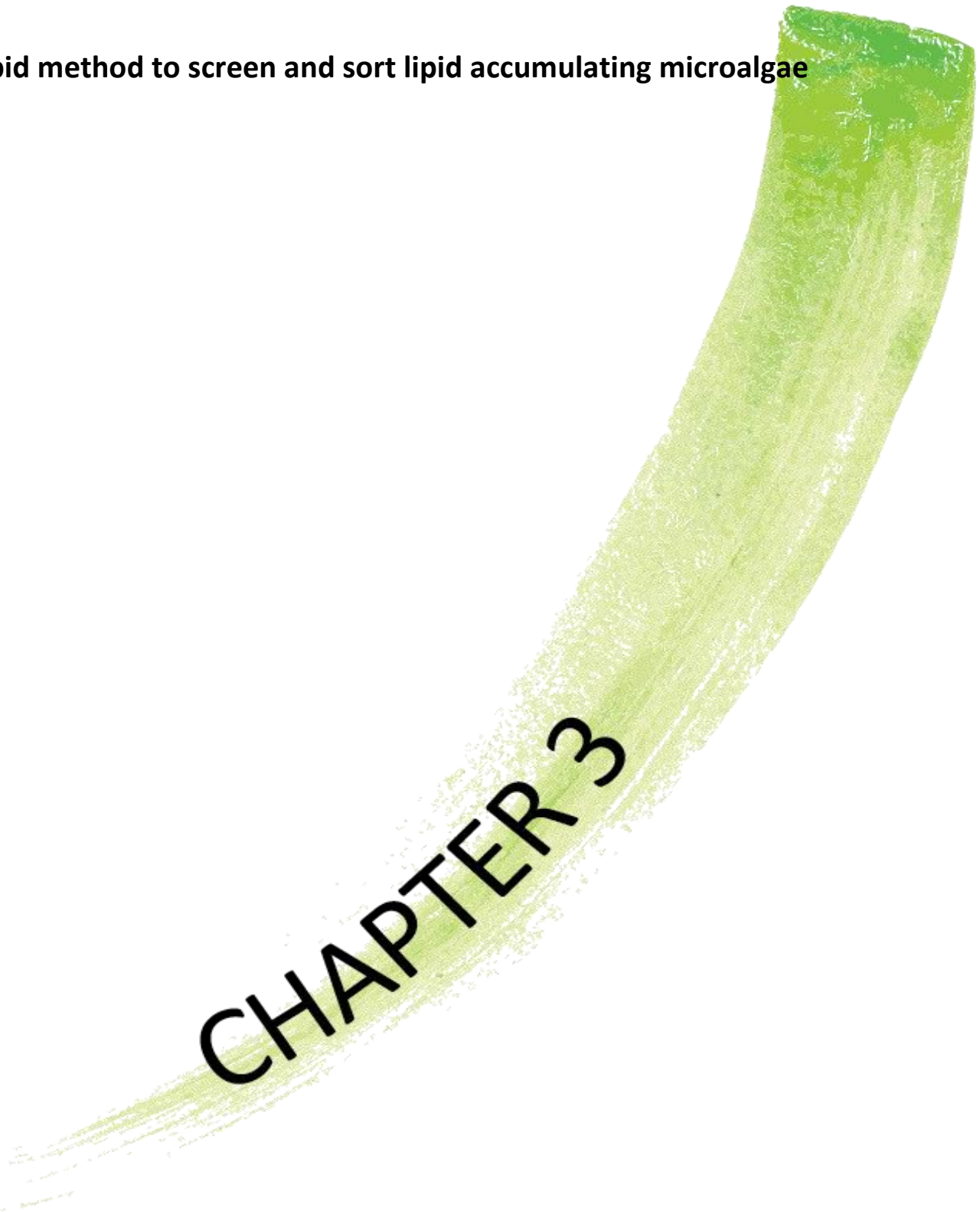

This chapter has been published as: Cabanelas, Iago Teles Dominguez; Zwart, Mathijs van der; Kleinegris, Dorinde MM; Barbosa, Maria J & Wijffels, René H. 2015. Rapid method to screen and sort lipid accumulating microalgae. Bioresource Technology 184, 47-52.

ABSTRACT:

The present work established an efficient staining method for fluorescence activated cell sorting (FACS) with *Chlorococcum littorale* maintaining cellular viability. The method was designed to detect high-lipid cells and to guarantee cellular viability. $BODIPY_{505/515}$ (BP) was more suitable to FACS when compared to Nile red. The optimum concentrations were 0.4 $\mu g.ml^{-1}$ of BP, 0.1 % DMSO or 0.35% ethanol. Both ethanol and DMSO were equally efficient and assured cellular viability after the staining and sorting. Here a method is presented to rapidly screen and sort lipid rich cells of *C. littorale* with FACS, which can be used to produce new inoculum with increased cellular lipid content.

Key words: Microalgae; Lipids; FACS; $BODIPY_{505/515}$; *Chlorococcum littorale*

3.1. Introduction

Microalgae are among the most promising and suitable sources to achieve sustainable production of commodities such as proteins, carbohydrates and specially oil as feedstock for food, feed, chemicals and biofuels [6,49,1]. However, the lipid productivity of the known strains needs to increase to make the production of algal lipids economically feasible [3]. Higher lipid productivity can be achieved with fast growing strains with high oil yield, which can reduce the costs of microalgae bulk production [3,1]. One option to develop an industrial culture of algae for production of lipids is via rapid sorting of lipid rich cells from a mixed population [50].

High throughput cell sorting can be done by coupling the fluorescence detection of intracellular lipid bodies (LB) with flow cytometry (FC) to carry out Fluorescence Assisted Cell Sorting (FACS) [10,24,51,52]. This technique allows the selection of a certain profile and the use of it to sort targeted cells, which can be grown and be used to establish a new cell lineage [10]. However, there are still challenges to apply it to sort lipid rich microalgae: (i) the staining must be designed to distinguish efficiently the high-lipid content cells; (ii) the dye must be homogeneously distributed in the population and (iii) the process must assure cellular viability to allow growth of sorted cells.

Nile red (NR - 9-diethylamino-5-benzo[α]phenoxazinone) is still the most common lipophilic fluorophore used for microalgae [10,14,52–55]. Yet, this dye has a series of drawbacks, especially when aiming at FACS. It may require a combination of cell destructive methods to increase dye homogeneity and the accuracy is highly strain dependent [53]. Also, it can interfere with the chlorophyll molecule on the lipid specific fluorescence, since it is also excited by a green laser (530/25 nm) and emits fluorescence in the yellow spectra (590/10)[56]. However, the ultimate inadequacy is its limited photo stability resulting in signal which is not constant in time. The application of $BODIPY_{505/515}$ (BP) probe in microalgae has become much more popular over the last few years [21,24,51,52,57–59]. $BODIPY_{505/515}$ (4,4-Difluoro-1,3,5,7-Tetramethyl-4-Bora-3a-Diaza-s-Indacene) has a high oil/water coefficient, which allows it to infuse membranes and makes the labelling of cell components faster than NR. It is excited by a blue 488 nm laser, with maximum emission in the green spectrum at 515 nm, which makes it spectrally distinguishable from algal chlorophyll spectra [51,52].

In the current research *Chlorococcum litorale* was the species of choice. Previous results of screening tests showed, under nitrogen stress: i) high photosynthetic efficiency, ii)biomass production (0.3 g $l^{-1}d^{-1}$) and iii) lipid accumulation (10 – 35 g fatty acids per g biomass l^{-1} d^{-1}) [37]. This strain was first described by Chihara et al. [39], *C. littorale* showed fatty acids accumulation of 34% DW high and a resilient CO_2 uptake (up to 50% CO_2) [40,60]. These features remark the potential - not thoroughly investigated - of this strain for lipid production. The aim of this work was to optimize a fluorescence method to efficiently assist cell sorting of *C. littorale,* assuring cellular viability.

3.2. Material and methods

3.2.1. Microorganism and culture conditions

Chlorococcum littorale (NBRC 102761) was acquired from the microbial culture collection of NIES, Japan [39]. For the optimization phase of the experiments it was cultivated batch-wise in the following medium (composition in g l^{-1}): NaCl 24.55; $MgSO_4.7H_2O$ 6.60; $MgCl_2.6H_2O$ 5.60; $CaCl_2.2H_2O$ 1.50; $NaNO_3$ 1.70; HEPES 11.92; $NaHCO_3$ 0.84; EDTA-Fe (III) 4.28; K_2HPO_4 0.13; KH_2PO_4 0.04; trace elements in mg l^{-1}: $Na_2EDTA.2H_2O$ 0.19; $ZnSO_4.7H_2O$ 0.022; $CoCl.6H_2O$ 0.01; $MnCl_2.2H_2O$ 0.148; $Na_2MoO_4.2H_2O$ 0.06; $CuSO_4.5H_2O$ 0.01). The cultivation was carried out in an incubator (Multitron Pro orbital shaker incubator INFORS HT, Switzerland) under controlled conditions and carried out in 0.2l borosilicate Erlenmeyer flasks. The operational conditions were: mixing at 120 rpm, light intensity 150 µmol m^{-2} s^{-1}, temperature at 25±0.2° C and CO_2 supply of 2% v/v over air flow in the headspace.

Non-stressed cultures were grown under nitrogen-replete conditions (i.e. with nitrogen available in de growth medium), while stressed cultures where kept under nitrogen-depleted conditions (i.e. no nitrogen available in the media). To carry out the stress experiments the progressive starvation approach was used, i.e. cells were allowed to consume all nitrogen available (150 mgN-NO_3/liter). Nitrogen starvation was used and a factor to stimulate lipid accumulation inside the cells. For the sorting and viability experiments, microalgae were cultivated in a flat panel reactor as described by [41] for both stressed (without nitrogen in the medium) and non-stressed cultures (with nitrogen in the medium). Both stressed and non-stressed experiments were performed aseptic and batch-wise. The liquid volume in the reactors was 380 ml with a light path of 14 mm. Operation was run at continuous illumination (incident light 410 µmol m^{-2} s^{-1}) using LED lamps with a warm white light spectrum (Bridgelux, BXRA W1200). The pH was set at 7.0 and controlled on demand by CO_2 addition to the airflow.

Nitrogen starvation was progressively imposed in the experiments. All available nitrogen was allowed to run out in the systems. Nitrogen replete experiments were carried out using samples from the exponential growth phase. The nitrogen content (N-NO_3 mg l^{-1}) was checked daily by the Sulphanilamide N-1-naphthyl method (APHA 4500-NO3-F) using the automatic analyser SEAL AQ2.

3.2.2. Experimental set-up and analytical methods

The experimental set-up followed the flow chart presented in figure 3.1. For every trial the measurements were performed on samples taken from the reactor under the same experimental conditions. All analysis were carried out with 3 to 5 replicates. Cytometer measurements were terminated when 10.000 individual particles were measured.

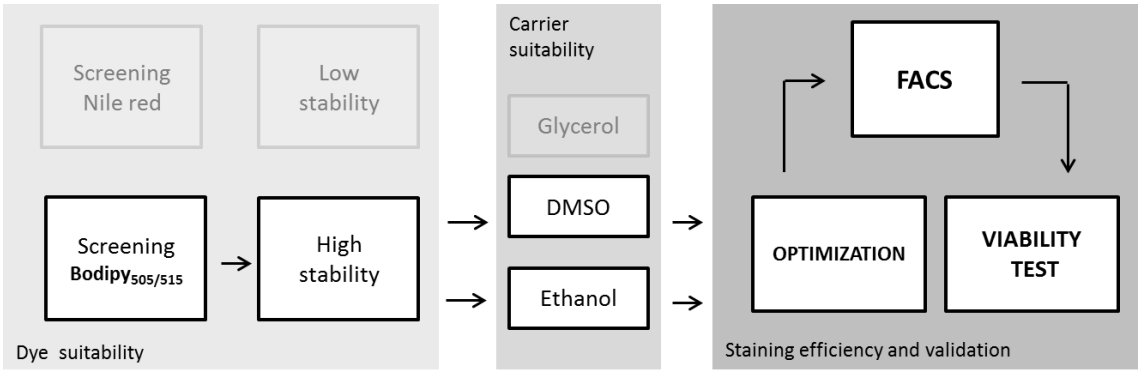

Figure 3.1: Experimental flow diagram. The shaded boxes represent negative results, thus they were put aside (supplementary materials for more information). The acronyms refer to dimethylsulfoxide (DMSO) and Fluorescence Assisted Cell Sorting (FACS from BD® flow cytometer).

The purpose of this approach was to select the best suitable protocol to effectively stain *Chlorococcum littorale*. The process also had to guarantee two key points: to detect high lipid content cells and to sustain the viability of the cells.

3.2.3. Fluorescence analysis

A Microplate reader FLx800 (BioTek Instruments) was used to assess fluorescence emission after excitation on predetermined wavelengths. For nile red (NR) (CAS#: 7385-67-3, Sigma Aldrich) a baseline protocol was established. Microalgae cell suspension was set at 0.8 of optical density (750 nm) and NR and glycerol (Sigma Aldrich, CAS#: 56-81-5) were directly added to the cell suspension. NR was kept in a stock solution, in acetone, at a concentration of 100 µg ml^{-1}. Fluorescence emission measurements were taken from 0 to 15 minutes, with 20 second intervals. The set of filters used were: excitation of 530/25 nm and emission of 590/10 nm. The sensitivity was set at 70 mV. The optimization approach tested the following parameters: NR concentrations: 0.4; 0.6; 0.8; 1.0 and 1.2 µg ml^{-1}, glycerol: 5; 10; 25; 50; 100; 125; 150 µg ml^{-1}.

A baseline protocol for $BODIPY_{505/515}$ (BP) (Life Technologies®) in the micro plate reader could not be established due to excessive noise (data not shown). For that reason the BP analysis was done directly in the flow cytometer (FACSCalibur, BD Biosciences, San Jose, California). BP stock solutions were prepared in all tested carriers: Dimethyl sulfoxide (DMSO, Sigma Aldrich CAS#: 67-68-5), ethanol (EtOH, Sigma Aldrich CAS#: 64-17-5) and glycerol ($C_3O_8H_3$, Sigma Aldrich CAS#: 56-81-5). The effectiveness of glycerol as a carrier was tested by addition of glycerol to the algae suspension in the following concentrations: 0; 0.10; 0.2; 0.3; 0.4; 0.5; 0.75 µg mL^{-1}.

Carriers were kept at the lowest possible concentration, in order to not affect the cellular viability. Microalgae samples were diluted until a concentration in which approximately 200 cells min^{-1} could be measured by the cytometer (between 1:50 and 1:200 dilution). Sterilized PBS (phosphate saline buffer - 1.0x) was used as sheath fluid. The readings were carried out with an argon ion laser with excitation at 488 nm and emission at 530/30 (BP, FL1 channel). All readings were logarithmic and the sensitivity of the apparatus was set at 300 mV. The cells were

sorted under these settings. To actually sort cells it is necessary to set a sorting gate, a selected fraction of the acquisition plot that establishes the thresholds which will be used to activate the sorting line, and perform the physical separation of targeted cells. An example of a sorting gate is given in Figure 3.4.

The flow cytometer cannot provide imaging of the assessed cell population. Therefore, the FlowCam (Fluid Imaging Technologies, Yarmouth, Maine) was used to provide both fluorescence measurements and imaging of the population. This approach had the objective to provide more descriptive information of the population: auto fluorescence and BP-dependent fluorescence per cell, cell diameter, presence of reproductive cells, contamination control and etc. For the FlowCam fluorescence measurements the following settings were used: samples dilution of 100-1000 times, 20x optical magnification, Trigger mode on (use of the argon laser to target particles) with Channel 2 (Ch2, Green).

The viability test was also carried out with the FlowCam (5 biological replicates). After being sorted in the FACS station, cells were immediately centrifuged (5000 x g) and followed by re-suspension with sterile growth media. Subsequently, they were kept under constant light in sterile falcon tubes (50ml). From day zero cells were counted with the FlowCam using the vitality dye Erythrosine B (4 mg ml^{-1} in 1xPBS) following the method of [61]. This staining is based on the differential uptake ratio of erythrosine between dead/alive cells. Erythrosine B can only be taken up by those cells whose plasma membranes have been damaged (considered nonviable). The differentiation can be assessed with light microscopy, since nonviable cells will appear pinkish-reddish. 20 µl of staining solution was added to 400 µl of microalgae suspension. After incubating for 10 minutes at room temperature, particles were counted in the FlowCam. The settings of the FlowCam were the same as before, with the exception of the reading mode that was set at Autoimage instead of Trigger mode. The viability was calculated accordingly with the following equation:

[1] $N_v \times 100/N$ [%]

where N_v is the number of viable cells and N is the total number of cells counted.

3.2.4. Triacylglycerides analysis

Samples of biomass (each approximately 30 mg) were harvested at 5 points in time of a batch cultivation of *C. littorale*. The time frame of sampling was from the second day after inoculation until the last day of stationary phase (10^{th} day), prior to fluorescence reading in the flow cytometer. The samples were centrifuged at 5000xg, washed to remove residual salts, frozen at -18 °C and freeze-dried for 24 h. Triacylglycerides (TAG) extraction and quantification were performed with the capillary column gas chromatographic method applied to the oil methyl esters, as described by [41].

3.2.5. Data analysis

Data from the micro plate reader, FlowCam and cytometer were exported to Microsoft Excel files with its basic statistics for editing. For further statistical analysis and graphs design SigmaPlot version 12.5 (STATSconsult, Netherlands) was used.

For statistical analysis the one-tailed Student's t-test was used to determine the difference between two groups, and one-way analysis of variance (ANOVA) was used to compare the significance of data among groups (≥ 3). A p-value lower than 0.05 ($p < 0.05$) was considered significant. A Linear regression approach was carried out to assess the correlation between variables (R^2 results are shown in the text and/or displayed in the charts).

For the viability assay stained (EtOH and DMSO) and non-stained (control) sorted cells were compared by growth rates - μ (d^{-1}) - according to [62] using the equation

[2] $\mu\ (d^{-1}) = \ln(C_2) - \ln(C_1) / (t_2 - t_1)$

where C_2 is the number of cells at the end of the growth phase and C_1 is the number of cells at the start of growth phase. The time of growth is represented by t_2 (final) and t_1 (initial).

3.3. Results and discussion

3.3.1. Screening two potential probes: BODIPY$_{505/515}$ and Nile red

The process optimization followed the steps presented in figure 3.1. The results with NR were positive but not suitable enough due to low signal stability (Figure 3.2). Full details of the optimization process with NR are available in the supplementary material.

Results showed optimal concentrations for Nile red (NR, 0.8 µg ml^{-1}) and assistant/carrier (glycerol, 125 mg ml^{-1}) close to values reported by [24]. Since the cellular viability of microalgae may be affected by the toxicity of DMSO [24], glycerol was chosen as carrier due to its low toxicity and previous applicability to fluorescence methods with microalgae [10,51]. However, the retaining time of the NR fluorescence signal started to decrease substantially after 3 minutes in the stressed cells (Figure 3.2, $p < 0.001$). The stability of the dye is a crucial factor when using FACS [59]Pick et al. [63] states that NR signal shifts between cytoplasmic plasma membrane and lipid globules fluorescence, and that such effect is more intense in cells with increased lipid content (i.e. N-starved). Also the fluorescence quenching (pronounced drop in the signal of high-lipid cells) can result from self-association of NR [63]. It has been shown that NR staining can be feasible with microalgae for lipid determination [55] and for fluorescence activated sorting [10]. However, due to a fast decrease in the fluorescence signal the application of NR to FACS is limited (Figure 3.2). A decreasing signal may lead to losses in the sorting process, since the values used to establish the sorting gate may not be found when sorting the cells. Henceforward, nile red was put aside

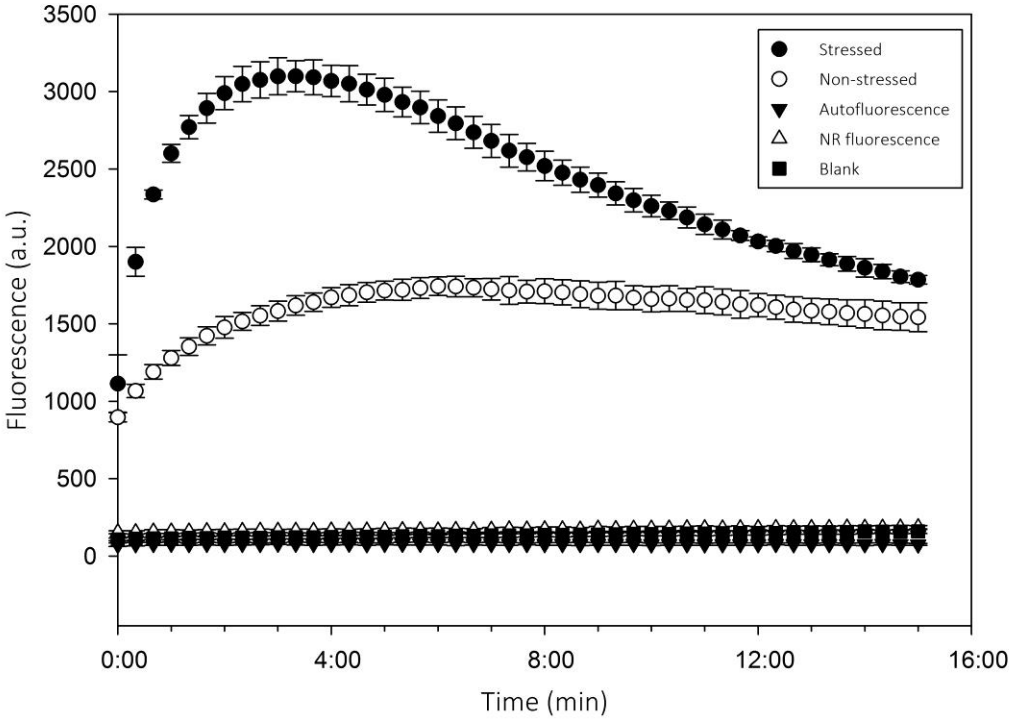

Figure 3.2: Final optimized protocol of nile red (NR) with *C. littorale* using stressed and non-stressed cells. The result was positive but not suitable enough, when compared to bodipy, due to a low signal stability. The following parameters were measured to remove interferences: Auto fluorescence regards to microalgae chlorophyll signal, NR fluorescence refers to the signal of NR solution alone (without algae) and as a blank it was used the same media that was used to dilute all other samples.

BODIPY gave a more stable fluorescence signal and is therefore more suitable for FACS when compared with NR. The fluorescence peaked after 5 minutes and was kept constant for 30 minutes consecutive readings (Figure 3.3A). Such findings are in agreement with values reported elsewhere [24,51]. The interval of 30 minutes was considered enough for average sorting gates (2- 10 minutes) and longer sorting periods (if very narrow sorting gates are selected, 20 - 30 minutes).

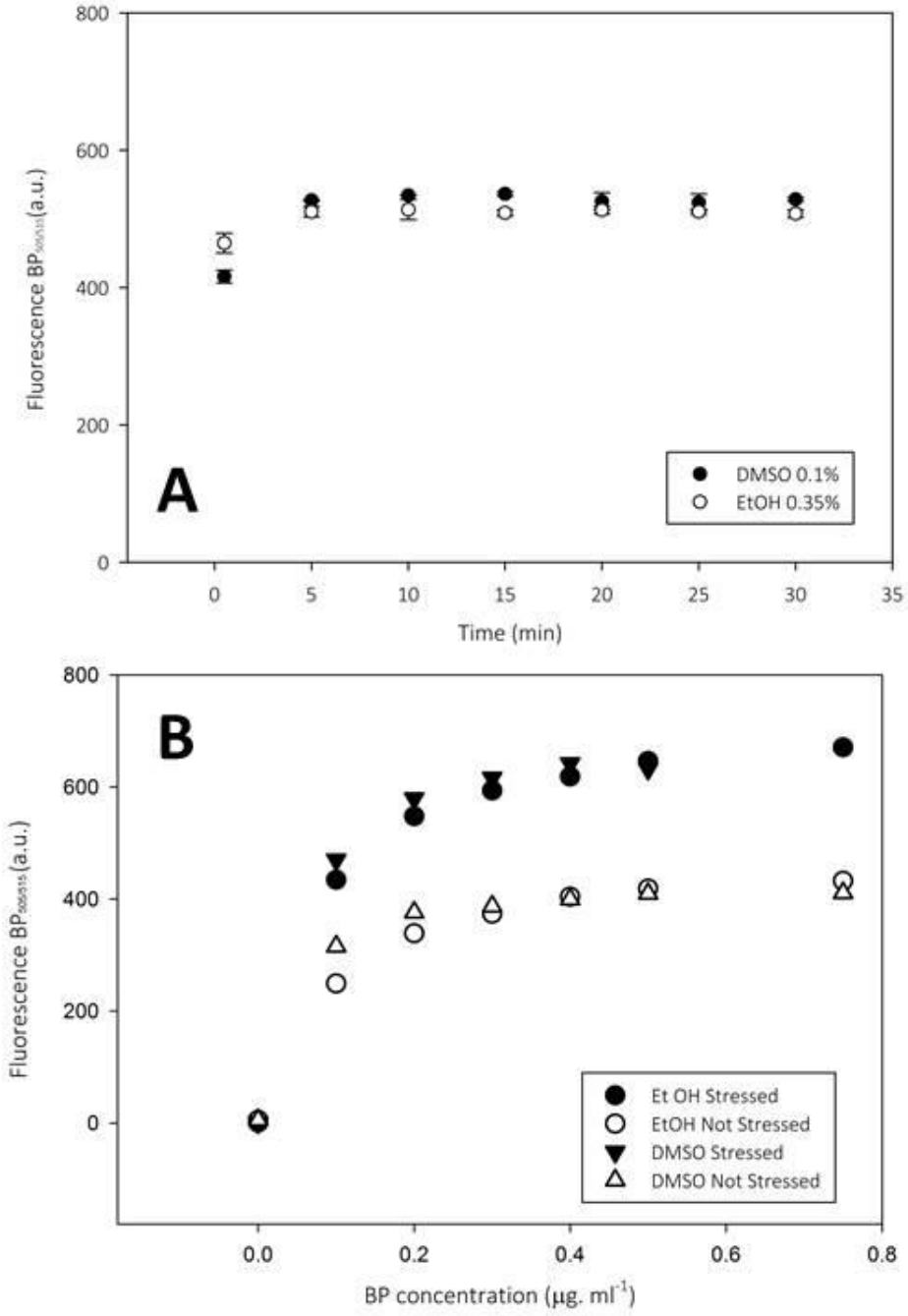

Figure 3.3: Optimization of BP with *C. littorale* with both carriers: EtOH and DMSO. (A) Assessment of BP retaining time within 30 minutes with 5 minutes intervals; conditions: 0.8 µg ml^{-1} BP (based on [7, 8]), 0.1% DMSO and 0.35% EtOH).(B) Effect of different BP concentrations on fluorescence intensity, assistants at: 0.35% EtOH and 0.1% DMSO.

The next step was to check the correlation between BP fluorescence and the content of neutral lipids (triacylglycerides, TAGs). The correlation presented a positive trend line (R^2 = 0.94, section 4 of supplementary materials) and confirms BP as an estimator of the cellular concentration of TAGs. This showed the reliability of BP - and of the present method - for screening the intracellular neutral lipids of *C. littorale*. The TAG profile and content is in accordance with [64] with isomers of C16 and C18 as the most abundant (for the full TAG profile: supplementary materials).

3.3.2. Optimization of the best probe: $BODIPY_{505/515}$

The results showed an optimum concentration of 0.4 µg ml^{-1} for BP, which is close to previous results with other microalgae species [51,53,59]. Nonetheless, this factor is highly strain dependent, particularly due to cell wall thickness and membrane permeability [59].

To achieve a high throughput sorting method for viable cells carriers/solvents concentrations were kept at the feasible minimum: 0.1% DMSO and 0.35% EtOH. DMSO is regarded as suitable and necessary for BP [52,65,66], but likewise it is known for its toxicity at high concentrations [24,59]. Ethanol was used as a solvent of BP considering its overall low toxicity. We hypothesized that BP could require only a polar solvent, therefore, the performances of both EtOH and DMSO at basal concentrations were compared (Figure 3.3).

Both carriers showed positive outcomes, with no differences between each other (Figure 3.3B, $p > 0.05$). There was a clear differentiation in fluorescence between the populations of N-stressed (high lipid) and non-stressed (low lipid) cells ($p<0.001$; Figure 3.3B). $BODIPY_{505/515}$ has been reported to need DMSO in order to permeate cells, but clearly the response is strain dependent and requires testing before application [51,52]. Until present date there is no report of successful staining with $BP_{505/515}$ without assistance of either DMSO or glycerol.

Elliot and collaborators [24] reported the use of $BP_{493/503}$ dissolved in EtOH (at 0.95%) with negative results for some strains. This result lead the authors to abandon the use of FACS to screen for naturally lipid rich strains in order to avoid possible toxic effects of DMSO [24]. However, the present results with EtOH suggest that for some strains a polar solvent may be enough to guarantee cell penetration. Glycerol was also assessed as carrier for BP, considering previous positive results [51,67]. However in the present experiments a negative correlation between BP fluorescence and glycerol addition was observed (supplementary materials).

The result of the optimization established a staining process that allows maximum fluorescence signal coupled with efficient detection of the target cells (lipid rich). The conclusions drawn from this stage of the research pointed towards positive application of the protocol to FACS approach.

3.3.3. Cell sorting and viability assay

In this section the protocol was applied to sort cells using the sorting station of the cytometer. The first step was to check the sorting efficiency using the scatter plot of auto- and BP-fluorescence to set-up a gate (Figure 3.4). The gate represents the thresholds used by the sorting unit to physically separate the target cells. The sorted cells were re-analysed with FACS immediately after sorting and the results confirmed the effectiveness of the sorting procedure (92.93%, figure 3.4). After that the cellular viability during the different steps of the entire process was assessed.

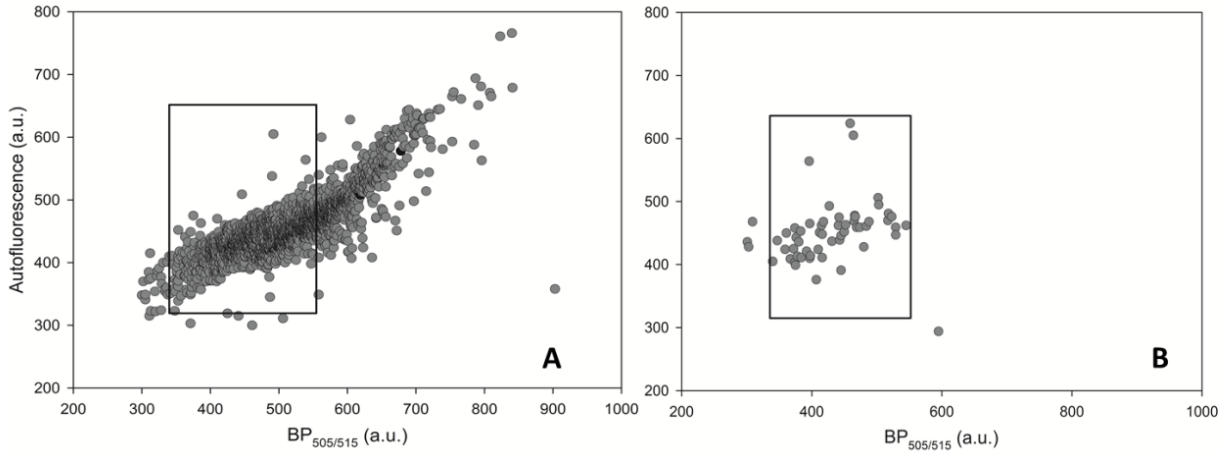

Figure 3.4: Scatter plot of *Chlorococcum littorale* population (A) and of sorted cells (after recovery) based on the gate set in the FACSCalibur (dark squares). The sorting efficiency calculated after re-analysing the sorted cells was 92.93% (53/57 events within the gate).

Some strains have been reported to be sensitive to the stress of the selection station [24], thus the effect of the FACS sorting procedure on *C. littorale* recovery was also checked. The variables that could affect the cell viability in the current work were: the dye, the carriers (DMSO and EtOH) and the sorting process. The growth of sorted cells was compared with a control – non-stained but sorted cells – to assess differences in the growth performance (Figure 3.5 A and B). The control group was subjected to the same process through the flow cytometer sorting unit.

There were no differences in the growth among the tested groups (specific growth rates μ (d^{-1}): control (0.60), EtOH (0.60) and DMSO (0.57)). Also, no statistical difference was detected in the cell numbers along the growth curve (ANOVA between groups, p=0.631). The viability was also checked daily using the erythrosine B staining (details given in section 5 of supplementary materials), showing positive results without significant difference between groups. Although the percentage of viable cells was lower at the first 48 hours (between 89 and 93% for all

treatments), it increased and remained constant from the second day onward (above 98%). It is possible that the nonviable section detected at the start of the experiment was due to cellular damage caused by the sorting process [24].

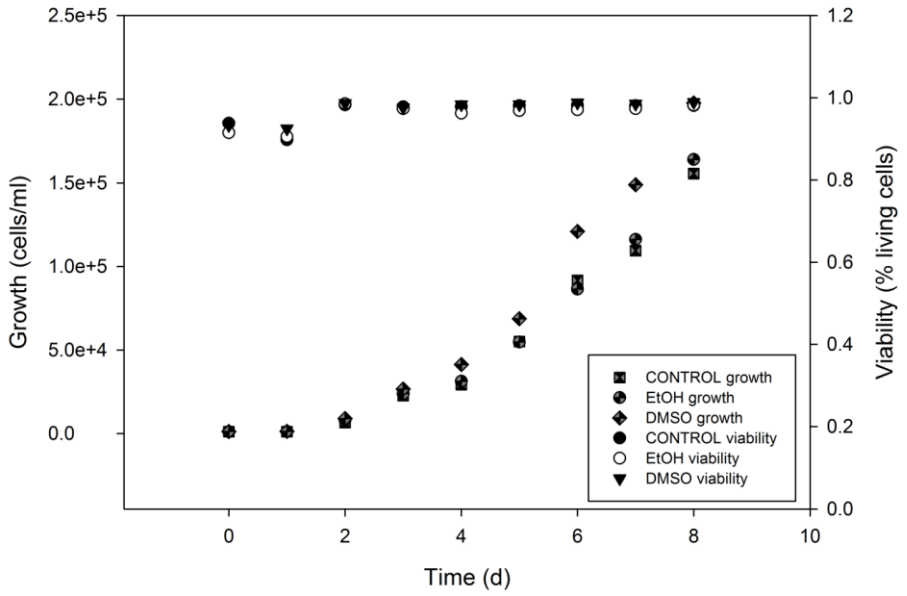

Figure 3.5: Results of viability test of *C. littorale*: Percentage of living cells per day (right y-axis) and growth curves (left y-axis) of all three treatments: control (without staining but sorted based on autofluorescence), DMSO and EtOH (sorted groups).

Previous results have highlighted that FACS could be an effective tool to increase the lipid content in microalgae cultures [10,52,53,56,67]. Positive results with re-grow of sorted cell lines of microalgae have been reported [52,53,56], but not yet with *C. littorale*. Moreover, up to date, the viability assay regarding FACS was not yet reported in literature with any species of microalgae.

3.4. Conclusions

A staining process was optimized to efficiently detect high-lipid cells in N-stressed populations of *Chlorococcum littorale*. Effective staining was achieved with $BODIPY_{505/515}$ and ethanol, with the same performance as with DMSO as carrier. It was designed for fluorescence assisted cell sorting (FACS) and was tested to assure cellular viability. Here a high throughput staining for *C. littorale* is presented, which can be used to actively sort high lipid producing cells. The selected new population could be used to establish inoculum with an increase cellular lipid content.

3.5. Supplementary materials

3.5.1. Nile red optimization steps

The glycerol concentration was optimized using different concentrations of glycerol. NR was kept at 0.4 µg/mL, the results are available in Figure S6.3.1A. The graph shows that glycerol concentrations of 50 mg.mL^{-1} or lower have no effect on dye uptake in *C. littorale*. Concentrations of 100 mg.mL^{-1} and higher enhance dye uptake significantly, with a maximum fluorescence at 125 mg.mL^{-1} glycerol. This is in similar with the results of Doan and Obbard (2011), who found an optimum at 100 mg.mL^{-1} NR for *Nannochloropsis sp*.

The NR concentration was optimized using 125mg.mL^{-1} glycerol as carrier. These results are displayed in Figure S6.3.1B. These results show that 0.8 ug.mL^{-1} NR results in maximum lipid dependent fluorescence. This is in range with findings of other studies, where 0.5 µg.mL^{-1} [53] or a range of 0.3 to 1.3 µg.mL^{-1} was proposed [10].

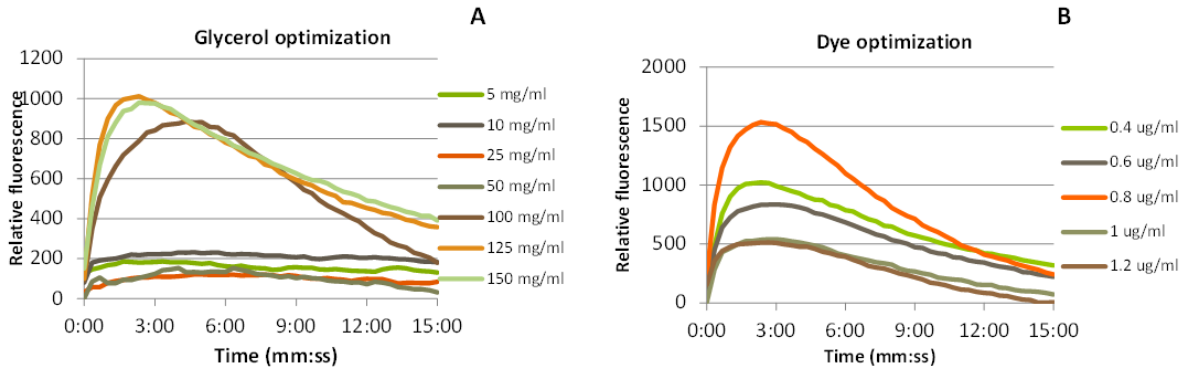

Figure S6.3.1: Both stressed and unstressed cells of C. littorale, lipid dependent emission was calculated by subtracting the emission of unstressed cells from the emission of stressed cells.
A: Lipid dependent emission after staining with 0.4 µg.mL^{-1} NR, using different concentrations of glycerol. B: Lipid dependent emission after staining with different concentrations of NR, using 125mg.mL^{-1} glycerol as a carrier

3.5.2. Glycerol effect on $BP_{505/515}$ staining:

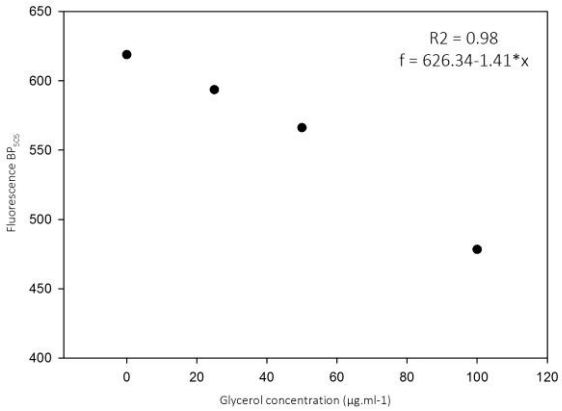

Figure S6.3.2: Effect of glycerol addition to BP505/515 lipid dependent fluorescence. Correlation coefficient (R2=0.98) and line equation (f=626.34-1.41*x) displayed in the chart.

Glycerol was also evaluated as a carrier/assistant for $BP_{505/515}$ staining with *C. littorale* (figure S6.3.2). Different from the effect of the previous assistants (DMSO and ethanol), a negative effect was observed in the present experiments. As it can be seen in figure S6.3.2, increments in the glycerol concentration were negatively correlated with the fluorescence signal of $BP_{505/515}$ (R^2 = 0.98). Although Brennan et al.[51] have reported successful staining using glycerol as a replacement for DMSO, Velmurugan et al. [68] reported similar negative effect of glycerol in assisting $BP_{505/515}$ dyeing. Hence, we have decided to take the current positive outcomes with DMSO and EtOH into consideration and to put the option of glycerol as carrier aside.

3.5.3. FA/TAG profile of *C. littorale*

Triglycerides (TAGs) profile of *Chlorococcum littorale* under the proposed experimental conditions. The profile is derived from the biomass at the stationary phase of growth.

TAG	TAG concentration (DW%)	Standard deviation (SD)
C8	0.01	0.000
C10	0.01	0.000
C12	0.09	0.000
C14	0.13	0.000
C16	8.09	0.002
C16:1	0.86	0.000
C16:2	0.38	0.000
C16:3	0.55	0.000
C16:4	3.98	0.001
C18	0.81	0.000
C18:1	7.08	0.020
C18:2	3.88	0.018
C18:3	7.33	0.001
C18:4	0.42	0.000
TOTAL	**33.62%**	**0.043**

3.5.4. Linear regression analysis between the triglycerides content (TAG, %DW) and BP-dependent fluorescence (a.u.), with the ethanol optimized protocol. R^2 and line equation are displayed on the chart.

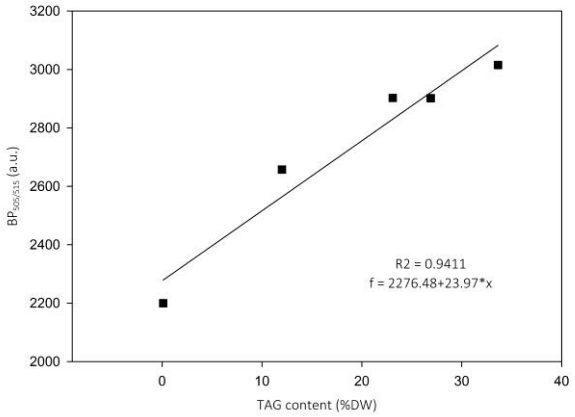

Does the cell size of *Chlorococcum littorale* matter?

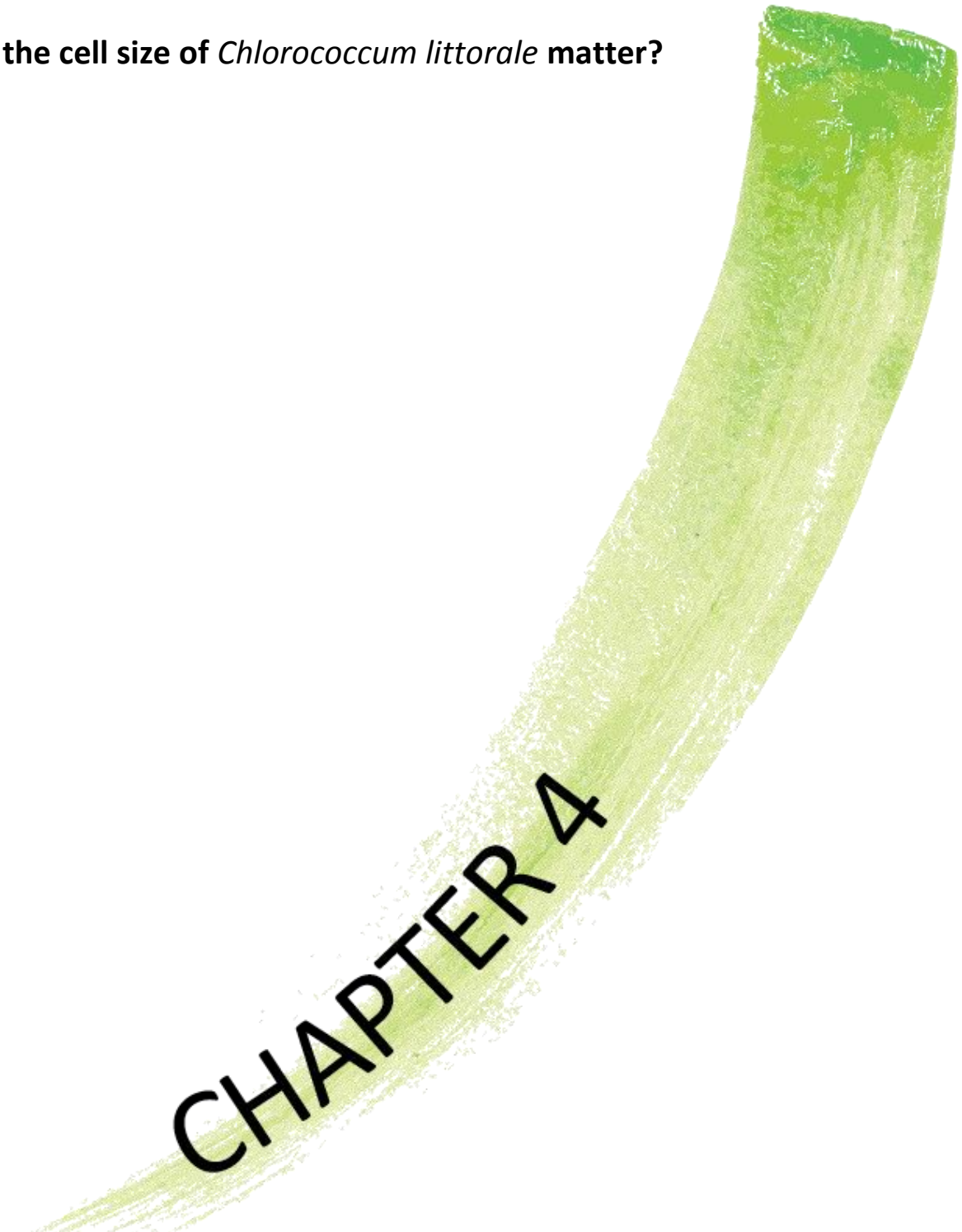

This chapter has been published as: Cabanelas, Iago Teles Dominguez; Fernandes, Carolina; Kleinegris, Dorinde MM; Wijffels, René H; Barbosa, Maria J. 2016. Cell diameter doesn't affect lipid productivity of *Chlorococcum littorale*. Algal Research, accepted, doi:10.1016/j.algal.2016.02.002

Highlights

- Successful cell sorting based on light forward scatter as proxy for cell diameter
- Single and multiple-cell sorting lead to populations with similar size distribution
- Cultures started with different diameters had similar final lipid productivities
- Cell size, as sorting criterion, had no effect on biomass and lipid productivity

ABSTRACT

We hypothesized that cells with different diameter have different division rates, which could affect lipid productivity (lipid content x biomass productivity). In the present work we assessed the influence of cell diameter, as a sorting parameter, on both biomass and lipid productivity of *Chlorococcum littorale*. Prior to sorting, cells were grown in a batch-wise nitrogen run-out including a long nitrogen depleted phase (N-) to stop cell division, thus only having vegetative cells (Pre-sorting). Cell sorting was done at the end of this N- phase using FACS (fluorescence assisted cell sorting) based on forward scatter as a proxy for diameter (size ranges (µm): 5-6 (small), 8-9 (medium), 11-14 (large) and 5-14 (control)). The sorting was done in 2 pools: multiple-cell (100 cells) and single-cell. After sorting, cells were recovered under low-light for 2 weeks, and used to start the Post-sorting experiment (analogous to Pre-sorting). The populations derived from different sorted pools, single-cell and multiple-cell, showed similar size distributions after re-growth. No difference was observed in biomass and lipid productivities among Post-sorting cells and when compared to Pre-sorting cells under nitrogen depletion. We concluded that cellular size had no effect on both biomass and lipid productivity of *Chlorococcum littorale*.

Key-words: microalgae**;** *Chlorococcum littorale*; cell sorting (FACS); cell diameter; biomass productivity; lipid productivity

4.1. Introduction

Microalgae have shown potential to replace current feedstock for bulk commodities [1,69]. The positive aspect of microalgae bulk production include sustainability and versatility of the production chain when compared to land crops [70]. Nevertheless, reported biomass and lipid productivities need to be improved to make bulk production economically feasible for commodity products, such as plastics or fuels [3,71].

One approach to increase productivity is to develop more productive strains. This can be done taking advantage of the natural genetic variability of a parental population to screen and sort cells with different features (e.g. high lipid producers) [10,72]. Another possibility is to increase genetic variability by inducing mutations in a parental population and screen and sort for mutants with abnormal improved features [9,14,21,73]. Fluorescence assisted cell sorting (FACS) is a method which allows rapid screening and sorting of cells with desired characteristics. Sorted cells can be regrown, possibly leading to a new improved culture [9,10,14,21]. FACS can sort cells based on multiple fluorescence and light scattering parameters, which makes it a versatile technology.

Chlorococcum littorale has a high lipid content [40], high photosynthetic efficiency under nitrogen stress [37], and has been used in FACS before [15] and for this reason has been chosen in this study. *C. littorale* is a unicellular microalga whose cell size can range from 5 to 14 µm in the vegetative stage [39]. *C. littorale* can reproduce sexually and asexually by multiple-fission of the mother cell, into 2 to 16 daughter cells (in the shape of spores that can be haploid or diploid, in case of asexual or sexual reproduction, although there is no morphological differences between the two kinds of spores) [39]. The formation of spores is relevant for the sorting, since dividing cells could be mistaken for a large vegetative cell. Up to now the regulation of cell size in microalgae is not completely understood [74–76]. Studies with *Chlamydomonas,* a genus with multiple-fission cell division, showed a positive correlation between mother cell's sizes and the number of generated daughters [75]. Other authors have shown that cells might even continue their division without doubling their cell volume. Hence, such cells would produce bigger daughter cells, that would generate more and smaller cells in the next division [74]. Both studies point to a possible influence of cell diameter on the growth patterns of following generations. Up to date, no report has focused on the possible effect of size of vegetative cells on the biomass productivity of bulk cultures. We hypothesized that cells with different diameter have different division rates, which could affect biomass productivity. Hence, differences in biomass productivity could consequentially affect lipid productivity (lipid content x biomass productivity).

In the present work we assessed the influence of cell diameter, as sorting criterion, on both biomass and lipid productivity of vegetative cells of *C. littorale. C. littorale* was grown in a batch-wise nitrogen run-out followed by a long nitrogen-depleted phase to stop cell division and to induce lipid accumulation, thus having only vegetative, lipid-rich cells. At the end of the nitrogen-depleted phase (15 days, after cell size was stable) cells were sorted in four groups of different diameters: small (5-6 µm), medium (8-9 µm), large (11-14 µm) and a control (5-14 µm). We compared both biomass and lipid productivities of sorted cells of *C. littorale* with the growth of the parental population. Additionally, we compared the daily differences in cell size

distribution, photosystem II quantum yield, autofluorescence and intra-cellular lipid fluorescence.

4.2. Materials and methods

4.2.1. Inoculum preparation, cultivation and culture screening with FACS

Inoculum of *Chlorococcum littorale* (NBRC 102761) was prepared from samples preserved under low light conditions (16 µmol m^{-2} s^{-1}) in borosilicate tubes containing growth medium and agar (12 g l^{-1}). Small samples were transferred from agar to 200 ml sterile borosilicate Erlenmeyer flasks, containing 100 ml of sterile growth medium. *Chlorococcum littorale* was grown in salt water-like medium with the following composition (g l^{-1}): NaCl 24.55, $MgSO_4 \cdot 7H_2O$ 6.60, $MgCl_2 \cdot 6H_2O$ 5.60, $CaCl_2 \cdot 2H_2O$ 1.50, $NaNO_3$ 1.70, HEPES 11.92, $NaHCO_3$ 0.84, EDTA-Fe(III) 4.28, K_2HPO_4 0.13, KH_2PO_4 0.04. The medium also contained the following trace elements (mg l^{-1}): $Na_2EDTA \cdot 2H_2O$ 0.19, $ZnSO_4 \cdot 7H_2O$ 0.022, $CoCl \cdot 6H_2O$ 0.01, $MnCl_2 \cdot 2H_2O$ 0.148, $Na_2MoO_4 \cdot 2H_2O$ 0.06, $CuSO_4 \cdot 5H_2O$ 0.01.

The sequence of experiments performed in this work is represented in Figure 4.1. After inoculum preparation we set-up a preliminary test to determine the boundaries for the sorting gates based on cell size using fluorescence assisted cell sorting (FACS). The preliminary test was performed before but analogous to the experiment explained in the next section.

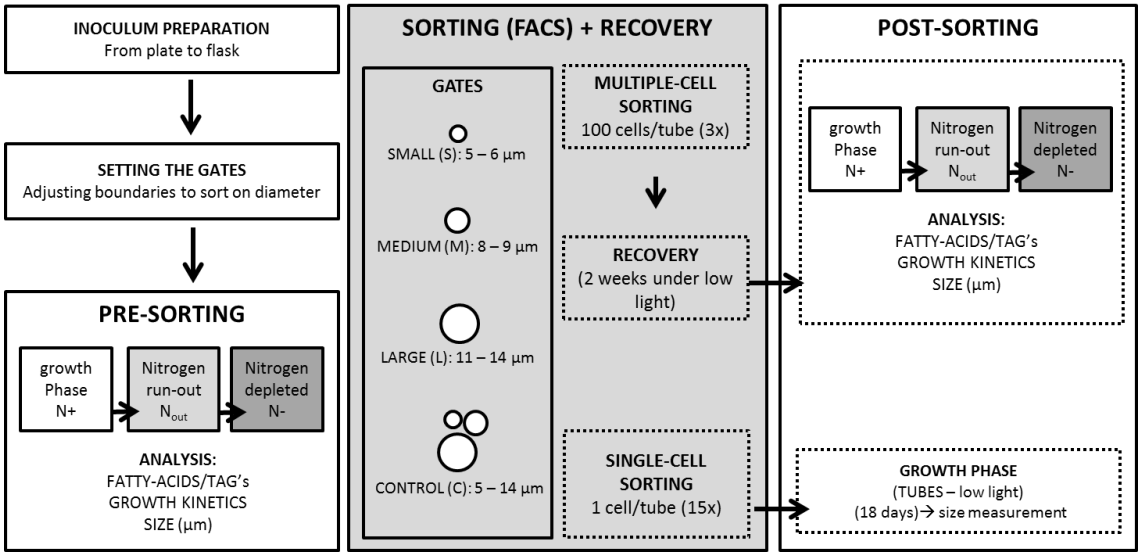

Figure 4.1: **Experimental flow diagram followed in this work**. **Inoculum preparation**: fresh cultures were prepared from agar plate's cultures and kept under controlled conditions. **Setting the gates**: a preliminary test was done to set the boundaries of the gates used for the actual sorting. **Pre-sorting**: Batch nitrogen run-out cultivations were done in flasks including a growth phase (N+, in white), a nitrogen run-out (N_{out}, in light grey) and a nitrogen depleted phase (N-, in dark grey). The same colors were used in Figure 4.4 and Figure 4.7. **Sorting**: after cell size was stabilized during nitrogen depletion (3 days with the same size distribution) the multiple-cell sorting was done with 4 different gates based on size (3x 100 cells/replicate). **Post-sorting**: experiments analogous to Pre-sorting to compare biomass and lipid productivities; the single-cell sorted cells were readily analyzed after 18 days of re-grow. **Acronyms**: FACS (fluorescence assisted cell sorting) and TAG's (triacylglycerides).

4.2.2. Experimental set-up

The experimental set-up was the same for both Pre-sorting and Post-sorting experiments (Figure 4.1). Experiments were inoculated with an initial OD_{750} value of 0.5 (~0.7 g DW l^{-1}). The algae were cultivated in 200 mL borosilicate Erlenmeyer flasks (100 mL medium per flask) and kept in an Infors Multitron Pro orbital shaker incubator. Growth conditions were: 25±0.2 °C, 120 rpm, 60% humidity, 2% CO_2 enrichment on air, and 120±2 µmol m^{-2} s^{-1} continuous light (24 h).

Both experiments had 2 phases: a growth phase (N+) and a nitrogen depleted (N-) phase. During the growth phase nitrogen (N-NO_3) was allowed to run-out progressively (at day 5 NO_3 was completely consumed by the cells). After reaching stationary phase, the cultures were diluted 5x to a biomass concentration of 1.4±0.1 DW g L^{-1}, in sterile medium without NO_3^-, to allow further light penetration in the culture and enhance lipid production. After dilution, cells were monitored until maximum size was achieved, and was constant for 3 days (after 15 days from start experiment). All daily measurements were done at the same time every day and are described in the following section.

Multiple-cell sorting (3x 100 cells) was done based on cell size in four groups, at the end of the stationary phase (Figure 4.3). After sorting, cells were re-suspended in 50 ml sterile falcon tubes containing fresh and sterile nitrogen-replete medium into. Cells grew for 2 weeks in the tubes under low light conditions (16 µmol m^{-2} s^{-1}). After this, cells were transferred to sterile borosilicate Erlenmeyer's, where Post-sorting experiments were conducted under similar conditions as the Pre-sorting experiments and with the same daily measurements.

Additionally single-cells were sorted from the same parental population on the same day (Figure 4.1**Figure**). Fifteen replicates per group of single-sorted cells were taken to increase sample size and to assure reproducibility of Post-sorting results. Single cell sorting was done analogous to and immediately after the multiple-cell sorting. After 18 days of growth under low-light conditions (16 µmol m^{-2} s^{-1}) the sorted cells were centrifuged at 1224 x g for 10 minutes, washed with sterile medium and readily analyzed for size and autofluorescence using the FlowCAM® fluid imaging system (settings are presented in the next section).

4.2.3. Daily measurements

All daily measurements were done at the same time every day. Optical densities were measured on a daily basis using a spectrophotometer (HACH, DR5000) on two different wavelengths: 680 and 750 nm. Samples were diluted within the range of the detection limit (0.1 – 1 units of OD). OD_{750} was used as a proxy for biomass concentration and OD_{680} was relative to the chlorophyll fluorescence [62].

Quantum yield of photosystem II (PSII) – ratio between the number of photons emitted and the number of photons absorbed by the cells – was measured daily with a fluorometer (AquaPen-C AP-C 100, Photon System Instruments, Czech Republic). The measurements were done with cultures at OD_{750} values between 0.2-0.4 after a dark period of 10 minutes at room temperature. The quantum yield was used to infer the photochemical efficiency of the cells. The F_v/F_m ratio gives the maximum quantum yield of PSII (Equation 1, [37]), where F_0 is the minimal

level of fluorescence (after dark-acclimation) and F_m is the maximum fluorescence after exposing the cells to a pulse of actinic light.

$$(F_V/F_m) = \frac{F_m - F_0}{F_m}$$ Equation 5

FlowCAM® analyses were performed daily to follow-up the cell's diameter, autofluorescence (chlorophyll fluorescence) and lipid-dependent fluorescence ($BODIPY_{505/515}$ fluorescence). For FlowCAM® analyses samples were first diluted 100 to 1000 times and then stained for neutral lipids to achieve a final concentration of 0.4 µg/mL of BODIPY $_{505/515}$ and 0.35% of ethanol, following the protocol of [15]. After 5 minutes the samples were run in the FlowCAM® (Fluid Imaging Technologies, Yarmouth, Maine) using the following settings: 20x optical magnification and Trigger-mode-on with channels 1 and 2, autofluorescence (650nm long pass filter) and $BODIPY_{505/515}$ (525/30 filter), respectively. The trigger mode activates the system to take a camera image when a particle produces a fluorescence signal. Diameter (µm), autofluorescence (Ch1) and $BODIPY_{505/515}$ fluorescence (Ch2) of each sample were taken for further analyses.

Daily samples were taken for measurement of nitrogen content ($N\text{-}NO_3$ mg l^{-1}) in the medium. 1 ml of culture was centrifuged at 13.000 x g and the supernatant was used for analysis. Nitrogen content was measured daily with the Sulphanilamide N-1-naphthyl method (APHA 4500-NO3-F) using the SEAL AQ2 automatic analyzer.

4.2.4. Cell sorting using FACS

At the end of the nitrogen-depleted phase of the Pre-sorting experiment, a sample was collected and diluted to an OD_{750} of approximately 0.3, to keep cell concentration in the flow cytometer at 200 cells/min. The sorting was carried out with a FACScalibur® flow cytometer (BD Biosciences, San Jose, California). FACScalibur® is equipped with an argon ion laser with excitation at 488 nm and in our work the emission at 670LP (FL3 channel) was used, relative to the cells autofluorescence (Chlorophyll-*a* emission). FL3 channel was read in logarithmic scale and the sensitivity was set at 300 mV while FSC channel was read on linear scale. Cells were collected in sterile 50 mL falcon tubes and sterile PBS was used as sheath fluid (phosphate saline buffer; composition: NaCl 137 mM, KCl 2.7 mM, Na_2HPO_4 10.0 mM, KH_2PO_4 1.8 mM).

The sorting was done in two steps: multiple-cell sorting and single-cell sorting. For multiple-cell sorting 100 cells were collected per tube to produce inoculum for the Post-sorting experiments (in triplicate). Subsequently, single-cell sorting was carried-out using the same sample and same machine settings as the multiple-cell sorting (with 15 replicates for each size). After sorting, cells were centrifuged at 1224 x g for 5 minutes and re-suspended in sterile growth medium (both multiple and single-cell sorting). The tubes with sorted cells were placed under constant light at 16 $\mu mol \cdot m^{-2} \cdot s^{-1}$, allowing cells to recover for 2 weeks. After the recovery time, triplicates containing 100 cells each were transferred to Erlenmeyer flasks to produce inocula for the Post-sorting experiments. The cultures originating from the single-cell sorting experiments were readily analyzed with the FlowCAM® after 18 days of growth in the tubes.

4.2.5. Fatty acid and TAG analysis

Biomass samples were collected at the end of both nitrogen replete (N+) and nitrogen depleted (N-) phases of Pre- and Post-sorting experiments. Biomass was centrifuged twice and washed with MilliQ water (3134xg for 10 minutes at 4°C) and followed by freezing at -20°C and freeze-drying for 24 h.

Fatty acid and triacylglycerol's (TAGs) extraction and quantification were performed as described by Breuer et al. (2013) [77], using GC/MS column chromatography of the chloroform fraction of lipids.

4.2.6. Data analysis

Data from FlowCAM and cytometer were exported to Microsoft Excel to be edited and analyzed. For statistical analysis, one-way analysis of variance (ANOVA) was used to access the significance of differences between and among sorted groups (SigmaPlot, v. 12.5). The premises of ANOVA, i.e. the homogeneity of variances and the normality of the data, were also measured with SigmaPlot. A *p*-value lower than 0.05 was considered significant.

Calculations

The biomass dry weight was used to calculate the growth rate of C. *littorale*, as given in [Equation 6],

$$\mu = \frac{\ln(DW_{t_{final}} - DW_{t_0})}{t_{final} - t_0} \qquad \text{Equation 6}$$

where, DW stands for the dry weight of biomass (g l^{-1}), from the first (t_0) and the last time point (t_{final}) considered. For the growth rate under nitrogen replete conditions (N+) the 5th day of cultivation (d=5) and the day of inoculation (d=0) were used as final and initial values, respectively.

The increase in BODIPY cellular fluorescence was used to calculate the BODIPY accumulation rate (BP_r), relating to the increase of cellular neutral lipids in time. The BP_r was estimated with an similar approach as used for equation 2, only that the values of DW where replaced with the values of BP fluorescence (relative fluorescence units, RFU). The period of time used for calculation was the period between the start (d=5) and the end (d=10) of the nitrogen run-out (being d=0 the inoculation day). This period was chosen because it shows the first increase in intracellular lipid content; hence it is an estimate of the first metabolic response of the intracellular lipid accumulation.

The decrease in photosystem II quantum yield (QY_r) was calculated using an identical approach to the one used in equation 2, but replacing DW values by QY measurements. Two QY_r were calculated: at the end of the nitrogen run-out (between d=5 and d=10), and at the end of the nitrogen depleted phase (between d=10 and d=25).

The volumetric biomass productivity (P_X, g l^{-1} d^{-1}) is given by [Equation 7],

$$P_X = \frac{DW_{tfinal} - DW_{t_0}}{t_{final} - t_0}$$ Equation 7

where, two time intervals of the dry weight (DW, in g per liter) were used: between the end (d=10) and the beginning (d=5) of the nitrogen run-out (N_{out}) and at the end (d=25) and the beginning (d=10) of the nitrogen depleted phase (N-).

The final TAG volumetric productivity (P_{TAG}, mg l^{-1} d^{-1}) was estimated using [Equation 8],

$$P_{TAG} = (P_X \times TAG) \text{ x } 1000$$ Equation 8

where P_X is the biomass volumetric productivity calculated above and the TAG (triacylglycerides) content in the biomass (g g^{-1}). The P_{TAG} was calculated using the P_x and the TAG content from both N_{out} and N- phases.

4.3. Results and Discussion

4.3.1. Gate set-up to sort cells on size

A preliminary test was done to check 2 assumptions: 1] that the intracellular lipid content is not correlated with the cell diameter and 2] that FACS could be used to sort cells based on cell size. The first assumption is relevant not to include the lipid content as a sorting criteria. As stated in the introduction, we hypothesized that cells with different diameters can have different division rates and we want to evaluate the effect of such differences on lipid productivity. We found no correlation between cell diameter and intracellular lipid-fluorescence, as it can be seen from the R^2 value in Figure 4.2. The preliminary test was done using the same experimental set-up as it was used for the actual experiments (Figure 4.1 and section 4.2.2 of methods).

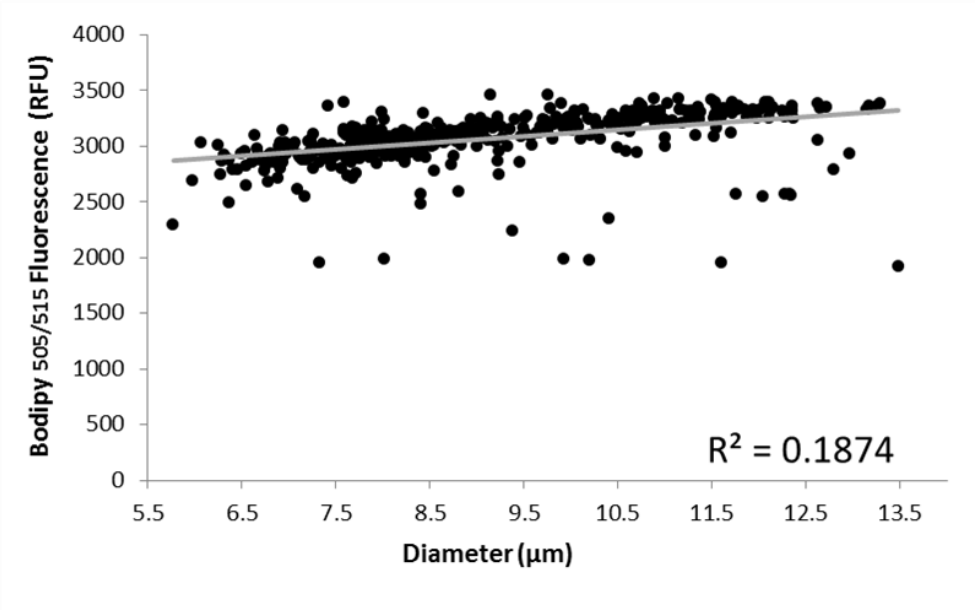

Figure 4.2: Nitrogen stressed cells show no correlation between diameter and intracellular lipid-fluorescence: Scatter plot between Bodipy dependent fluorescence (Y-axis) and cellular diameter (x-axis) (n=500 cells). Data derived from the preliminary test, with cells exposed to 15 days of nitrogen depletion. R^2 represents the coefficient of determination, evidencing the lack of correlation between lipid-dependent fluorescence and cellular diameter.

Once the first assumption was checked we used the same sample to do a preliminary sorting test to check the second assumption: Can FACS be used to sort cells based on diameter? Cell diameter cannot be directly measured in FACS. However, measurements of the forward light scattering (FSC) of every cell can be used as a proxy for cell size [10,78]. Although calibration beads are available to convert FSC into diameter [79], we decided not to use calibration beads due to intrinsic differences in e.g. surface smoothness between the calibration beads and microalgae cells. Furthermore, we worked with size intervals that differed from each other in only 2 µm. Hence we decided not to use calibration beads to convert FSC to cell size, instead we decided to use FSC as a proxy for cell size and to perform a test to confirm the results of the set gates boundaries by measuring the cell size of sorted cells immediately after the sorting (using FlowCAM fluid imaging).

A histogram of FSC was firstly established to show the distribution of size within the population and to identify the different size groups (Figure 4.3B). The information from the histogram (Figure 4.3B) was crosschecked with simultaneous plotting of autofluorescence (AF) versus FSC (Figure 4.3A) as a positive control for algae cells (to avoid gating non-fluorescent particles. Autofluorescence was used as a proxy for cellular chlorophyll content to confirm the identity of the particles as microalgae cells. We kept the ratio AF/FSC the same for all gates to avoid AF as a second sorting criteria (Small: 1.2, Medium: 1.1, and Large: 1.1). The gates used for sorting were established on the dot-plot shown on Figure 4.3A. This approach was important to avoid the inclusion of cell debris, especially for the group containing small cells.

Once the gates were established, as shown in Figure 4.3A, the cells were sorted (100 cells per group, in triplicate) and subsequently analyzed for size. The cell size was assessed with the FlowCam imaging, which provides direct measurement of cell diameter (µm) and autofluorescence, supplementing the analysis from FACS. The results from the preliminary test (Figure 4.3) confirmed the suitable gate boundaries to sort cells based on size: small (5-6 µm), medium (8-9 µm), large (11-14 µm) and a control including all previous sizes (5-14 µm). Detailed pictures of the cells from all different groups can be found in the supplementary materials (SM1).

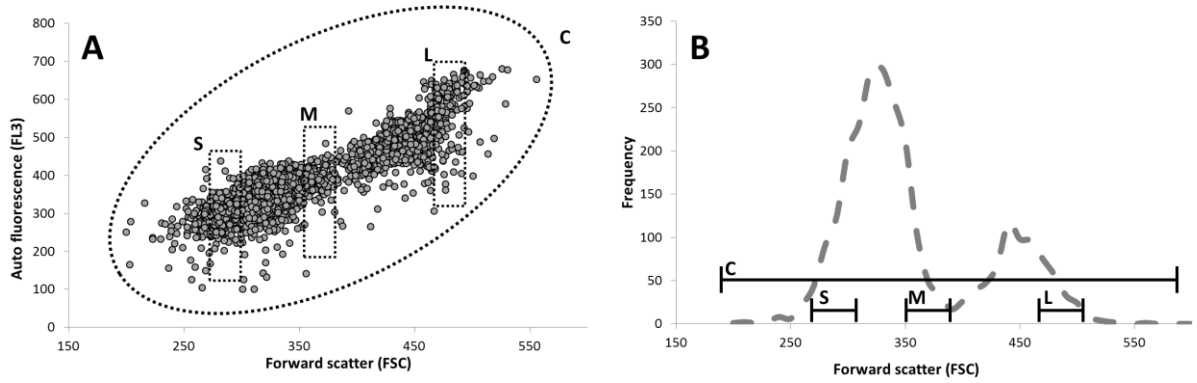

Figure 4.3: **Preliminary test done to set the boundaries to sort cells based on size**. **A:** Dot-plot of nitrogen depleted cells of *Chlorococcum littorale* using Autofluorescence (FL3) vs forward scatter (FSC), both parameters are in relative fluorescence units (RFU). **B:** Histogram of frequency of the FSC of nitrogen depleted cells of *Chlorococcum littorale.* The gates are depicted as rectangles and an ellipse (A) and range-lines (B) and stand for small (S), medium (M) and Large (L) and control (C).

4.3.2. Growth of *C.littorale* before cell sorting

C. littorale was cultivated phototrophically, batch wise in nitrogen replete medium (Pre-sorting experiment). At day 5 the concentration of nitrogen in the medium was zero (Figure 4.4A, light grey area marks the 5th day). We kept the cultivation for 5 additional days after nitrogen run-out, until biomass concentration reached its maximum, meaning that the cells had consumed their internal nitrogen pools while finishing to divide (which can also be noticed on the size evolution, Figure 4.4C). At this point, the cultures were diluted in nitrogen depleted medium to

increase the light intensity inside the culture necessary to further stimulate lipid accumulation in microalgae [45,80–82] (Figure4.4A), and a consequent increase in size (Figure 4.4C).

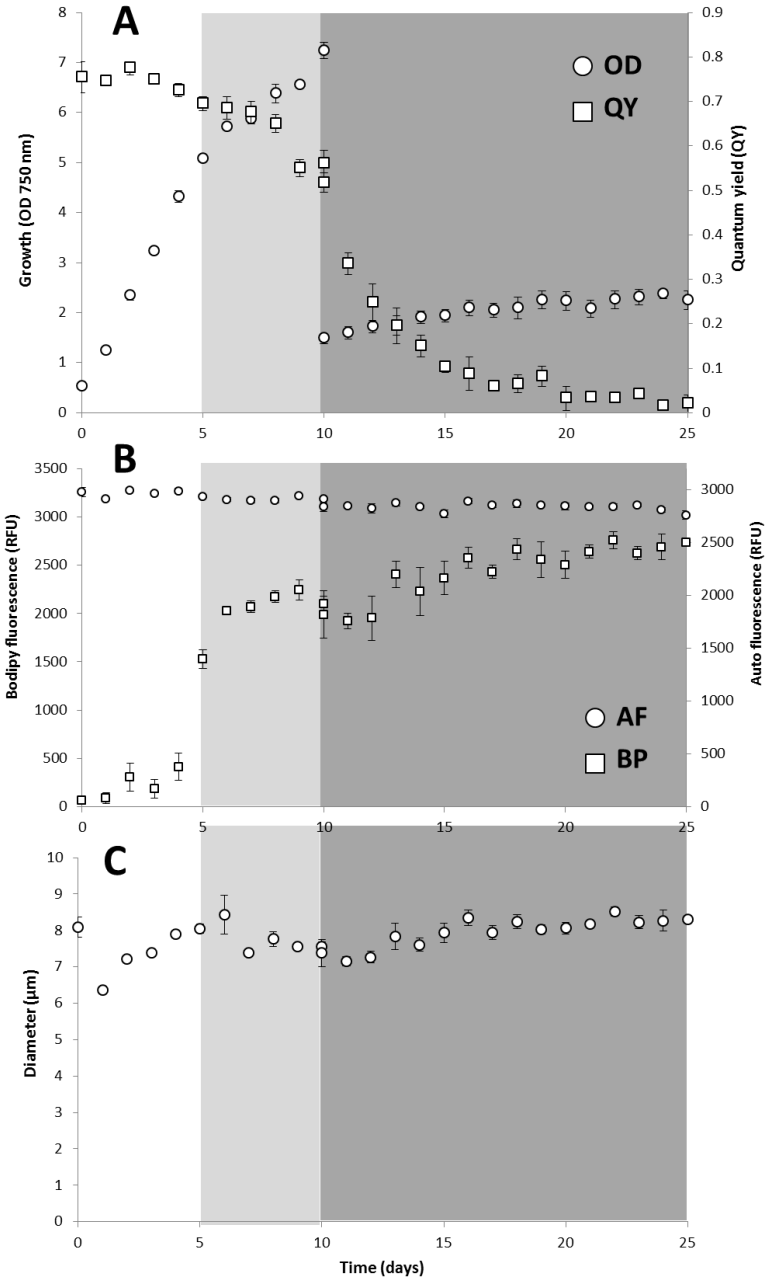

Figure 4.4: Evolution of *C. littorale* **growth parameters before cell sorting**. The white area of the chart indicates the growth phase (N+), the light grey area marks the point in which N runs out (N_{out}), and the dark grey area indicates the phase in which the culture is diluted in nitrogen depleted medium (N-). For every plot the standard deviation is present, (n = 3). **A:** Evolution of biomass production of *C. littorale* (circles, primary y-axis) and evolution of the quantum yield of photosystem II over time (QY, squares, secondary y-axis). **B:** Evolution of autofluorescence (circles, primary y-axis) and BODIPY-fluorescence (squares, secondary y-axis) of *C. littorale* cells over time. The averages of two measurements of fluorescence were plotted (500 cells were assessed per measurement). The measurements are represented as relative fluorescence units (RFU). **C:** Evolution of average (per cell) diameter of *C. littorale* cells over time.

Table 4.1 presents the growth rate, biomass and TAG volumetric productivities and fatty-acid and TAG content (%DW biomass). The growth rates and productivities calculated in the present work were used to compare the Pre-sorting with the Post-sorting populations.

In the growth phase we observe that the quantum yield (QY) of photosystem II remained above 0.5, supporting the hypothesis that the cells were not under photochemical stress (Figure 4.4A). The QY is an indicator of stress at values below 0.4 [83,84]. We can detect a drop in the QY after the nitrogen run-out (light grey area, Figure 4.4A) and a further drop to half of the initial value during the nitrogen depleted phase (dark grey area, Figure 4.4A). Low values of QY are an indirect indication of lipid formation, because under nitrogen stress no biomass can be produced and the photochemical energy is used to produce storage lipids [44]. The experiment was kept until values of QY close to 0 were achieved (Figure 4.4A).

Both autofluorescence and lipid-related fluorescence (Bodipy) were monitored during the experiment. The autofluorescence was stable throughout the experiment, showing only a reduction of 6.8% in autofluorescence from the beginning to the end of the experiment (Figure 4.4B). The autofluorescence is related to the fluorescence of both photosystems in the chloroplast [85], hence it can be used as a proxy for the chlorophyll content per cell. We can infer that almost no chlorophyll degradation took place, since only a small fraction of autofluorescence was reduced.

Fluorescence of the Bodipy dye was used as a proxy for cellular lipid content [15,51,59,86]. $BODIPY_{505/515}$ is a dye used to stain non-polar lipid bodies in microalgae cells [15,51,52]. The average $Bodipy_{505/515}$ fluorescence per cell is presented in Figure 4.4B, where it is possible to see an accumulation of neutral lipids from the moment of nitrogen run-out onward (Day 5). The increase in cellular lipid content is a survival mechanism in most microalgae, which directs the energy converted from photosynthesis to the synthesis of storage lipids in the absence of substrate (nitrogen) to grow [44,87,88].

4.3.3. Single-cell and multiple-cell sorted populations exhibited similar size distribution

Sorting based on cell size took place at the end of the nitrogen-depleted phase (d=25), after vegetative cells had reached their maximum size (As showed in 4.4C). Size measurements were plotted in a histogram after the regrowth phase (Figure 4.5). The overlap of the curves indicates that, after sorting, cells showed the same behavior as before the sorting. We also measured the distribution of cell diameter in the population originated from sorted single-cells to compare the 4 sorted populations among each other. The comparison of the average cell diameter among the sorted cells showed no statistical difference (Figure 4.6, $p>0.05$, one-way ANOVA).

These results were the first evidence that cell size might be an intrinsically regulated phenotypical distribution of *Chlorococcum littorale*. Cell cycle studies with *Chlamydomonas,* a microalgae strain with multiple-fission division as *Chlorococcum littorale*, showed that there is a positive correlation between mother cell's sizes and the number of generated daughters [75].

Other authors, however, have shown that cells might divide without doubling their cell volume. Hence, such cells would produce bigger daughter cells, that would generate more and smaller cells in the next division, which is an evolutionary advantage for natural unstable conditions [74].

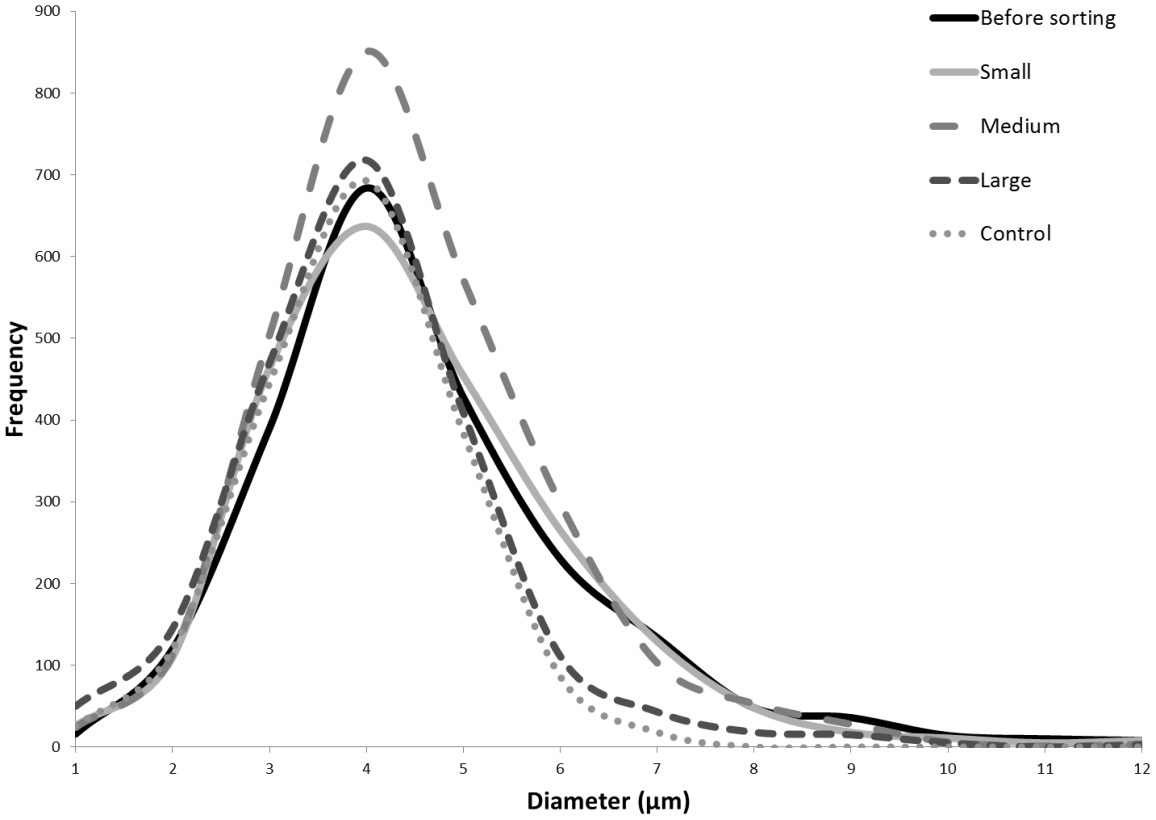

Figure 4.5: Cell size distributions of the different sorted populations overlap with the distribution of the parental population To assess early differences in cell size distribution we measured cell size from all sorted samples after re-growth (after two weeks recovery, as shown in Figure 4.1). A sample from the growing inoculum (early exponential phase) from the Pre-sorting experiment was also taken for comparison.

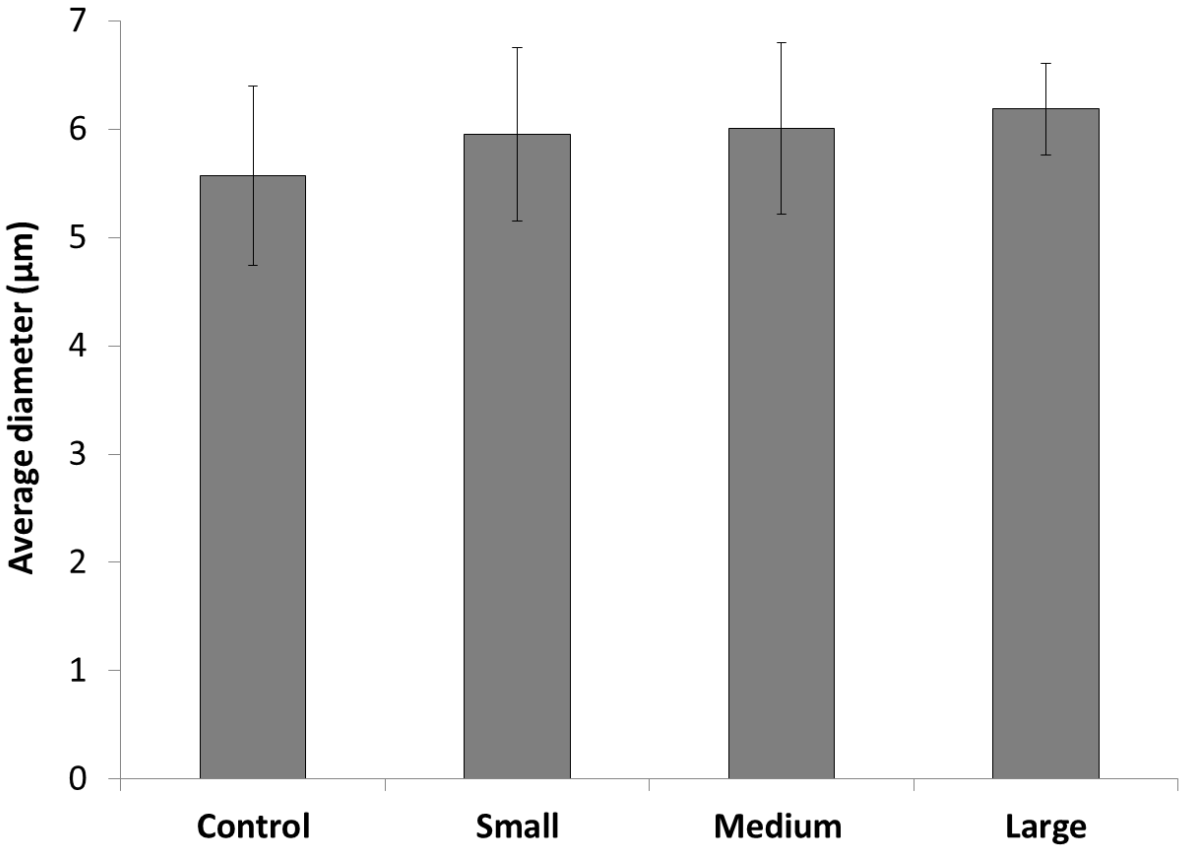

Figure 4.6: Single-cell sorted populations showed similar average diameters after re-growth. Grey columns represent the average cell diameter (n=500, per replicate) of each sorted population (originated from a single-cell) after re-growth for 18 days in nitrogen-replete medium and constant light (16 µmol m^{-1} s^{-1}). Error bars represent the standard deviations between replicates. Statistical analysis showed no significant differences ($p>0.05$, one-way ANOVA).

4.3.4. Cell size showed no effect on the growth dynamics of *C. littorale* after sorting

All sorted populations were grown batch wise in similarity to the Pre-sorting experiment (Figure 4.4) in order to be able to compare the Pre- with the Post-sorting culture on biomass and lipid productivity. All populations, including the parental population, showed similar growth (Figure 4.7 and Table 4.1).

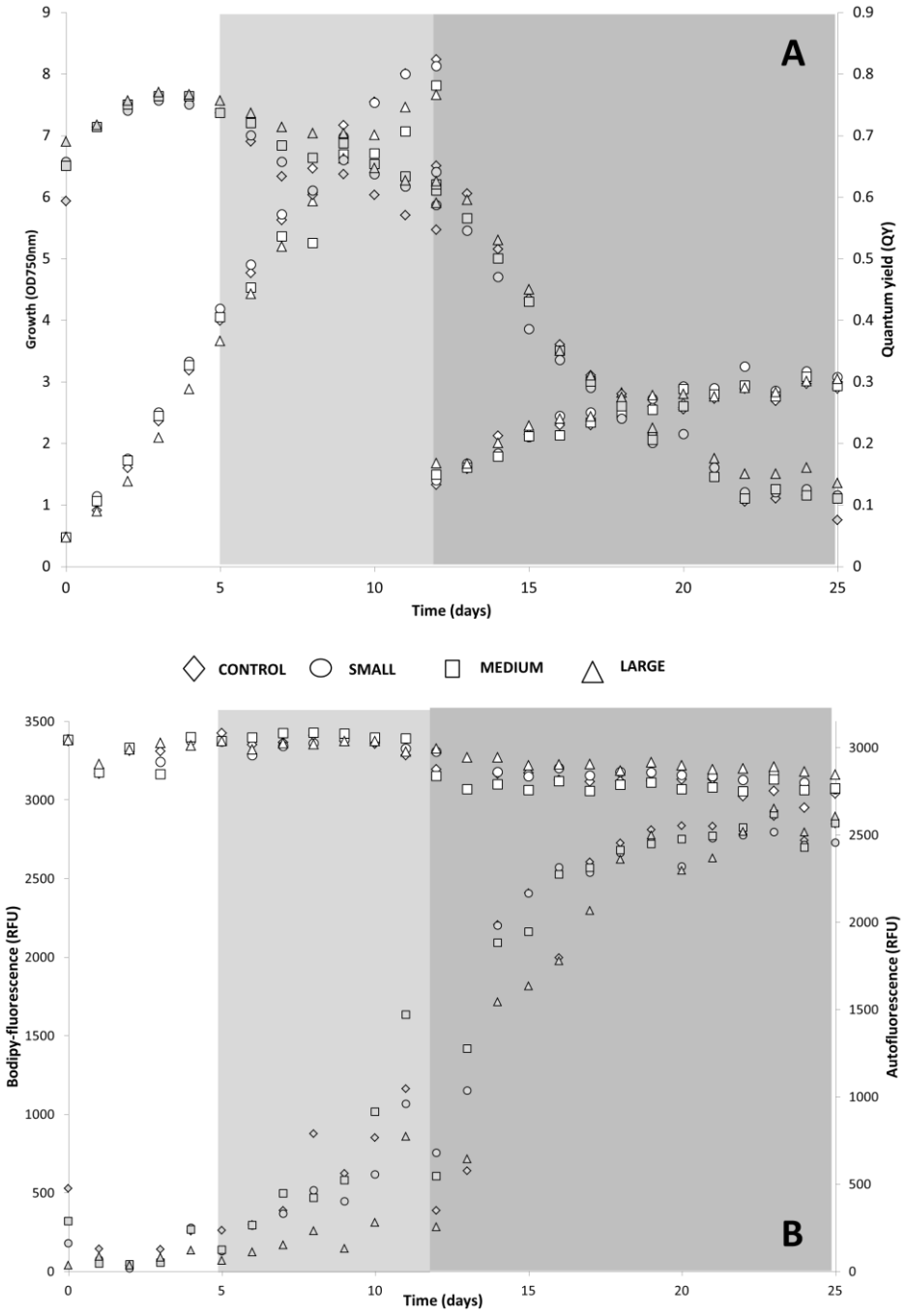

Figure 4.7: Different sorted populations exhibited similar growth dynamics among each other: The white area of the chart indicates the growth phase, the light grey marks the start of the nitrogen run-out, and the dark grey area of the chart indicates the phase in which the cultures were diluted in nitrogen-depleted medium. All sorted populations are represented in the graphs: small (○), medium (□), large (Δ) and control (◊). **A:** The evolution of biomass production of *C. littorale* (OD_{750}) (primary y-axis) and the evolution of the quantum yield (QY) of photosystem II (secondary y-axis) over time. **B:** The fluorescence of Bodipy (BP) (primary y-axis) shows a sigmoid curve, while the autofluorescence (AF) (secondary y-axis) shows a smooth curve. Both fluorescence signals were measured with the FlowCAM and are given in relative fluorescence units (RFU; values are the average fluorescence per cell of an analyzed population of 500 cells).

All four groups showed similar biomass productivities during the nitrogen run-out phase, ranging from 0.32 to 0.35 g l^{-1} d^{-1} (P_x N_{out}, Table 4.1). The lack of statistical difference among the groups confirms the previous results from the size distribution of single cell and multiple-cell sorting's (Figure 4.5 and Figure 4.6). The Post-sorting populations showed, however, a higher value of P_x at N_{out} when compared with the Pre-sorting population (P_x N_{out}, Table 4.1, $p<0.05$). The higher P_x values from Post-sorting could be a result of the low light acclimation that the cells experienced during recovery (Figure 4.1), before being again cultivated, which is known to increase photosynthetic efficiency, hence, the biomass production [89]. Another observation that could corroborate this effect is the evolution of the photosystem II quantum yield (QY) (Figure 4.7). The QY values dropped at a faster rate in the Pre-sorting experiment when compared with the Post-sorting experiment (Figure 4.4 and Figure 4.7). The evolution of the QY, however, showed no difference when Post-sorting populations were compared among each other (Figure 4.7). This effect can also be seen with the similar QY decrease rates (QY_{rate}) between experiments at the end of both N+ and N- phases (from 0.3 to 0.4, Table 4.1).

Despite an apparent physiological change possibly due to photo-acclimation during nitrogen replete conditions, no difference was observed in the P_x among the sorted groups and in comparison with the Pre-sorting population at nitrogen depleted conditions (P_x N-, Table 4.1). These results are evidence that cell size of vegetative cells has no effect, as sorting criteria, on biomass productivity.

Table 4.1: Growth parameters of *C. littorale* **Pre- and Post-sorting.** Growth rate (μ) is presented only for the growth phase (N+) (white area of figures 4.3 and 4.6). Decrease rates of photosystem II (QY_r) are presented for the nitrogen run out period (N_{out}) and N-depleted phase (N-) (As depicted in figure 4.3 and 4.6: N_{out} refers to the light grey area while N- refers to the dark grey area). Bodipy accumulation rate (BP_r) is related to the lipid accumulation after nitrogen run-out (N_{out}). The volumetric productivities of biomass (P_X) and TAG's (P_{TAG}) and also the total fatty acids and TAGs content (%DW) are presented for both growth phase (N+) and nitrogen depleted phase (N-). Superscript letters (a, b and c) mean statistical significance (ANOVA, $p<0.05$). Statistical analysis was carried out to detect differences between the Pre- and Post-sorting experiments.

			POST-SORTING			
PARAMETER	PHASE	PRE-SORTING	CONTROL	SMALL	MEDIUM	LARGE
μ (d^{-1})	N^+	0.19 ± 0.00	0.19 ± 0.00	0.17 ± 0.00	0.17 ± 0.00	0.18 ± 0.00
QY_r (d^{-1})	N_{out}	-0.34 ± 0.05	-0.40 ± 0.04	-0.46 ± 0.09	-0.49 ± 0.10	-0.44 ± 0.05
	N^-	-0.04 ± 0.00	-0.04 ± 0.01	-0.05 ± 0.00	-0.05 ± 0.00	-0.05 ± 0.00
BP_r (d^{-1})	N_{out}	1.27 ± 0.05	1.39 ± 0.05	1.29 ± 0.08	1.46 ± 0.05	1.33 ± 0.02
P_X (g l^{-1} day^{-1})	N_{out}	0.29 ± 0.02 ^{a}	0.32 ± 0.06 ^{b}	0.32 ± 0.01 ^{b}	0.35 ± 0.02 ^{b}	0.31 ± 0.02 ^{b}
	N^-	0.07 ± 0.00 ^{a}	0.07 ± 0.00 ^{a}	0.09 ± 0.00 ^{a}	0.08 ± 0.00 ^{a}	0.07 ± 0.05 ^{a}
P_{TAG} (mg l^{-1} day^{-1})	N_{out}	38.25 ± 2.15^a	23.25 ± 1.51 ^{b}	22.62 ± 1.80 ^{b}	23.87 ± 1.01 ^{b}	18.17 ± 1.30 ^{c}
	N^-	14.50 ± 0.15^a	12.35 ± 0.20^a	14.82 ± 0.70^a	13.65 ± 0.12^a	13.10 ± 0.11^a
Total TAGs (%DW)	N_{out}	13.19 ± 0.01^a	7.36 ± 0.73^b	7.07 ± 0.35^b	7.46 ± 0.17^b	5.68 ± 0.25^c
	N^-	33.77 ± 0.15^a	25.00 ± 0.07^b	25.6 ± 0.06^b	24.3 ± 0.00^b	24.4 ± 0.02^b

The evolution of BP fluorescence over time (Figure 4.7**Figure**B) is related to the values of lipid productivity (Table 4.1). All sorted populations showed similar trends among each other (Figure 4.7) and when compared to the Pre-sorting experiment (Figure 4.4B) in the evolution of lipid/cell accumulation. However, all sorted populations reached lower values of BP fluorescence at the end of the N_{out} phase when compared with the Pre-sorting experiments (Figure 4.3 and Figure 4.7). Such lower values of BP fluorescence match the results of lipid content in biomass: both TAG/total fatty-acids content and TAG productivity (P_{TAG}) were similar among Post-sorting populations at the end of the N_{out}, but statistically different when compared to the Pre-sorting experiment (Table 4.1, ANOVA $p<0.05$). An exception was for both TAG/total fatty-acids content and TAG productivity (P_{TAG}) of large cells (Table 4.1), which showed values statistically lower than the other Post-sorted populations and the parental population. However, such differences were not found in the N- phase, indicating that the delay in lipid accumulation was temporary during the N_{out}. These differences may be an effect of the low-light acclimation period the sorted cells went through for 2 weeks before growing under the same conditions as the Pre-sorting experiment (as shown in Figure 4.1). The photo-acclimation effect is corroborated by the above-mentioned slower decrease in the QY values (Figure 4.7A and Table 4.1). Due to photo-acclimation cells produced more biomass in comparison to the Pre-sorting experiment, which explains the different TAG fluorescence per cell (Figure 4.7B) and the lower TAG content/productivity in biomass (Table 4.1) in the Post sorting experiment.

These results point to a temporary change in the physiological response of sorted cells, seen in the lower values of BP at the beginning of the nitrogen run-out in comparison with the Pre-sorting experiment (Figure 4.4 and Figure 4.7). However, the accumulation rate of BP fluorescence (BP_r d^{-1}) shows that the biological mechanism still responded at the same rates. Likewise, the P_{TAG} at the end of the nitrogen depletion phase (N-) showed no differences among the Post-sorting populations and no difference when compared with the Pre-sorting population (Table 4.1). We conclude that sorting vegetative cells of *C. littorale* according to cellular diameter does not result in differences in biomass and lipid productivity.

4.4. Final remarks

We established the gates for cell sorting based on size using the FSC as a proxy for diameter in combination with autofluorescence. A Pre-sorting experiment was performed including a growth phase (N+), a nitrogen run-out (N_{out}) and a long nitrogen depleted phase (N-). The N- phase assured that cells stopped dividing, thus resulting only in vegetative cells, and assured that cells only increased their size due to lipid accumulation. Vegetative cells of *C. littorale* were sorted at the end of the Pre-sorting experiment based on cell size. Both single-cell and multiple-cell sorted populations showed similar size distributions after re-growth. The growth rates and productivities (biomass and lipid) were calculated to compare Pre- and Post-sorting populations. No difference among Post-sorting populations was detected, however, Post-sorting cells showed a higher value of biomass productivity (P_x) when compared with Pre-sorting cells. This result could be due to the low light acclimation that the cells experienced during recovery after sorting. Nevertheless, no difference was observed in the TAG's productivity (P_{TAG}) among Post-sorting cells and when compared to Pre-sorting cells at the nitrogen depletion phase. We conclude that cellular size of vegetative cells has no effect on both biomass and lipid productivities of *Chlorococcum littorale*.

4.5. Supplementary materials

S4.6.1. Photomicrography's of nitrogen depleted cells of *Chlorococcum littorale* at the day of the sorting. Images were acquired with the FlowCAM. Images are bright field micrograph's and display the cell diameter under each picture (magnification: 200x).

A] small cells

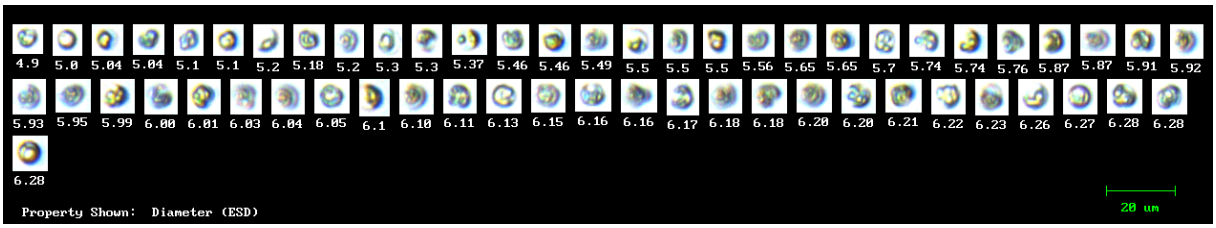

B] medium cells

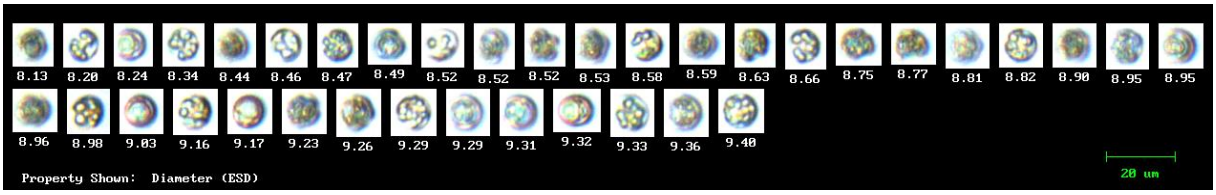

C] large cells

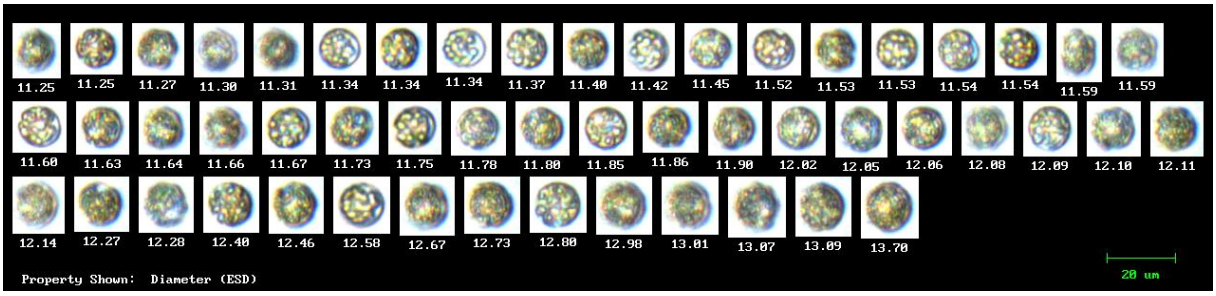

S4.6.2] Photomicrography's of the cell cycle of *Chlorococcum littorale*. **A:** vegetative cell at the end of nitrogen depletion phase; **B:** cell division into two daughters cells; **C:** cell division into four daughters cells; **D:** cell division into eight daughters; **E:** a zoospore with the two equal flagella. All pictures were at a magnification of 1000x, with a bright field microscope. Scale bar is equivalent to 12 µm.

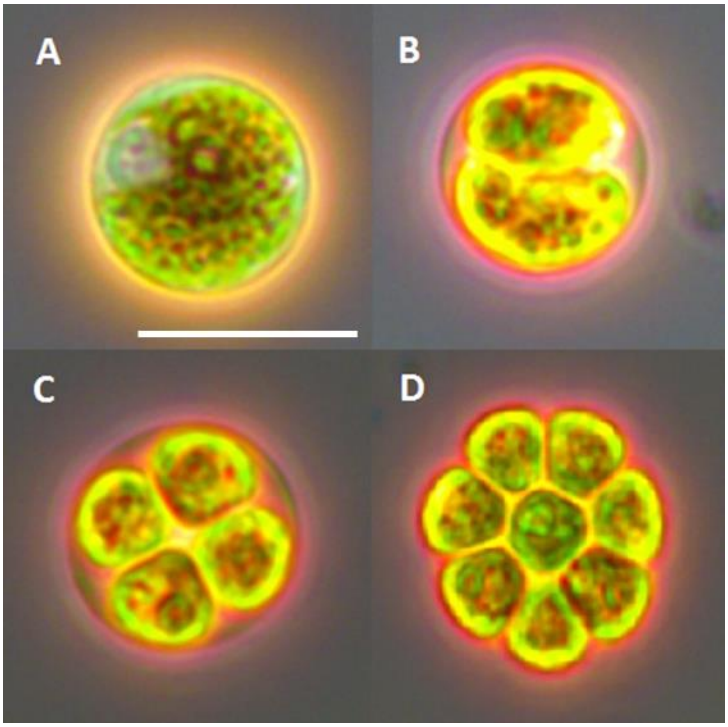

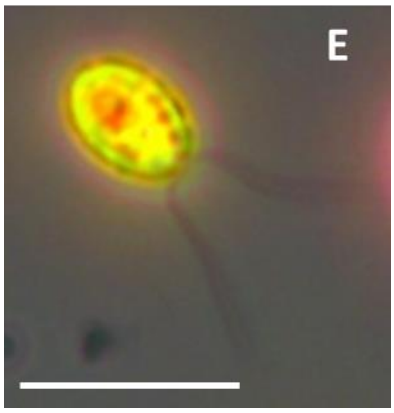

Sorting microalgae cells with increased TAG productivity

This chapter has been published as: **Cabanelas, I.T.D.**, Zwart, M.V.D., Kleinegris, D.M., Wijffels, R.H., Barbosa, M.J., 2016. Sorting cells of the microalga *Chlorococcum littorale* with increased triacylglycerol productivity. Biotechnology for Biofuels. doi:10.1186/s13068-016-0595-x.

Highlights

- Successful sorting of cells of *C. littorale* with increased TAG productivity using FACS
- Sorted population showed doubled TAG productivity in comparison with original
- Sorting removed cells with low efficiency (TAG/light) from original population
- Sorted phenotype shows stability after 1.5 years after sorting
- TAG productivity of sorted population is among the highest in literature

GRAPHICAL ABSTRACT:

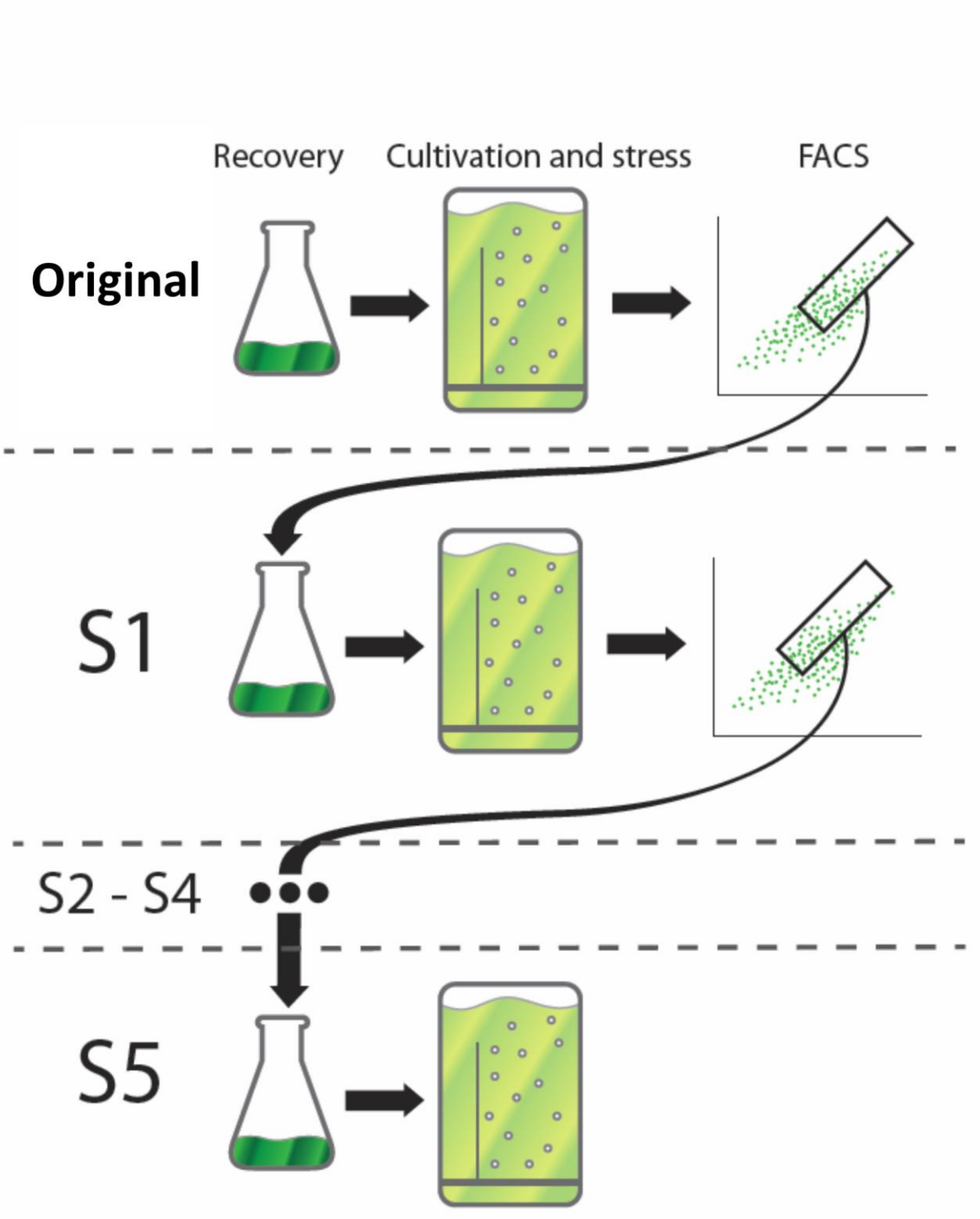

ABSTRACT:

A strategy to sort microalgae cells with increased TAG productivity is demonstrated. [1] We successfully identified sub-populations of cells with increased TAG productivity using Fluorescence assisted cell sorting (FACS). [2] We sequentially sorted cells after repeated cycles of N-starvation, resulting in 5 sorted populations (S1-S5). [3] The comparison between sorted and original populations showed that S5 had the highest TAG productivity (0.34 against 0.18 g L^{-1} d^{-1} [original], continuous light). [4] Original and S5 were compared in lab-scale reactors under simulated summer conditions resulting in a 2-fold increase in TAG productivity (0.4 against 0.2 g L^{-1} d^{-1}). Biomass composition analyses showed that S5 produced more biomass under N-starvation because of an increase only in TAG content and, flow cytometry showed that our selection removed cells with lower efficiency in producing TAGs. Literature review showed that S5 has a superior TAG yield on light compared to the most common wild type oleaginous strains (0.32 against 0.16-0.20 g mol^{-1}), and that S5 competes with an starchless strain of *Scenedesmus obliquus* that was improved via random mutagenesis (0.32 (S5) against 0.37 g mol^{-1}). All combined, our results present a successful strategy to improve the TAG productivity of *Chlorococcum littorale*, without resourcing to genetic manipulation or random mutagenesis.

Key-words: microalgae**;** *Chlorococcum littorale*; cell sorting (FACS); strain improvement; lipid productivity

5.1. Introduction

Microalgae are a versatile feedstock with applications ranging from animal feed to high-end products like nutraceuticals [1]. Economic analyses show production costs from 5-6€ per kg of dry biomass [3], which clearly require further reduction if aiming at low-value market products (e.g. biofuels). Despite extensive research in the last decades, microalgae are still only economically feasible for high valued markets, e.g. nutraceuticals and also as feed for aquaculture [5–7].Cost reduction can be achieved by 2 ways: [1] decreasing capital and operational costs of the cultivation systems) and [2] increasing microalgae productivity (thus increasing the yields on light). The yields can be increased via process optimization to improve the light usage by the cells [8] or via developing new strains with superior performance [9]. Strain improvement has multiple approaches that could be used: selection of cells [10], adaptive laboratory evolution [11], random mutagenesis [14] and genetic manipulation [9,13].

In the present work we focus on microalgae selection: taking advantage of the natural biological variability of species to select variations based on desired characteristics [9]. Microalgae are microscopic phototrophs with unicellular species ranging from 1 to 30 µm in size [71]. Due to their size we need a technology that can quickly analyze and select cells of interest. Fluorescence activated cell sorting (FACS) is a well-established technology that has been used since the 1970's for single cell analyses of mammalian and plant cells. A few research groups have recently applied FACS to microalgae with different approaches and outcomes, mainly focusing on selecting lipid-rich cells [10,21]. Most of the works on FACS to improve lipid content of microalgae strains present also a combination with different mutagenesis techniques [9,14,22,23].

All above mentioned articles, however, presented results that were carried out in small volumes (well-plates or shake flasks) and do not refer to biomass productivity or growth rates of the sorted/improved strains. Hence, estimation of industrial performance of strains is limited. The exception was the work of Beacham et al. (2015) [23], that reported a reduction in biomass productivity in all high-lipid sorted/mutated strains, resulting in only one sorted/mutant cell line with increased lipid productivity when compared to their original culture. Another work reported a 3.2 times slower growth rate in their high-lipid sorted strain [21]. Clearly, using FACS (with or without mutagenesis) to select lipid-rich cells may lead to undesirable results to cell growth, which would affect directly lipid productivity. Hence, it is necessary to evaluate the effect of the sorting on biomass/product productivity to assess the industrial potential of developed strains.

In the present work we present a strategy to find and sort microalgae cells with increased TAG productivity. Our approach was developed in the following steps: [1] to analyze cell properties at population level to identify sub-populations with potentially increased TAG productivity; [2] to sequentially sort (5x) cells under N-starvation as a selective pressure towards increased TAG productivities; [3] to confirm the increased lipid productivity of our sorted populations with lab-scale photobioreactors experiments, to measure biomass accumulation and also biomass composition; [4] the sorted population with the highest lipid productivity (S5) was run in comparison with the original strain in an indoor photobioreactor under simulated Dutch summer conditions.

5.2. Materials and methods

5.2.1. Inoculum preparation, cultivation and culture screening with FACS

Chlorococcum littorale (NBRC 102761) was used as the original strain. Inocula from the original strain was prepared from samples preserved in petri dishes containing growth medium and agar (12 g l^{-1}), under low light conditions (16 µmol m^{-2} s^{-1}). Homogenous samples were taken from agar to 200 ml sterile borosilicate Erlenmeyer flasks, containing 100 ml of sterile growth medium. Artificial seawater was used as grown medium with the following composition (g l^{-1}): NaCl 24.55, $MgSO_4 \cdot 7H_2O$ 6.60, $MgCl_2 \cdot 6H_2O$ 5.60, $CaCl_2 \cdot 2H_2O$ 1.50, $NaNO_3$ 1.70, HEPES 11.92, $NaHCO_3$ 0.84, EDTA-Fe(III) 4.28, K_2HPO_4 0.13, KH_2PO_4 0.04. additionally, the medium contained the following trace elements (mg l^{-1}): $Na_2EDTA \cdot 2H_2O$ 0.19, $ZnSO_4 \cdot 7H_2O$ 0.022, $CoCl \cdot 6H_2O$ 0.01, $MnCl_2 \cdot 2H_2O$ 0.148, $Na_2MoO_4 \cdot 2H_2O$ 0.06, $CuSO_4 \cdot 5H_2O$ 0.01.

Initially, N-starved cells (using the experimental set-up as shown in 5.2.4) of *C. littorale* were used to analyze cell properties at population level. The population analyses were done to choose the boundaries of the sorting gate. Samples were run in a FACS Calibur® to measure autofluorescence (FL3, 670nm LP), lipid fluorescence (FL1, 530/30 nm) and forward scatter (full settings given at section 5.2.4). FlowCAM® fluid imaging was used to complement the assessment of the population characteristics, providing the actual cell diameter (µm)and photomicrographs of the cells (the same parameters as the FACS were also measured , autofluorescence and lipid fluorescence). The lipid fluorescence was measured using the Bodipy 505/515 (BP) stain following the protocol developed previously [15].

5.2.2. Experimental set-up

For the N-runout/sorting experiments *C. littorale* was cultivated in a 0.4 L flat panel photobioreactor under controlled and sterile conditions (25˚ C, air flow at 1 v/v/m, pH set at 7.0 controlled on demand via CO_2 addition to air, constant light at 400 µmols m^2 s^{-1}), specifications of the photobioreactor can be found at Breuer et al., (2013) [64]. The cultivations were nitrogen run-out batches, i.e. nitrogen was added at an initial concentration of 10.7 mM (as KNO_3) and was allowed to be taken up by the cells. All nitrogen was consumed within the first 48 hours, after which the N-starvation phase is considered. At the end of the nitrogen starvation phase (after 8 days of cultivation), when the cells reached the maximum lipid-fluorescence, a sample was taken to the FACSCalibur to be measured and sorted. At each sorting round 1000 cells were sorted into a sterile falcon tube (50 ml) and subsequently centrifuged (1050 x g, 10 minutes) and transferred to a new sterile falcon tube containing 20 ml of fresh sterile medium.

The sorted cells were allowed to recover and grow under low light conditions for 2 weeks (constant at 16 µmols m^2 s^{-1}). After 2 weeks of growth the cells were transferred to a sterile Erlenmeyer flask containing 100 ml of fresh sterile medium, to continue the cycles of starvation/sorting. The algae were grown in a INFORS shake incubator under controlled constant conditions for 2 weeks (25 C, 120 rpm, 50% air moist and 120 µmols m^2 s^{-1}). After two

weeks in the incubator the cells were used as inoculum to re-start the N-runout/sorting procedure. Additionally, a sample of the sorted populations was plated on agar plates (with N replete medium) for long term preservation (refreshed every 3 months). Additionally, samples from the sorted populations were plated in agar plates for storage and for producing inocula for the comparison experiment.

A second experiment was done to compare the sorted populations with the original population in parallel, using the same experimental set-up as described above. The original population was compared with 4 different sorted population (S2, S3, S4 and S5; the numbers refer to the round of N-starvation/sorting). The first sorted population (S1) was kept out of this experiment because it showed no differences when compared with the original population in the first experiment (data not shown). For this new experiments all the different populations (original, S2, S3, S4 and S5) were transferred from agar plates to Erlenmeyer flask and next to photobioreactors and cultivated under the similar conditions as above mentioned. Biomass samples from each reactor were taken at the end of the N-starvation phase for analyzing the biochemical composition (as showed below at section 5.2.5).

A final experiment was conducted to compare the original with the S5, which was the best population in the previous experiments. The goal of the experiment was to compare both populations under simulated Dutch summer conditions (day length of 16 hours), hence the light was supplied with an sinus function with a solar noon at 1500 µmols m^2 s^{-1} supplied as a day/night cycle (resulting in an average daily incident light intensity of 636 µmols m^2 s^{-1}). This experiment was done in a flat panel reactor with a working volume of 1.9 L, light path of 0.02m, and 0.08 m^2 surface area (Labfors, Infors HT, 2010). Air flow as set at 1.0 L min^{-1} and mixed with CO_2 on demand to keep the pH constant at 7.0. Temperature was kept constant with an integrated water-jacket at 25 ˚C.

5.2.3. Daily measurements

Daily samples were taken always at the same time. Optical densities were used as a proxy for cell density (750nm) and chlorophyll (680nm) using a spectrophotometer (HACH, DR5000) [62]. FlowCAM® fluidic imagining was daily used to follow-up the cell's diameter, autofluorescence (chlorophyll fluorescence) and lipid-dependent fluorescence ($BODIPY_{505/515}$ fluorescence). Samples were diluted to meet a PPUI (particle per use image) between 1.0-1.2 and then stained for neutral lipids using BODIPY $_{505/515}$ at 0.4 µg/mL diluted in 0.35% ethanol [15]. After 5 minutes of dark incubation the samples were run in the FlowCAM® using the following settings: 20x optical magnification and Trigger-mode-on based on the fluorescence of channels 1 (autofluorescence , 650nm long pass filter) channel 2 ($BODIPY_{505/515}$, 525/30 nm filter).

Samples were also taken for analyses of extracellular nitrogen content ($N\text{-}NO_3$ mg l^{-1}). Hence, 1 ml of culture was centrifuged at 13.000 x g and the supernatant was separated to be analyzed. Sulphanilamide N-1-naphthyl method was used (APHA 4500-NO3-F) by an SEAL AQ2 automatic analyzer.

5.2.4. Cell sorting using FACS

FACSCalibur® (BD life technologies) was used to measure cell properties and to sort cells. The measurements were lipid-dependent fluorescence (Bodipy 505/515, FL1 channel) and chlorophyll-dependent (autofluorescence, FL3 channel). Both channels were measured at log scale and the sensitivity was set at 300mV. All samples were diluted to a concentration of 200 events/second (OD_{750} of approximately 0.1). Measurements of 10,000 and 1,000 cell's per sample were saved and further used for analyses. 1,000 cells were sorted and used in the experiments.

Sorting was done using the same settings as above, using the gate depicted in Figure 5.1. The system was fluxed for 10 minutes with ethanol 70% to reduce contamination. Autoclaved and filtered (0.2µm) PBS was used as sheath fluid (phosphate saline buffer (1x PBS); composition: NaCl 137 mM, KCl 2.7 mM, Na_2HPO_4 10.0 mM, KH_2PO_4 1.8 mM).

Cells were centrifuged immediately after the sorting (1224 x g for 5 minutes) and re-suspended in sterile growth medium. The tubes containing sorted cells were placed under constant light at 16 $\mu mol \cdot m^{-2} \cdot s^{-1}$, allowing cells to recover and grow for 2 weeks. The tubes were transferred to flasks, after the growth time, to make inoculum for the next round of N-runout/sorting.

5.2.5. Biomass analyses

Biomass samples were collected at the end of the N-runout for composition analysis, all results are expressed as %DW. Biomass was centrifuged twice and washed with MilliQ water (3134xg for 10 minutes at 4°C) and followed by freezing at -20°C and freeze-drying for 24 h.

Polar lipids and triacylglycerol's (TAGs) were extracted and quantified using GC/MS column chromatography of the chloroform fraction of lipids [77]. Total carbohydrates were analyzed with the phenol-sulfuric acid method[90]. Total starch was analyzed after extraction with 80% ethanol followed by quantification using the colorimetric/enzymatic method with the commercial kit from Megazyme (K-STA kit, UK). Total proteins were measured using the colorimetric method developed by Bradford (1976) [91].

5.2.6. Data analysis

Cell analyses from the FlowCAM were exported to Microsoft Excel to plot graphs and estimate descriptive statistics. Flow cytometry data (FSC files) were analyzed with the software FlowJO v 10. Null hypothesis significance testing (NHST) was used to compare the results between and among samples. One-way analysis of variance (ANOVA) was used to access the significance of differences between different groups (SigmaPlot, v. 12.5). The premises of ANOVA, i.e. the homogeneity of variances and the normality of the data, were also measured with SigmaPlot (for all testes α was set at 0.05). For population-wide data (flow cytometry) the large data set (10,000 measurements per sample) was compared using size-independent parameters, i.e. the median and the coefficient of variation (CV). Confidence intervals (CI) and histogram overlapping were used to compare populations.

Calculations

The biomass dry weight was used to calculate the growth rate (μ, d^{-1}), as given in [Equation 6],

$$\mu = \frac{\ln(DW_{t_{final}} - DW_{t_0})}{t_{final} - t_0}$$ Equation 9

where, DW stands for the dry weight of biomass (g l^{-1}), from the first (t_0) and the last time point (t_{final}) considered. For the growth rate under nitrogen replete conditions (N+) the 2nd day of cultivation (d=2) and the day of inoculation (d=0) were used as final and initial values, respectively.

Relative lipid production was measured by BODIPY cellular fluorescence to calculate the BODIPY accumulation rate (BP_r), relating to the increase of cellular neutral lipids in time. The BP_r was estimated with an approach similar to Equation 6, however the values of DW where substituted with the values of median BP fluorescence. The time interval used for calculation was the period between the start (d=2) and the end (d=8) of the nitrogen run-out.

The volumetric biomass productivity during the growth phase (N+; P_X, g l^{-1} d^{-1}) was estimated with [Equation 7],

$$P_X = \frac{DW_{tf} - DW_{t_0}}{t_f - t_0}$$ Equation 10

where, the values of dry weight (DW, in g per liter) were used between the end (t_f=2) and the beginning (t_0=0) of the growth phase (for both experiments as presented in 5.3.2 and 5.3.3).

The maximum average TAG volumetric productivity (P_{TAG}, g l^{-1} d^{-1}) was estimated using [Equation 8],

$$P_{TAG} = \frac{TAG_f - TAG_0}{t_f - t_0}$$ Equation 11

where, TAG_f is the TAG concentration at the end of the production period (in g L^{-1}) and TAG_0 is the TAG concentration at the start of the N-starvation (also in g L^{-1}). The corresponding time period was represented by the final and initial days of TAG production (respectively, t_f and t_0). For the first experiment (section 5.3.2) we used the total N-starvation period, hence between t=8 and t=2. For the second experiment (section 5.3.3), comparing original and S5, we used the period which showed the maximum TAG productivity, hence between t=4 and t=2. TAG yields (g mol^{-1}) on light were calculated using the areal TAG productivity (g m^2 d^{-1}) divided by the corresponding total amount of light impinging on the surface of the reactor (in mol m^2 d^{-1}).

5.3. Results and Discussion

5.3.1. Gate set-up to sort lipid-rich cells

Our approach started by choosing the sorting criteria. Besides the obvious choice of lipid-dependent fluorescence (Bodipy, BP) we also included chlorophyll-dependent fluorescence (Autofluorescence, AF). We included AF for two reasons: the first reason is because AF correlates to cell size, hence it can be used to estimate the ratio lipid/cell. Secondly, we hypothesized that cells that could keep their levels of AF after a period of N-starvation would be cells with low levels of chlorophyll degradation, hence cells that could grow again if N is re-supplied.

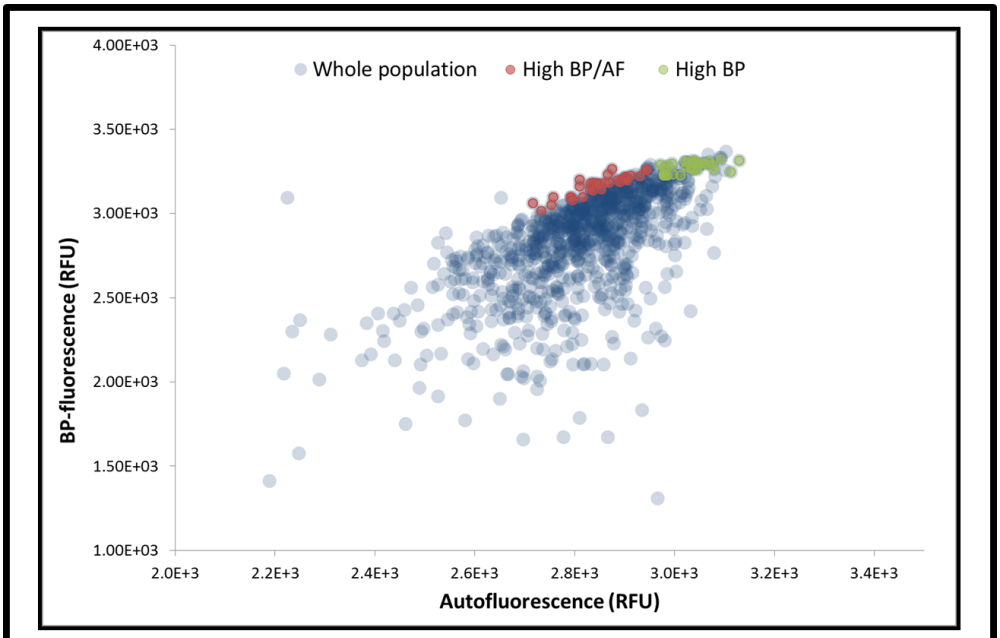

	AF (RFU)	BP (RFU)	BP/AF ratio	Size (µm)	BP/cell (RFU/µm)
Whole population	2.83E+03	2.91E+03	1.01	6.66	4.37E+02
High BP/AF:	2.85E+03	3.18E+03	1.12	7.01	4.54E+02
High BP:	3.03E+03	3.28E+03	1.08	8.11	4.04E+02

Figure 5.1: Flow cytometry data can identify high-lipid content cells among the population. The graph shows a scatter-plot between lipid fluorescence (Bodipy, BP; y-axis) and chlorophyll fluorescence (Autofluorescence, AF, x-axis), in which we can see the whole population (in blue) and two sub-populations marked as relevant: cells with the highest values of lipid fluorescence (High BP; in green), and cells that show the highest ratio between lipid and chlorophyll (High BP/AF; in red). The colored sections in the graph correspond to the rows with the same color in the table. The table shows the median values of AF, BP, cell size and the ratios between median values of BP/AF and BP/cell.

To establish the sorting gate we first carried out a screening test in which N-starved cells (under the same conditions to be used in the experiments to follow) were analyzed with flow cytometry. The scatter-plot between autofluorescence (chlorophyll-dependent, AF) and Bodipy fluorescence (lipid-dependent, BP) (Figure 5.1) shows that there are some regions of the population in which these two variables correlate more. Hence, we included the BP/AF ratio as a criterion to estimate the amount of lipids (BP) per cell size (AF). Our analyses of the population of N-starved cells pointed to 2 interesting sub-populations, as showed in Figure 5.1.

The first sub-population to be analyzed were the cells that presented the highest values of lipid fluorescence (High BP). These cells, however, show high values of BP because they are also the biggest cells within the population, which can be evidenced by its bigger size in comparison with the whole population (8.11 against 6.66 µm; Table in Figure 5.1). Cell size could be a misleading variable since bigger cells might have, proportionally, the same lipid content as the population's median. When normalizing the median BP fluorescence by the median cell volume of each population it is clear that the sub-population marked as High BP doesn't have more fluorescence per cell volume than the whole population (4.04 against 4.37E+03 BP/cell; Figure 5.1).

The other sub-population was chosen using the BP/AF ratio as criterion (High BP/AF,Figure 5.1). We hypothesized that BP/AF ratio would lead to a sub-population of cells with a higher lipid content per cell. At the same time this sub-population selects the top lipid producers while keeping the median AF value, hence avoiding the AF as a cofounding variable (either due to cell size or relative chlorophyll content). The normalized BP/cell volume show us that indeed the High BP/AF sub-population has a higher value of BP/cell volume in comparison with the whole population (4.54 versus 4.37E+03, Figure 5.1). Thus, the gate depicted in red on Figure 5.1 as BP/AF was chosen as sorting criteria.

5.3.2. Sorting lipid-rich cells

The sorting's were done as depicted in the graphical abstract. After each round of sorting the cells were transferred to shake flasks to produce new inoculum to start a new N-runout (and consequently a new round of sorting). Additionally, an aliquot of the sorted cells was transferred to an agar plate and kept under low light conditions for long term storage and further use for comparing all sorted populations. All sorting rounds had a period of one month in between to grow the inoculum after sorting. Hence, each new round of N-runout was started with cells that came from different acclimation conditions than the Wt. Therefore, we produced inoculum from original and all sorted populations that were kept on plate, at the same time and started parallel runs with an independent reactor for each population. The population from the first round of sorting (S1) was kept out of the parallel runs because preliminary data from flow cytometry showed that the cells of S1 had the same distribution of lipid fluorescence as the original (data not shown).

Original was run in parallel with S2, S3, S4 and S5 to compare growth rates, biomass and lipid productivities and biomass composition. Figure 5.2 shows the overlapped growth curves for all 5 populations with a clear similarity among all populations during the growth phase (during the first 2 days N was available, green area). Table 5.1 gives the values of specific growth rates (µ)

and biomass productivities (P_X) among all sorted populations, which were similar to each other. Since cells were sorted based on their lipid content per cell size, the first parameter to be investigated was the relative lipid accumulation rate (BPr, d^{-1}), showing that all sorted populations presented higher accumulation of lipids in comparison with the original (1.15-1.20 against 1.09 d^{-1}, Table 5.1). Next, the median fluorescence values (both AF and BP) were compared, revealing an progressive increase in median BP fluorescence while the AF was reduced (Figure 5.3A). This resulted in a progressive increase in the BP/AF ratio, the aim of our sorting criteria. The parameter BP/cell was calculated dividing the median value of BP-fluorescence by the total cell number (at the end of the N-runout, thus at day 8), resulting in a similar trend as the BPr. These parameters were used to decide to continue/stop the sorting in the early stage of the research as an indication of the lipid productivity. It should be highlighted that they are relative measurements, hence not capable of replacing the actual measurement of lipid productivity, which can only be determined after sorting a new population when enough biomass is produced. Biomass samples of all populations were taken at the end of the comparison runs to measure the TAG productivity.

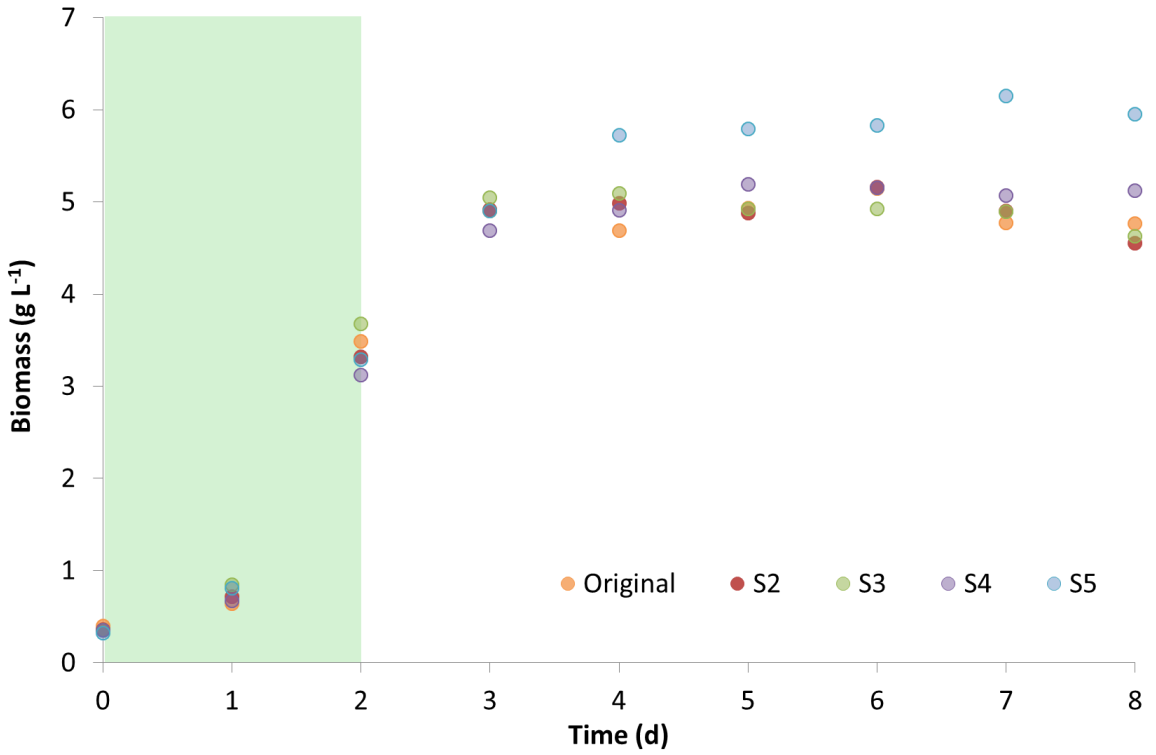

Figure 5.2: All sorted populations are similar to the wildtype (Wt) in the growth phase. The graphs shows the biomass concentration per day (g L^{-1}). The green area (days 0 to 2) marks the growth phase, after which all nitrogen was taken up by the cells. From day 2 onwards it should be considered as starvation phase (N-).

TAG productivity (P_{TAG}) was measured for all populations, showing increased P_{TAG} values among all sorted populations (Table 5.1). Compared to original, S2 and S3 showed a discrete increase (from 0.18 in original to 0.20 g l^{-1} d^{-1} in S2 and S3) and S4 showed an increase of 38% (from 0.18 to 0.25 g l^{-1} d^{-1}). S5 showed the highest P_{TAG0}, resulting in an 88% increase in P_{TAG} when compared with original (from 0.18 to 0.34 g l^{-1} d^{-1}). The biomass produced by all sorted populations was analyzed for its content as total starch, total carbohydrates (minus starch), total proteins, polar lipids and TAGs (Table 5.1). The biomass composition of all sorted populations and the original population was similar among each other, with the exception of TAGs. The analyses of biomass composition showed that the extra biomass produced by the sorted populations was caused only by an overproduction of TAGs (Table 5.1).

We would like to highlight that the sorted criteria used in the current research didn't affect the TAGs composition of all sorted populations, which showed the same saturation degree (Figure 5.3B). This finding was intentional and expected, considering the staining used in the current research. Bodipy (505/515) is a hydrophilic fluorophore that binds to neutral lipids, being a relative measurement of total TAGs [59,86]. Hence, in our work cells were selected based on total TAGs content per cell, without applying any pressure that would favor a change in TAGs composition. Two previous works on microalgae strain improvement with cell sorting have reported a change in lipid composition [9,14]. Both works however, have used random mutagenesis, which could explain the change in lipid composition.

Table 5.1: Comparing kinetic parameters and biomass composition between original and sorted populations. The kinetic parameters are: specific growth rate (μ) and biomass productivity (Px), both under growth conditions (between t=0 and t=2). TAG productivity (Ptag) and lipid fluorescence accumulation rate (BPr) consider the whole N-starvation period (t=2 to t=8), while lipid fluorescence per cell was measured considering the values at the end of the starvation phase (t=8). All analyzed biomass components are expressed as relative to biomass dry weight (g/g/ DW). Standard variation of measurements is not depicted because the technical error was always around 5%.

Kinetic parameters	**μ (d^{-1})**	**Px ($g\ L^{-1}d^{-1}$)**	**Ptag ($g\ L^{-1}d^{-1}$)**	**BPr (d^{-1})**	**BP/cell (RFU/cell)**
Original	0.69	1.54	0.18	1.09	1.09
S2	0.67	1.48	0.20	1.15	1.12
S3	0.73	1.66	0.20	1.22	1.14
S4	0.64	1.39	0.25	1.19	1.20
S5	0.67	1.48	0.34	1.20	1.23
Biomass composition	**Starch (g/g)**	**Carbs (g/g)**	**Proteins (g/g)**	**PL (g/g)**	**TAG (g/g)**
Original	0.24	0.10	0.14	0.05	0.23
S2	0.24	0.12	0.15	0.06	0.27
S3	0.25	0.12	0.14	0.05	0.26
S4	0.24	0.13	0.16	0.06	0.29
S5	0.25	0.12	0.16	0.06	0.34

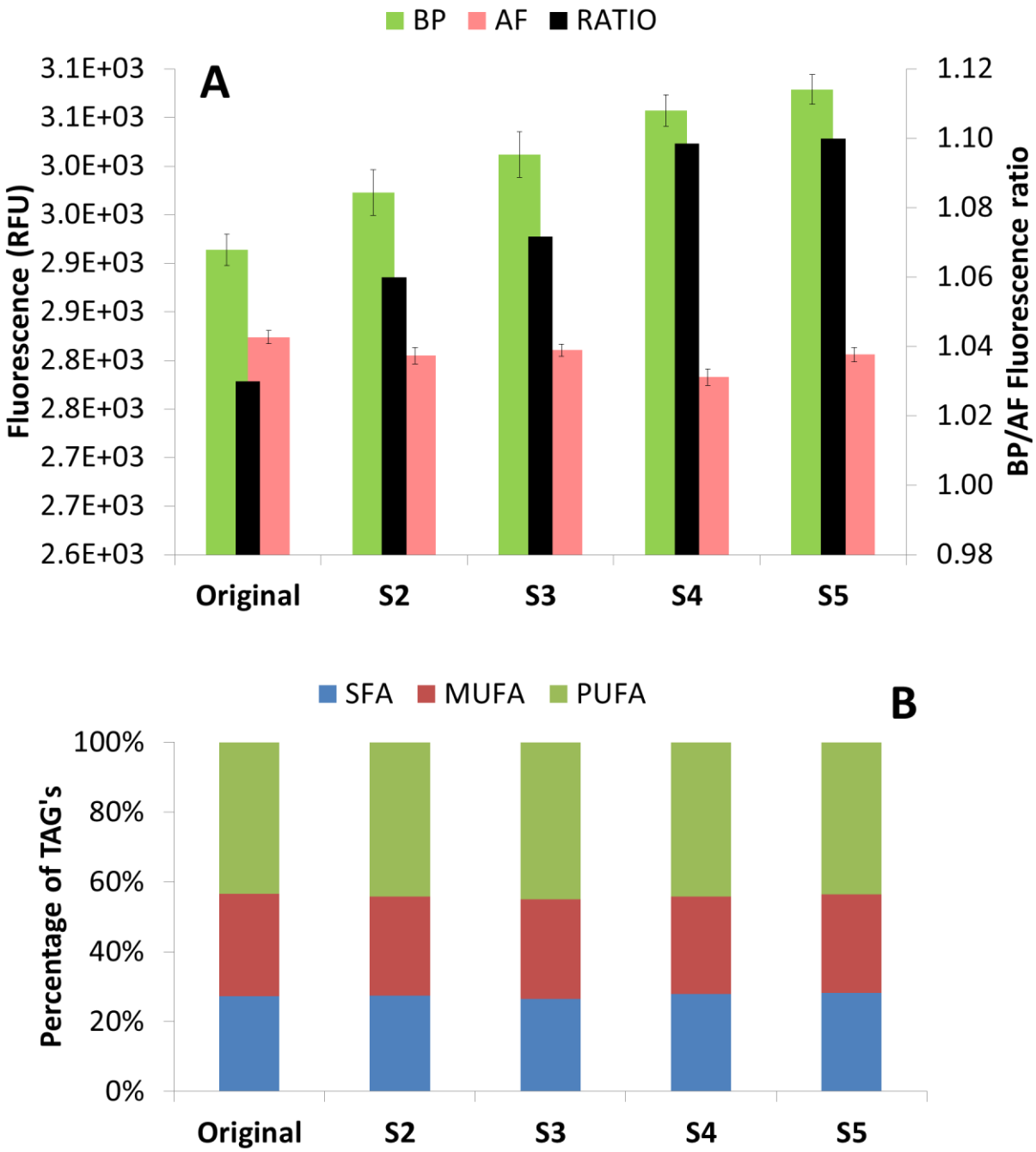

Figure 5.3: A progressive increase in lipid fluorescence leads to a progressive increase in BP/AF ratio without changes in the saturation degree of TAG's. Fluorescence measurements of both Bodipy (BP) and autofluorescence (AF) on the primary y-axis and the BP/AF ratio on the secondary y-axis in all populations (x-axis)(A). All populations showed similarities in the TAG's saturation degree (SFA, MUFA and PUFA's as % of total TAG's) (B).

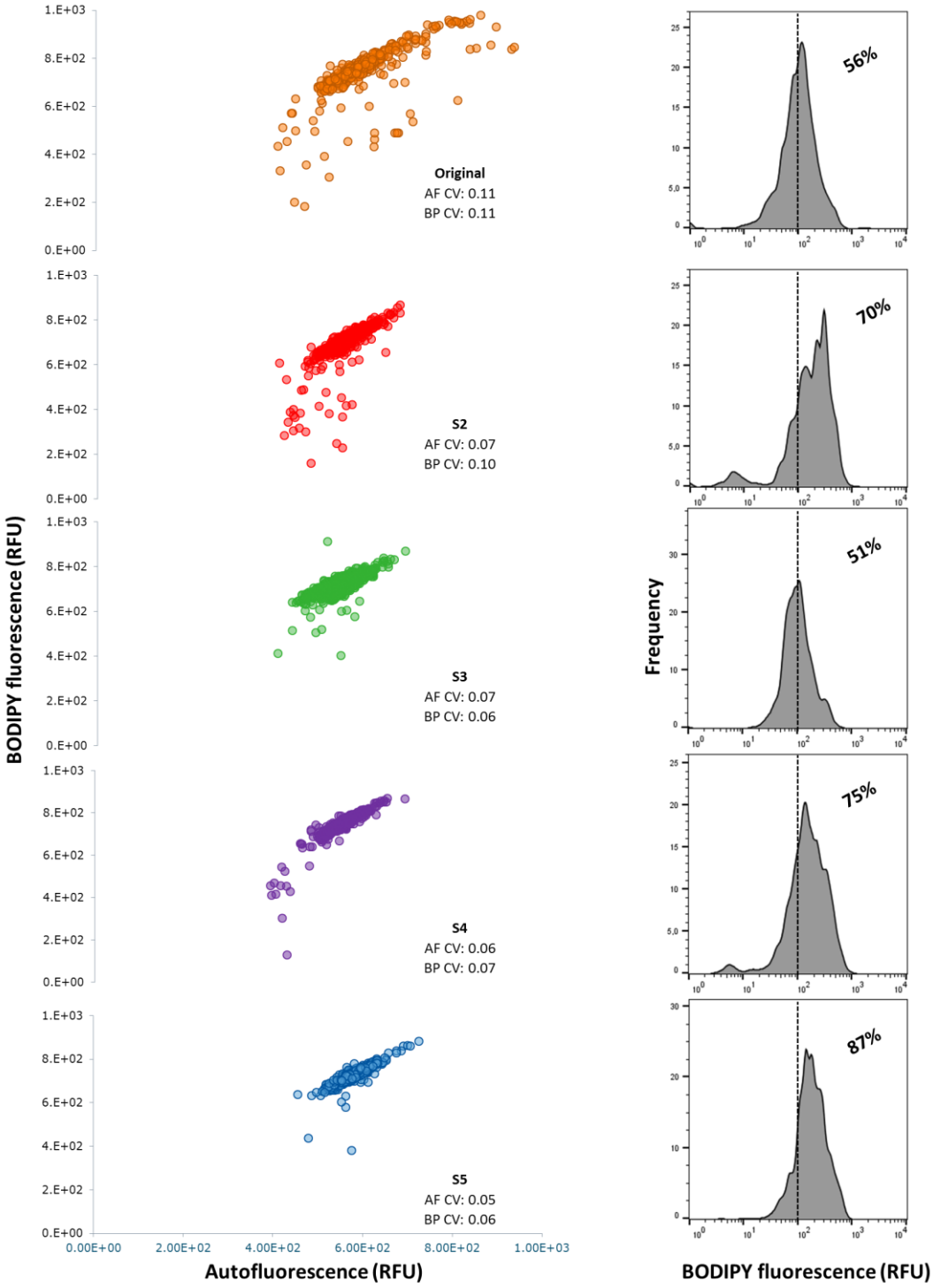

Figure 5.4: Sorted populations show a progressive increase in lipid productivity due to an increase in the proportion of lipid-rich cells within the populations. Scatter plots represent the relation between autofluorescence (AF, x-axis) and lipid fluorescence (BP, y-axis). On all scatter-plots the coefficient of variation (CV) of both AF and BP are depicted. Each populations has a histogram plotted showing the frequency distribution of lipid fluorescence (BP, x-axis). Additionally, each histogram is market to show the percentage of cells that have fluorescence signal above 10^2. All graphs represent the readings of 1000 cells.

Flow cytometry data were used to see the relationship at cellular level, between relative lipid content and autofluorescence (Figure 5.4, scatter plots). From such relation we can see that the sorted cells don't show fluorescence values above the maximum already exhibited by the Original. We hypothesized that our sorted cells would achieve higher values of BP-fluorescence than the Original, similar to what has been reported by Doan & Obbard (2011) [10]. What we see, however, is that we increased the lipid/cell ratio by progressively removing the cells with a low lipid/cell ratio, hence increasing the median BP fluorescence of the population. This effect can be visualized in numbers using the coefficient of variation (CV) of both auto and BP-fluorescence, which were progressively reduced in all sorted populations (values available on the scatter plots, from 0.11 (Original) to 0.06 (S5), Figure 5.4). The results from the scatter plots (Figure 5.4) can be combined with the histograms of frequency of BP (right side, Figure 5.4). The histograms show that the populations have a higher median TAG content because they show a higher proportion of the population composed of lipid-rich cells (percentage values on the charts show the proportion of cells within the population that have fluorescence values above 10^2 RFUs). We can conclude, combining all results above, that the sorting carried out in the present research was successful in producing new cell lines with increased lipid productivity.

Previous research articles have also reported successful sorting of microalgae cells to produce populations with increased lipid content [9,10,14,22]. All these publications, however, do not measure the impact of the sorting on biomass or lipid productivity. Furthermore, all these publications were done at small laboratory scale, many using well-plates or shake flasks, hence the estimation of industrial performance of strains is limited. One exception was the work of Beacham and co-authors, which assessed both growth rate and lipid productivity of *Nannochloropsis salina* and sorted mutants [23]. The combination of mutagenesis and cells sorting lead to 4 mutants, all exhibiting an overproduction of lipids, but all mutants also exhibited a reduction in biomass productivity (from -18 to -95% growth). In their results only one mutant showed a final lipid productivity higher than the original strain (from 0.40 to 0.49 x 10^{-4} g mL^{-1} d^{-1}).

Another important remark when comparing sorted cells/mutants is the timing in between sorting rounds, which may cause an effect on growth and lipid kinetics of sorted populations. Most of other works above mentioned compared the lipid content of cell populations cultivated immediately after being sorted, hence ignoring a possible effect of the post-sorting period of re-growth on the physiological response of microalgae [9,10,21–23]. Previous research has found a 3.2 times longer growth phase in sorted populations in comparison with the original [21]. Since the growth was measured immediately after sorting, it is impossible to say if the slower growth was a feature of the new population or a longer lag phase caused by the sorting process. The effects of the sorting process itself could decrease growth rate and/or affect the lipid metabolism response since it represents a source of stress and the cellular response is strain-specific [15,78,68]. The above discussed results highlight the importance of assessing cellular growth after a long period post-sorting, to guarantee the stability of the sorted population to industrial cultivation.

5.3.3. Comparing original and S5 under simulated Dutch summer conditions

The parallel runs with sorted populations and original population showed S5 as the population with the highest TAG productivity. The next step was to cultivate original and S5 under simulated outdoor conditions. This is an important step since part of the biomass (carbons sources, e.g. starch and TAGs) can be respired during dark periods for cellular maintenance, leading to possible changes in the productivity of different biomass components when comparing to experiments under continuous light [92]. The goal of this comparison was to evaluate how superior the productivity of S5 was in comparison with original under day/night cycles, hence we simulated an average Dutch summer day in an indoor flat panel reactor.

We also used the comparison experiment between S5 and original to estimate the stability of the sorted phenotype as the comparison experiments were carried out 1.5 years after the population had been sorted. original and S5 were kept under low light in agar plates containing growth medium in the time between the sorting and the comparison experiments (cultures were transferred to new plates every 3 months). Therefore, original and S5 were compared using inoculum that came from similar conditions, and both were done in biological replicates, all combined to make the comparison more accurate.

Figure 5.5A shows the growth (as biomass DW,g L^{-1}) of original and S5, confirming our results from the parallel runs: under growth conditions (days 0 to 2, Figure 5.5) S5 shows similar growth kinetics as the original (μ and Px, Table 5.2

Table). Previous research articles have reported that cells with improved lipid content presented also a reduction in growth [14,23]. Our results, however, highlight that the sorting criteria used in the current work didn't affect cell growth.

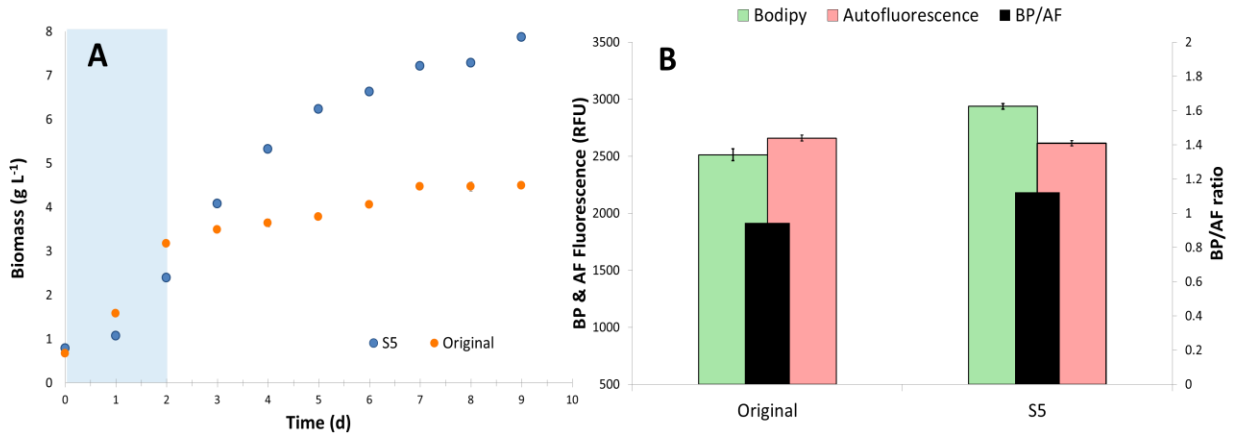

Figure 5.5: Comparing growth and lipid accumulation of original and S5 under simulated Dutch summer conditions. Graph A shows that the S5 strain produces more biomass under nitrogen starvation than the Wt. The grey area represents the period of the cultivation in which N was available, from day 2 onward the N-starvation phase (N-) is considered. Graph B shows the difference between S5 and original at cellular level (at the end of the N-starvation period): the S5 population has higher values of Bodipy fluorescence than the Wt, leading to an increase in the BP/AF ratio. Both populations had the same number of cells analyzed (n=500). Error bars represent confidence intervals.

Differences, however, were observed after the start of the N-runout (Figure 5.5, after day 2). Biomass composition shows again that TAGs were the biochemical fraction that explained the increase in biomass accumulation in the N-starvation period (Table 5.2). The TAG content of S5 was 1.7 x higher than original (0.36 against 0.21 g/g DW, Table 5.2), while other biomass components (starch, carbohydrates (minus starch) and polar lipids) were similar between original and S5. The increase in TAG content resulted in a 2-fold increase in the P_{TAG} of S5 when compared with original (Table 5.5), thus confirming the results of the first experiments. Cytometry data were used to evaluate the cause for increase in lipid productivity at cellular level. Flow cytometry data from the cells at the end of the cultivation corroborate the previous results since we observe once again an increased median lipid fluorescence (BP) being the responsible variable that results in an increased BP/AF ratio (Figure 5.5B). Additionally, Figure 5.6 shows that S5 has a higher percentage of lipid-rich cells under similar conditions when compared with Wt. The amount of lipid-rich cells in S5 was 99% while in the original population it was 66% (arbitrarily chosen as cells with fluorescence signals above the half of the scale; numbers derived from the histograms on Figure 5.6). Added to that, biomass composition indicates that S5 has no alterations in the carbon partitioning between TAG and starch (Table 5.1 and Table 5.2), but only an doubled TAG yield on light when compared to the original population. Hence, the strategy here presented was successful in selecting microalgae cells with increased TAG yield without affecting the metabolism of other cellular components.

Table 5.2: Comparing kinetic parameters and biomass composition between original and S5 under indoor simulated Dutch summer conditions. The kinetic parameters are: specific growth rate (μ), biomass productivity (Px), TAG productivity (Ptag) and TAG yield (Y_{TAG}). All analyzed biomass components are expressed as relative to biomass dry weight (g/g/ DW).

Populations	**μ (d^{-1})**	**P_X ($g\ L^{-1}\ d^{-1}$)**	**P_{TAG} ($g\ L^{-1}\ d^{-1}$)**	**Y_{TAG} ($g\ mol^{-1}$)**
Original	0.52±0.08	1.03±0.19	0.2±0.02	0.16±0.01
S5	0.48±0.03	1.08±0.08	0.4±0.06	0.32±0.03
	Starch (g/g)	**Carbs (g/g)**	**Polar lipids (g/g)**	**TAG (g/g)**
Original	0.25±0.04	0.20±0.04	0.07±0.01	0.21±0.02
S5	0.29±0.01	0.19±0.05	0.06±0.01	0.30±0.04

The results from our experiments were compared with other researches with batch-wise TAG production. A review of TAG production is given by Benvenuti et al. (2016)[93], comparing different microalgae strains using the yields of TAG on light to compensate for different growth/stress conditions. We calculated the TAG yields on light of both original and S5 as being 0.16 and 0.32 g mol^{-1}, respectively (under simulated summer conditions). First it is important to highlight that original *Chlorococcum littorale* showed an TAG yield close to other high-lipid microalgae, such as: *Scenedesmus obliquus*; 0.22 g mol^{-1}; *Nannochloropsis oculat*a, 0.17 g mol^{-1}; *Chlorella zofingiensis*, 0.19 g mol^{-1} and *Nannochloropsis sp*., 0.14 g mol^{-1} [73,94,47]. The work of Breuer et al., (2014)[73] also presents the TAG yield of an starchless mutant of *Scenedesmus obliquus* at 0.37 g mol^{-1}, close to the yields measured for the S5 in the current work (0.32 g mol^{-1}).

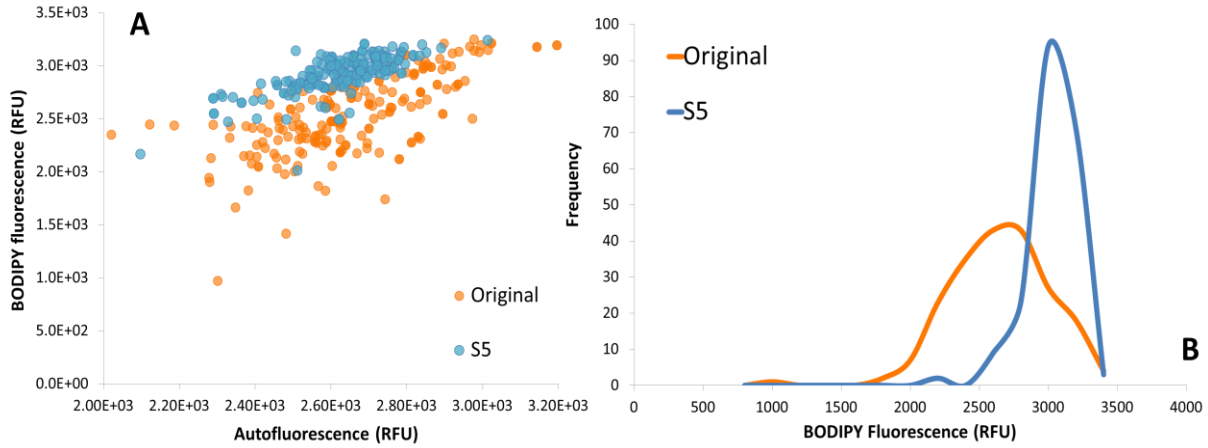

Figure 5.6: S5 population has a higher percentage of lipid-rich cells than the original population. Graph A shows a scatter-plot between autofluorescence and Bodipy fluorescence at the end of the N-runout. Each dot represents one-cell measurement. Graph B shows the distribution of frequency of Bodipy-fluorescence of both original and S5. In both graphs a total number of 500 cells were analyzed per sample.

5.4. Final remarks

In the present work we presented an approach to select microalgae cells with increased lipid productivity under N-starvation. Our approach was successful because we successfully selected new cell lines with increased lipid content (under N-starvation) with no effect on growth (N supplied), resulting in progressive improved TAG productivities. S5, sorted after 5 cycles of starvation-sorting, showed 1.9x higher TAG productivity than the Wt. Hence, S5 and original were compared under simulated summer conditions in a flat-panel photobioreactor. The results from comparing S5 and original confirmed the results of the first experiment: S5 showed an 2x higher TAG productivity (from 0.2 to 0.4 g L^{-1} d^{-1}) because we have removed cells with low TAG yield (on light) in comparison to Wt. The experiments comparing S5 and original were done 1.5 year after the sorting, therefore indicating a stable phenotype. S5 showed superior TAG yields on light when compared with other Wt-high-lipid green microalgae (0.32 against 0.16-0.20 g mol^{-1}), being comparable to the highest yield registered with a starchless mutant (0.32 against 0.37 g mol^{-1}). Biomass composition indicates that S5 has no alterations in the carbon partitioning between TAG and starch, but only an doubled TAG yield on light when compared to the original population. All combined, our results present a successful strategy to improve the TAG productivity of *Chlorococcum littorale*, without resourcing to genetic manipulation or random mutagenesis. Additionally, the improved TAG productivity of S5 was confirmed under simulated summer conditions, highlighting the industrial potential of S5 for microalgal TAG production.

Outdoor performance of *Chlorococcum littorale* at different locations

This chapter has been submitted as: Cabanelas, Iago Teles Dominguez; Slegers, Petronella M; Böpple, Hanna; Kleinegris, Dorinde MM; Wijffels, René H; Barbosa, Maria J.

Highlights:

- Carbon partitioning (starch/TAG) of *C. littorale* Original and S5 under N-starvation
- Successful simulations confirmed doubled TAG yield of S5 compared to Original
- High irradiance locations show lower biomass yields on light compared to low irradiance
- TAG yields were not affected by location-dependent irradiance intensity

ABSTRACT:

Background: Our goal in the present study was to evaluate the potential for lipid production of two cell populations of the marine microalgae *Chlorococcum littorale* under different climate conditions. We have selected, in a previous study, a new cell population of *Chlorococcum littorale*, namely S5. S5 showed a stable doubled triacylglycerols (TAG) productivity in comparison with the original population. A previously developed model was expanded to include day:night cycles and validated to predict biomass and TAG productivities outdoors at different locations. Four different locations were chosen to simulate the response of *C. littorale* to different day lengths and light intensities (the Netherlands, Norway, Brazil and Spain).

Results: Indoor experiments (simulated summer) were carried out with Original and S5, confirming that both populations showed the same biomass productivity under growth conditions. However, S5 showed a doubled TAG productivity under N-starvation. A previously developed model was validated for *C. littorale* using the indoor experiments (Original and S5). Outdoor experiments with Original were used as input for the model to predict outdoor productivities. Finally, simulations of biomass and TAG productivities of Original and S5 at different locations were done. At locations with lower light intensities, Oslo and Wageningen, biomass productivities were higher than at locations with higher light intensities, Brazil/Spain. Such results might be associated with light-saturation effects. TAG productivities, however, showed no effect of local light intensity.

Conclusions: Locations at higher latitudes, Norway/Netherlands, cannot sustain microalgae phototrophic year-round production, which impacts the yearly average TAG productivities. Yearly average TAG productivities were doubled in Brazil/Spain when compared with Norway/Netherlands (from 1.4-1.6 to 3.0-3.2 g m^{-2} d^{-1}). Likewise, *C. littorale* S5 was simulated with doubled TAG productivities when compared with Original, at all locations (2.5-2.7 to 4.7–5.2 g m^{-2} d^{-1}, respectively). The present results confirm the industrial potential of *Chlorococcum littorale*, both original and S5, as a source of TAG. Furthermore, our results can be used for comparison and to estimate future production scenarios.

Key-words: microalgae; TAG; *Chlorococcum littorale*; strain improvement; model carbon partitioning; outdoor productivities; year round productivities

6.1. Background

Microalgae have been argued to be the next feedstock for energy, food and feed in the XXI century [70]. However, microalgae have high production costs, which makes production of microalgal biomass only economic feasible, to the present date, for high-value products, e.g. pigments, and food supplements [3,1]. Therefore, reducing production costs by increasing productivities are imperative, which can be achieved with a combination of strain improvement (biology) and reactor optimization (engineering) [1,95].

Our goal in the present study was to evaluate the potential of two cell populations of *Chlorococcum littorale* under different climate conditions. We have selected, in a previous study, a new cell population of *Chlorococcum littorale* using fluorescence activated cell sorting (FACS). This new population, namely S5, showed a stable doubled triacylglycerols (TAG) productivity in comparison with the original population due to an increased TAG content at the same growth rate. We can use models to estimate biomass and TAG productivities of both Original and S5 under controlled conditions. Models can further translate results from indoor and outdoor experiments at specific locations to different locations worldwide [96–98]

Modelling is a powerful tool to evaluate the potential of different variables on microalgae growth and metabolism [97–100]. A few models have been developed for microalgae, mostly describing biomass productivity as a function of light intensity [98,101,102]. The limitation of these models is that the concentration of intracellular components, neither the cellular response under starvation conditions, is described. Since it is known that green microalgae accumulate carbon storage compounds under N-starvation [88,103], we require a model that describes the carbon partitioning after N-starvation (i.e. the fate of the photosynthetically absorbed energy inside the cells after nitrogen is depleted). This carbon partitioning has been described and modelled for the green microalgae *Scenedesmus obliquus* under continuous light (both wildtype and a starchless mutant) [99]. This model can describe the dynamics between intracellular starch and TAG production rates of *Scenedesmus obliquus*, allowing estimations of productivities under different light intensities. Adaptations needed to be made in the model to include a day:night cycle to estimate more realistic scenario. Finally, we used this model to describe TAG and biomass productivity in *Chlorococcum littorale* under different climate conditions.

First we evaluated the performance *Chlorococcum littorale* (Original and S5) under simulated Dutch summer conditions (laboratory scale). Second, we used the lab scale experiments to derive biological parameters to be used as model inputs, and we evaluated the model performance to simulate the indoor experimental data. Third, indoor results (and simulations) were compared with outdoor pilot-scale results (and simulations), to evaluate the predictability of the model to estimate outdoor productivities. Finally, the model was applied to simulate biomass and TAG productivities of *C. littorale* (Original and S5) at four different locations, with different day lengths and light intensities (the Netherlands, Norway, Brazil and Spain).

6.2. Model description

A mechanistic model was previously developed for the green microalgae *Scenedesmus obliquus.* The model estimates yields and productivities of intracellular components using the carbon partitioning towards carbohydrates and lipids under N-starvation and continuous light [99]. Carbon partitioning of green microalgae refers to the fate of the photosynthetically converted photon energy into the cell. We included a day:night cycle in the model, which required adaptations to account for night biomass losses (dark respiration). Microalgae under phototrophic growth need to respire part of their biomass to provide energy for maintenance (ms) during dark periods. To validate the model for *C. littorale* (Original and S5) input biological parameters were estimated. Briefly, the input parameters are growth rate, initial biomass composition, intracellular compounds production rates and biomass degradation rate. A full list of parameters and how they were calculated can be found at supplementary materials (section 6.7.1, Table S6.7.1). The experiments were done in flat panel photobioreactors under Dutch summer simulated conditions (section 6.2 of methods). Figure 6.1 describes the structure of the model, in which energy is first allocated to cover the maintenance requirements (ms). Once ms is covered two scenarios are distinguished: nitrogen is available (N+, growth phase) or not (N-, starvation phase).

Under N+ conditions the photosynthetic energy is first used to cover ms and is then directed to build functional biomass (X, Figure 6.1). Functional biomass (X) accounts for biomass produced until nitrogen depletion, including biomass constituents as starch, TAGs and carbohydrates (non-starch). Under N- conditions the photosynthetic energy, after covering ms, is used to produce carbon derived compounds. First a fixed amount of CHO (structural carbohydrates, non-starch) is produced. This amount is assumed to be constant throughout the starvation period. Following, the available energy is used to produce STA (starch) and TAG. The model also accounts for conversion from STA to TAG. Additionally, STA is used as an energy source to cover maintenance during dark periods. Hence, a fraction of STA in the biomass is used for dark respiration; arrow STA →ms on Figure 6.1. The model accounts for respiration of STA in functional biomass (X) to cover maintenance if all STA produced under N- conditions is respired (arrow X → ms on Figure 6.1; conditions not found in the current research).

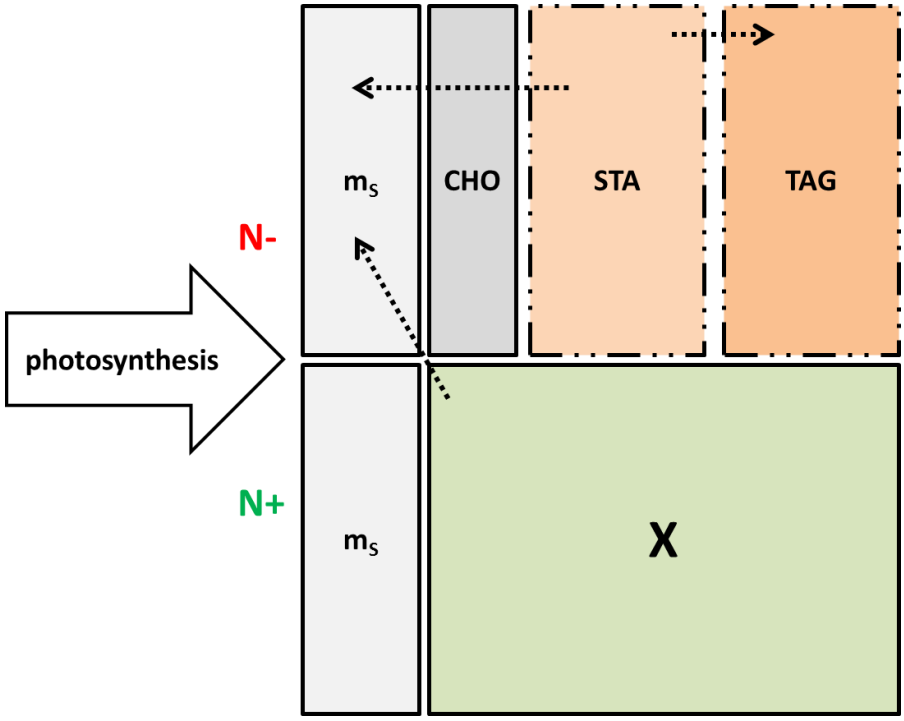

Figure 6.1: Scheme of partitioning of photosynthetic energy which depends on extracellular nitrogen presence: N-replete (N+) and N-deplete (N-) scenarios. Maintenance requirements (ms) are firstly covered by the energy photosynthesis. In dark respiration ms energy is covered by starch (STA) degradation (STA → ms). During N-depletion, accumulation of carbohydrates (CHO, non-including starch) takes place and once produced it is assumed constant. After CHO is produced, cells will accumulate TAG and STA as storage compounds. The model also describes conversion from STA to TAG (STA → TAG). If there is no accumulated STA available, ms will be covered from the starch fraction of the functional biomass X (X → ms), which was produced previously when N was available.

6.3. Results and discussion

6.3.1. Comparing indoor and simulated performances of Original and S5

Indoor experiments were carried out with Original and S5 to compare the performance of both populations. Secondly, the experiments were used to derive the biological parameters necessary to model productivities. Original and S5 were cultivated in a N-runout batch, which means that functional biomass was produced up to the time point at which N was depleted from the growth medium (green area, Figure 6.2). Both growth rate and biomass productivity showed no differences between Original and S5 in this period (Table 6.1). After all nitrogen was consumed by the cells (green area, Figure 6.2), starch and TAG are produced as a known biological response of microalgae to N-starvation [29,94]. During N-starvation, S5 showed an increased biomass accumulation in comparison with Original (maximum biomass concentration 7.7 g L^{-1} against 4.6 g L^{-1} from Original, Table 6.1), which was accounted for by an increased TAG content (0.30 g g^{-1} against 0.21 g g^{-1} from Original, Table 6.1).

Table 6.1 also provides a comparison of TAG productivities and yields between Original and S5. The average TAG productivity ($P_{TAG,ave}$), which considers the entire N-starvation period of 7 days was 1.9x higher in S5 in comparison with Original. The maximum time average productivity ($P_{TAGmax,time,ave}$) is calculated considering only the period of starvation in which maximum TAG daily productivity takes place. For both Original and S5 the $P_{TAGmax,time,ave}$ was measured 48h after N-starvation, confirming a 1.9x higher performance by S5 (Table 6.1). These results showed the industrial potential of S5 for TAG production, since this cell population has been developed 1.5 years before the current experiments, highlighting a stable phenotype.

The experimental data presented above were used to calculate the necessary input parameters for the model simulations. The mechanistic model [99] had to be validated for *C. littorale* under simulated Dutch summer conditions, as it was originally developed for *S. obliquus* under continuous light. The model was modified to include a day night cycle, which requires inclusion of dark respiration (night biomass losses, NBL). Dark respiration means that part of the biomass that was produced during the day is used during dark periods to cover maintenance [104,105]. Average night biomass losses (NBL_{ave}) were calculated for Original and S5 accounting the whole period of N-starvation. Both Original and S5 showed similar rates of NBL_{ave} (0.25 and 0.23 g_{Cx} L^{-1} $night^{-1}$ respectively, Table 6.1). According to experimental data only starch is degraded during night to cover maintenance requirements of both Original and S5 (and simulated data follows closely). This conclusion can be derived from the average starch night respiration (SNR), which presented similar values and the NBL (0.20 g_{STA} L^{-1} $night^{-1}$ for Original and 0.23 g_{STA} L^{-1} $night^{-1}$ for S5, Table 6.1).

Table 6.1: Overview of growth parameters, biomass and TAG productivities, yields of biomass and TAG on photons for indoor experiments with Original and S5 under simulated Dutch summer conditions, and of outdoor experiment with Original. Results are derived from 2 biological replicates. Standard deviations were not shown because all were below 5% variation from the mean, with the exception of starch for outdoors (13%).

	Unit	Time frame	Indoor (Original)	Indoor (S5)	Outdoor (Original)
PFD	mol m^{-2} d^{-1}		55.0	55.0	30.1
Biomass production (Cx)	g_{Cx} L^{-1}	Final day	4.65	7.71	4.28
Growth rate (μ)	d^{-1}	$t_0 - t_{N=0}$	0.69	0.72	0.45
Biomass productivity (Px)	g_{Cx} L^{-1} d^{-1}	$t_0 - t_{N=0}$	1.04	1.09	0.64
Biomass areal productivity ($P_{X,\ area}$)	g_{Cx} m^{-2} d^{-1}	$t_0 - t_{N=0}$	23.4	24.5	12.5
Biomass yield ($Y_{cx,ph}$)	g_{Cx} mol^{-1}	$t_0 - t_{N=0}$	0.43	0.45	0.42
Night biomass losses, average (NBL_{ave})	g_{Cx} L^{-1} $night^{-1}$	N-starvation period	0.25	0.23	0.42
Starch night respiration ($SNR_{,ave}$)	g^{-1}_{STA} L^{-1} $night^{-1}$	N-starvation period	0.20	0.23	0.19
TAG average productivity ($P_{TAG,ave}$)	g L^{-1} d^{-1}	N-starvation period	0.17	0.32	0.08
Max time average TAG productivity $P_{TAG\ max\ time\ ave}$	g L^{-1} d^{-1}	48h after start of N-starvation (indoor), between t=3 to t=6 (outdoor)	0.21	0.4	0.14
TAG yield ($Y_{TAG,ph}$) Max time average	g_{TAG} mol^{-1}		0.09	0.16	0.09
TAG areal productivity, maximum time average ($P_{TAG,area,\ max,\ ave}$)	g_{TAG} m^{-2} d^{-1}		4.72	9.00	2.74
TAG	g g^{-1}_{Cx}	End of N-starvation	0.21	0.30	0.15
STA	g g^{-1}_{Cx}	End of N-starvation	0.25	0.29	0.18
CHO	g g^{-1}_{Cx}	End of N-starvation	0.20	0.19	0.28

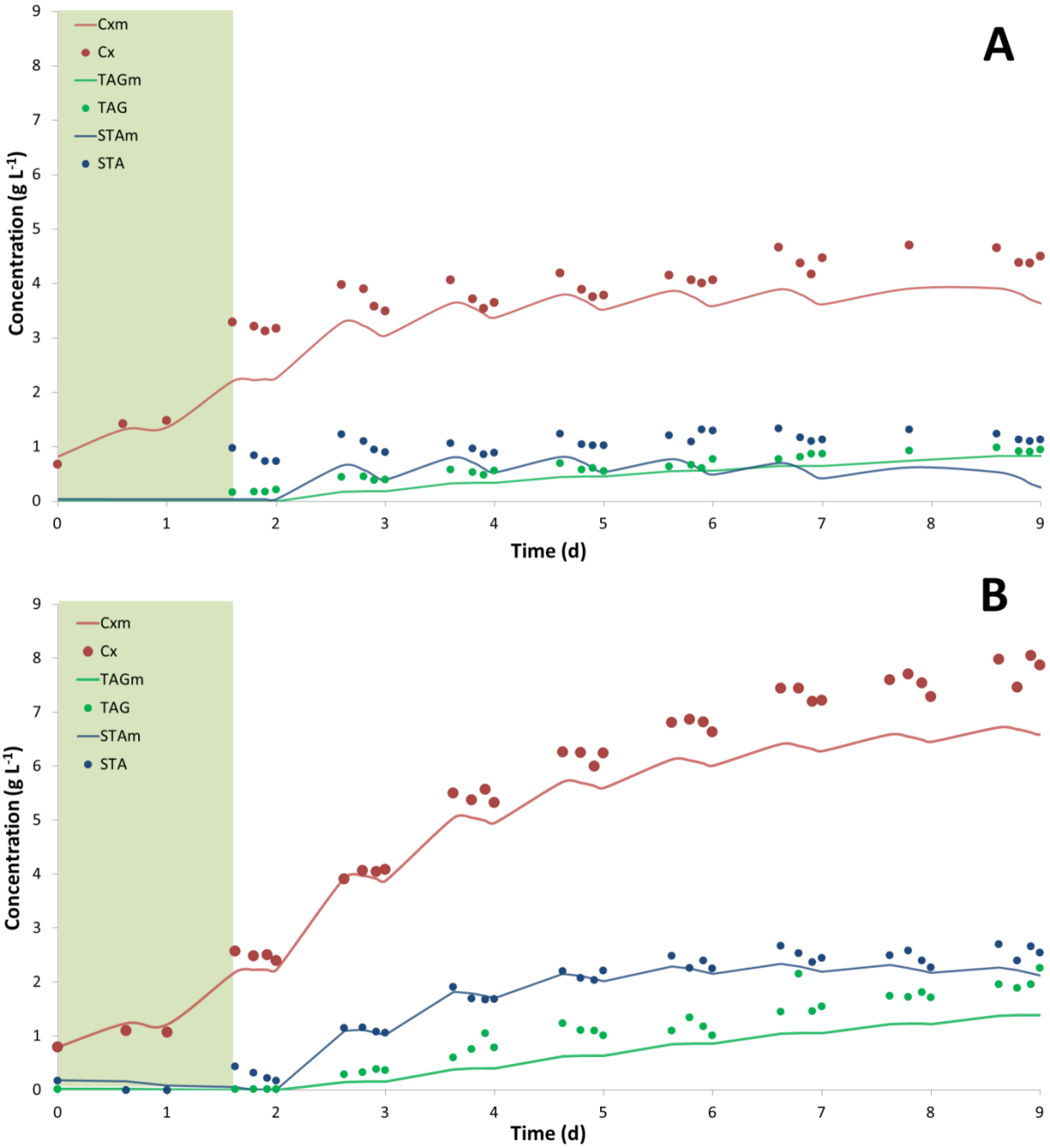

Figure 6.2: Concentration of biomass (cx), starch (STA) and triacylglycerides (TAG) for both original (A) and S5 (B). Symbols represent the experimentally obtained values, while the lines represent model simulation results. The green area represents the period of the cultivation in which nitrogen was available, i.e. the growth phase (N+ phase). From day 1.7 onward it is considered as nitrogen starvation phase (N-starvation).

The modelled data generally followed the trends of the experimental data (concentrations of biomass, TAG and starch, g L^{-1}, Figure 6.2). Extracellular nitrogen concentration (mg L^{-1}) was accurately simulated, since both experimental and modelled mark the start of the N-depletion phase at the same time point (green area, Figure 6.3). For both Original and S5 simulated biomass concentration is underestimated during N-starvation, which can be related to the underestimation of TAG concentrations also during the N-starvation phase (Figure 6.2). Starch concentrations, however, followed closely the experimental data including the night respiration of biomass (Figure 6.2). Additionally, the confidence intervals (CI) between simulated and experimentally measured data were calculated for biomass, TAG and STA concentrations (both Original and S5; figures S6.7.2, S6.7.3 and S6.7.4, supplementary materials). For all parameters almost all data points fell within the confidence intervals, with biomass and TAG concentrations showing higher accuracy than starch.

Chlorococcum littorale respires only starch during night to cover maintenance requirements, which is understandable considering the higher energy yield (on ATP) of starch in comparison with TAGs [106]. Such results have industrial implications when aiming to produce TAGs from *C. littorale* since no TAG respiration was observed in the current research, indicating the potential of both Original and S5 for TAG production under real light conditions. *C. littorale* Original is already among the most productive strains in the literature, for both biomass and TAG [35,107,108]. Recent studies register an areal TAG productivity of *Nannochloropsis* sp. (one of the most studied strains for TAG production) between 2.0 to 6.5 g_{TAG} m^{-2} d^{-1}, considering indoor and outdoor experiments [109–112]. *C. littorale* S5 showed the same biomass productivity as Original, but a 2-fold increased TAG productivity (S5: 9.0 g against Original: 4.7 g_{TAG} m^{-2} d^{-1}). The doubled TAG productivity of S5 makes it competitive for TAG production. In summary, we conclude that the model was validated for *C. littorale* using experiments under simulated summer conditions, which gives the possibility to estimate the performance under outdoors conditions. We also highlight that *Chlorococcum littorale* S5 showed indoor TAG productivities above the values reported to the most productive strain in literature. Furthermore, simulations indicate the potential of S5 to be produced at industrial scale.

6.3.2. Comparing simulations from indoor to outdoor

Results of the outdoor run with the wildtype of *Chlorococcum littorale* were used to estimate the parameters required to run simulations of biomass, TAG and starch concentrations (Figure 6.3). In figure 6.3 it is possible to see that, like the indoor experiments, the simulated data for the outdoor run also generally followed the experimental data. Differently from the indoor experiments, under outdoor conditions the amount of light available varies on a daily basis, causing a variability to the data set, decreasing the accuracy of the simulations. Both biomass and TAG concentrations showed acceptable confidence intervals, while starch showed much higher intervals (Figure S6.7.2-6.7.3, sup materials). These results are nevertheless remarkable considering that the model simulated a flat panel (2 cm depth reactor), while the experiments outdoors were carried out in a tubular pilot reactor (tubes diameter 5 cm). One explanation could be that the combination of biomass concentration and light intensity outdoors were close

to the optimum for *C. littorale*. The biomass concentration in the outdoor experiments was chosen considering the indoor experiments, to keep both experimental conditions comparable.

Chlorococcum littorale, in outdoors experiments, required twice the time (3 days, compared with 1.7 from indoor) to consume all extracellular nitrogen when compared with indoors experiment (i.e. growth phase, N+ phase, Figure 6.3). This resulted in a lower growth rate when compared with indoor experiments (from 0.65 indoor to 0.45 outdoor). The same interval (day 0 to day 3) was used to estimate the average biomass productivity outdoors, which was lower than under indoors conditions (0.64 against 1.04 g L^{-1} d^{-1}, Table 6.1). Such result was expected due to a lower light intensity outdoors (30 against 55 mol m^{-2} d^{-1}, Table 6.1). The same applies for TAG productivity, which was 0.14 g L^{-1} d^{-1} outdoors, against 0.21 g L^{-1} d^{-1} indoors ($P_{TAGmax,time,ave}$,Table 6.1). However, when comparing yields on light energy (g biomass/TAG per mol light), the values were the same. The comparison of the yields was done using the equivalent time intervals, which confirms that the biological functions responded similarly during indoors and outdoors cultivation.

Average night biomass losses (NBL_{ave}) under outdoor conditions were higher than under indoor conditions (0.42 against 0.23 g_{Cx} L^{-1} $night^{-1}$, Table 6.1). Differently from indoor, under outdoor conditions the NBL_{ave} could not be solely attributed to starch degradation (0.19 g_{STA} L^{-1} $night^{-1}$, table 6.1) and neither to any of the other analyzed biomass components (carbohydrates, TAGs and polar lipids all showed no night degradation). Additionally, lower biomass concentrations were achieved outdoors (4.28 against 4.65 g_{Cx} L^{-1} indoors, Table 6.1), hence It can be hypothesized that part of produced biomass (whole cells) are respired under outdoors conditions. The higher maintenance determined outdoor in comparison with indoors also corroborates this finding (Table S6.1, sup materials). The higher outdoor maintenance (ms) could be a consequence of more dark zones in the horizontal tubular reactor when compared with the flat panel (indoor). The reactor used in the outdoors experiment was a horizontal tubular reactor with 0.05m diameter tubes (section Experimental set-up, materials and methods), different from the 0.02m light path flat panel reactor used for the indoors experiments. This difference in design can explain the higher respiration rate, which can explain the increase in the measured maintenance (ms) [2,98].

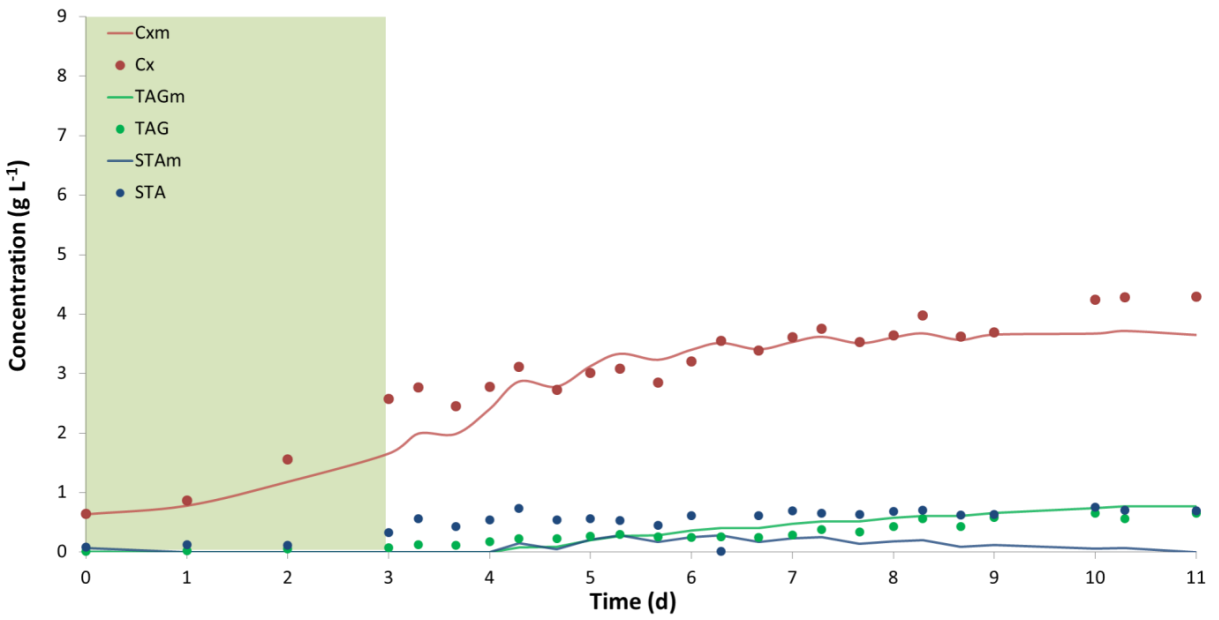

Figure 6.3: Concentration of biomass (Cx), starch (STA) and triacylglycerides (TAG) for the outdoors experiments with Original. Symbols represent the experimentally obtained values, while the lines represent model simulations. The green area represents the period of the cultivation in which nitrogen was available, i.e. the growth phase (N+ phase). From day 3 onward it is considered nitrogen starvation phase (N- phase).

An important factor that the model does not incorporate is the influence of temperature. The outdoor runs were carried out in a system with temperature control, but that showed limited capacity during peaks of high light intensity days with high temperature. Maximum temperatures of 32 °C with an average 6-9 h above 30° C each day (data not shown) have been reached. Chihara et al. (1994)[39] reported sub-optimal temperature above 28° C for *C. littorale*, which might have had a negative impact on biomass and TAG yields in the present study. This could explain why the model underestimated biomass production, because the effect of temperature fluctuation during the day is not included in the model (the model assumes controlled temperature) (Figure 6.3).

The simulated productivities under outdoor conditions are in the range of what has been registered for other strains and other climate conditions. In the current research, the maximum time-averaged TAG yield reached in outdoor experiments with *C. littorale* was 0.09 g_{TAG}/mol. The maximum TAG yields reported by Benvenuti et al. (2015) [109] with *Nannochloropsis sp*. cultivated in the same horizontal tubular reactors and using the same strategy (nitrogen runout batch) as in this work, were 0.06-0.09 g_{TAG} mol^{-1} photons (depending on initial biomass concentration) . Similarly, another research with *Nannochloropsis sp*. also registered a outdoors TAG yield on light of 0.06 g_{TAG} mol^{-1} [110]. These results highlight the industrial potential of *Chlorococcum littorale*, once it sustains similar yields as the most commonly used strain in literature. The doubled TAG productivity of S5 indicates the potential of this cell population to outcompete the most productive strains available.

The mechanistic model was validated for *C. littorale*, Original and S5 under indoors conditions. Simulations of indoor experiments followed closely the measured data, although with biomass and TAG slightly underestimated. The simulations of the outdoor experiments followed similar trends as the experimental data despite limitations to calibrate this model to different reactor design. The results are yet remarkable, considering the differences of reactor design between indoor and outdoor experiments. The biomass concentration during outdoor experiments was chosen to keep both experimental conditions comparable, which guaranteed that the described biological parameters could be used to simulate production. Further implementation of light use, correcting for the reflection angles on the surface of tubular reactors, could make the prediction of outdoor data more accurate in the future [98]. The yields of biomass and TAG on light, however, were similar for the indoor and outdoor experiments highlighting that the biological mechanism for biomass and TAG production were similar. This finding indicates the potential of the model validated with indoors simulations to estimate outdoors performance.

6.3.3. *C. littorale* productivities under different locations

After validation of the model for simulations on *C. littorale*, the potential for cultivation under different light regimes was tested. Hence, the biological parameters and growth conditions from indoor experiments were used to simulate the productivities of both Original and S5. The biological parameters were combined with the light values (light intensity and day length) at 4 different locations: Wageningen (the Netherlands), Oslo (Norway), Rio de Janeiro (Brazil) and Cádiz (Spain).

The simulations considered the average total daily light impinging on ground area and the duration of the day to simulate batch N-runout cultivations of *C. littorale* Original and S5. Figure 6.4 shows the average light intensity for each location (photon flux density, PFD; mol m^{-2} d^{-1}), in comparison with the indoors experiments. In figure 6.4 the amount of running months per year is also depicted, showing that while Cádiz and Rio de Janeiro can sustain year-round phototrophic microalgae production, Oslo and Wageningen were assumed to run phototrophic production from April until September (most sunny months). Accumulation of TAG and starch after nitrogen depletion depend on photosynthesis rate of each location. Hence, the yields of both biomass and TAG are solely dependent on light intensity and duration of the day.

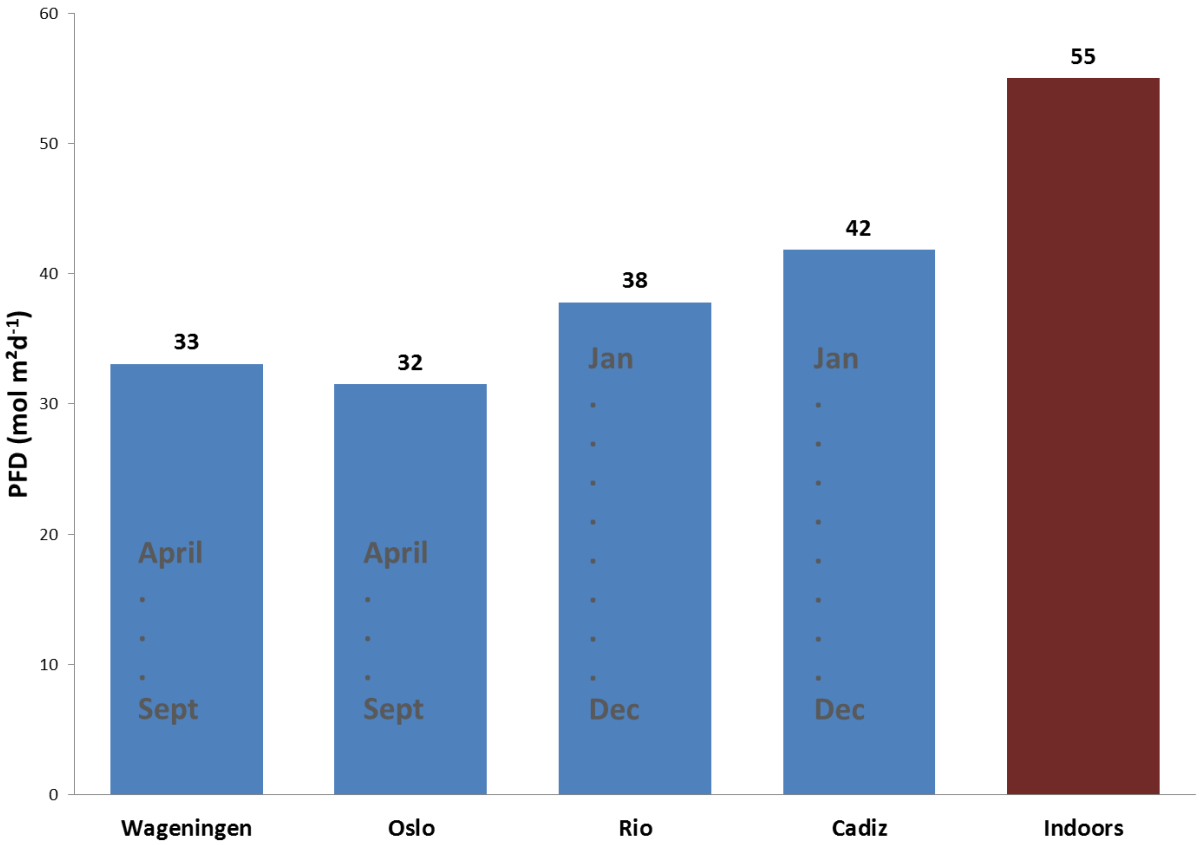

Figure 6.4: Photon flux density (PFD, mol m^{-2} d^{-1} for the locations Wageningen, Oslo, Rio and Cadiz as well as for the indoor experiments simulating a Dutch summer day). Wageningen and Oslo are averages for the cultivation period from April to September, while an average PFD of the whole year are shown for Rio and Cádiz. Details on the acquisition and calculation of light intensities are available in materials and methods. The different periods of production for Oslo/Wageningen impacted the year-round productivities, because the total amount of production days for Oslo/Wageningen was 150/year, while for Rio/Cádiz it was 300/year.

Table 6.2 summarizes the results of the simulations of biomass and TAG productivities at different locations. At locations with lower light intensities, Oslo and Wageningen, growth rates (μ) and biomass productivities (P_{Cx}) were higher (μ= 0.6 and P_{Cx}= 0.70-0.74 g_{Cx} L^{-1} d^{-1}) than at locations with higher light intensities, Rio de Janeiro and Cádiz (μ= 0.46 and P_{Cx}= 0.58-0.60 g_{Cx} L^{-1} d^{-1}). Such results might be associated with light-saturation effects, since most marine algae saturate at the peak hours of light intensity during the day, hence just a fraction of received irradiance is actually utilized for photosynthesis [2,92,113]. Additionally, Kurano & Miyachi (2005)[114] observed light saturation for *C. littorale* at light intensities above 300 μmol m^{-2} s^{-1}, which might explain why large increases in irradiance did not lead to increase in biomass productivities. This assumption can be corroborated comparing biomass yields on light of *C. littorale* Original between simulations and the outdoors experiments carried out in Wageningen (Table 6.1). This comparison shows that for Oslo/Wageningen slightly higher biomass yields were observed (0.42 g_{Cx} mol^{-1} outdoor experiment (Original, Table 6.1), 0.48/0.53 g_{Cx} mol^{-1} for Oslo/Wageningen, Table 6.2), than for Cádiz/Rio (0.32/0.36 g_{Cx} mol^{-1} , Table 6.2). The same trend was observed when comparing outdoors data from Wageningen with the simulations for *C. littorale* S5.

Table 6.2: Simulated of growth parameters, biomass and TAG productivities, yields of biomass and TAG on photons for both Original and S5, at four different locations worldwide. Yearly daily TAG productivity was calculated multiplying the maximal areal productivity (PTAG, yearly average areal productivity, g m^{-2} d^{-1}) by the amount of production days and further dividing by the days of the year (150 production days at Oslo/Wageningen and 300 days at Rio/Cádiz; for all cases the final result was divided by 365, thus normalizing the measurement.

		Oslo		Wageningen		Rio de Janeiro		Cadiz	
Parameters	**Units**	**Original**	**S5**	**Original**	**S5**	**Original**	**S5**	**Original**	**S5**
day length	h	16,45		15,17		11,98		12,03	
Photon flux density (PFD)	mol $m^{-2}d^{-1}$	31,51		33,07		37,77		41,83	
Growth phase	days	1,69	1,79	1,64	1,81	2,41	2,40	2,41	2,40
Growth rate (μ)	d^{-1}	0,62	0,53	0,61	0,50	0,46	0,46	0,47	0,46
Biomass productivity (P_{Cx})	g_{Cx} L^{-1} d^{-1}	0,74	0,71	0,70	0,64	0,58	0,67	0,60	0,67
Biomass areal productivity ($P_{Cx,\ areal}$)	g_{Cx} m^{-2} d^{-1}	16,6	15,9	15,7	14,4	13,05	15,08	13,50	15,08
Biomass $yield_{Cx}$ (Y_{Cx})	g_{Cx} mol^{-1}	0,53	0,51	0,48	0,44	0,34	0,40	0,32	0,36
P_{TAG}, ave (From t_2 to t_f)	g L^{-1} d^{-1}	0,11	0,17	0,12	0,17	0,14	0,18	0,14	0,18
P_{TAG}, max time ave (From t_2 to t_4)	g L^{-1} d^{-1}	0,14	0,22	0,15	0,22	0,17	0,23	0,18	0,23
TAG yield, max time ave ($Yield_{TAG}$)	g L^{-1} d^{-1}	0,10	0,15	0,10	0,15	0,10	0,13	0,10	0,12
P_{TAG}, max areal time ave	g m^{-2} d^{-1}	3,15	4,95	3,38	4,95	3,83	5,18	4,05	5,18
$P_{TAG,yearly\ area}$	g m^{-2} y^{-1}	473	743	506	743	1148	1553	1215	1553
P_{TAG}, Yearly average areal daily productivity	g m^{-2} d^{-1}	1,29	2,03	1,39	2,03	3,14	4,25	3,33	4,25

TAG productivities showed a different trend when compared with biomass productivities, for both Original and S5. No effect of local light intensity was observed on TAG productivity or Yields (Table 6.2). This result makes sense since the light intensities used for the simulations at all locations are all below what has been experimentally used in the current research (Figure 6.4). Additionally, the amount of light used in indoor experiments didn't show any measurable negative effect during N-starvation, since no negative yield was observed during N-starvation. Some algae strains show a considerable reduction in photosynthetic activity during N-starvation, but *C. littorale* has been chosen for the current research exactly for its resilience under N-starvation [109,115]. Furthermore, we would like to highlight that the yields simulated for other climate conditions (Table 6.2) are similar to the yields calculated for indoors experiments (both Original and S5, Table 6.1) and also for the outdoors experiment (for Original only, Table 6.1). Simulated TAG areal productivities (P_{TAG}, max areal time ave, Table 6.2) under different locations were between 3.1 and 4.0 $g_{TAG}\ m^{-2}\ d^{-1}$ for Original and between 4.9 and 5.2 $g_{TAG}\ m^{-2}\ d^{-1}$ for S5. Such values are in the same order as the values reported for the genus *Nannochloropsis* (2.0 to 5.2 $g_{TAG}\ m^{-2}\ d^{-1}$) under indoor and outdoor conditions [109–112]. The same research also reports no effect of different total irradiance (outdoors) on lipid yields [109]. Hence, for biomass production of *Chlorococcum littorale* photo-saturation might reduce the yields of biomass on photons under higher light intensities. On the other hand, for TAG accumulation such effect might not be seen, as long as light intensity is kept below the threshold of photo-damage.

Although no differences were observed among the simulated TAG productivities under different locations, attention should be paid when extrapolating the results to year-round projections. We reported the yearly average TAG productivities, which were calculated by multiplying the daily areal productivity by the amount of running days per year (150 for Oslo/Wageningen and 300 for Rio/Cádiz). Since the locations have different production periods, the yearly average TAG productivities were normalized by the amount of days per year, allowing comparison. Yearly average TAG productivities of 1.4-1.6 $g\ m^{-2}\ d^{-1}$ were simulated for *C. littorale* Original at Oslo/Wageningen, and 3.0-3.2 $g\ m^{-2}\ d^{-1}$ were simulated at Rio/Cádiz, hence doubling the year-round production. Likewise, *C. littorale* S5 was simulated with increased TAG productivities at all locations, increasing to 2.5-2.7 $g\ m^{-2}\ d^{-1}$ at Oslo/Wageningen and to 4.7–5.2 $g\ m^{-2}\ d^{-1}$ at Rio/Cádiz. Locations at higher latitudes (e.g. Wageningen and Oslo) can sustain microalgae phototrophic production during spring and summer, but not year-round production. We demonstrated that *C. littorale*, Original and S5, are competitive strains to produce biomass at large scale, competing with commonly used strains. S5, however, showed similar TAG productivities as *Nannochloropsis sp.*, with the potential to outcompete it. In summary, we believe that the estimated productivities can be used for comparison purposes and for future production scenarios.

6.4. Conclusions

We validated a model to predict biomass and TAG productivities of *Chlorococcum littorale* under summer conditions. The validation was done for *C. littorale* Original strain and for S5, a selected cell population with doubled TAG productivity. The simulations of outdoor experiments (with Original) followed the experimental data and the yields of biomass and TAG were similar to indoor experiments. Therefore, the model can be used to estimate biomass and TAG productivities under different climate conditions. Simulations of productivities under different locations showed that biomass yield was higher at locations with lower light intensity. TAG yields, however, showed no effect of local light intensity. Yearly average TAG productivities were estimated as 1.4-1.6 g m^{-2} d^{-1} for *C. littorale* Original at Norway/Netherlands, and 3.0 -3.2 g m^{-2} d^{-1} at Brazil/Spain. *C. littorale* S5 was simulated with increased TAG productivities at all locations, increasing to 2.5-2.7 g m^{-2} d^{-1} at Norway/Netherlands and to 4.7 – 5.2 g m^{-2} d^{-1} at Brazil/Spain. We demonstrated that *C. littorale*, Original and S5, are competitive strains to produce biomass at large scale, competing with commonly used strains. S5, however, showed similar TAG productivities as *Nannochloropsis sp.*, with the potential to outcompete it. In summary, we believe that the provided productivities can be used for comparison purposes and to estimate future production scenarios.

6.5. Materials and methods

6.5.1. Inoculum preparation

Two cell populations of *Chlorococcum littorale* were used: Original (NBRC 102761) and S5, which is a new cell line developed by us in a previous research (submitted for publication, chapter 5). S5 was developed using cell sorting (FACS), hence selecting cells with a specific phenotype (doubled lipid productivity) to make a separate new population. The phenotype of S5 is stable 1.5 years after the selection and more details can be found in the previous publication (Chapter 5). Inocula from both populations were prepared from samples conserved in petri dishes containing growth medium and agar (12 g l^{-1}). Homogenous aliquots from biomass were taken from petri dishes and transferred to 200 ml sterile borosilicate Erlenmeyer flasks, containing 100 ml of sterile artificial seawater medium. Artificial seawater had the following composition (g l^{-1}): NaCl 24.55, $MgSO_4 \cdot 7H_2O$ 6.60, $MgCl_2 \cdot 6H_2O$ 5.60, $CaCl_2 \cdot 2H_2O$ 1.50, $NaNO_3$ 1.70, HEPES 11.92, $NaHCO_3$ 0.84, EDTA-Fe(III) 4.28, K_2HPO_4 0.13, KH_2PO_4 0.04. The medium contained also trace elements (mg l^{-1}): $Na_2EDTA \cdot 2H_2O$ 0.19, $ZnSO_4 \cdot 7H_2O$ 0.022, $CoCl \cdot 6H_2O$ 0.01, $MnCl_2 \cdot 2H_2O$ 0.148, $Na_2MoO_4 \cdot 2H_2O$ 0.06, $CuSO_4 \cdot 5H_2O$ 0.01.

6.5.2. Experimental set-up

To compare both Original and S5 and to validate the previously developed model to *C. littorale*, simulated Dutch summer conditions were used in a lab-scale flat-panel photobioreactor. The simulated Dutch summer consisted of day length of 16 hours and light supplied with a sinus function with a solar noon at 1500 µmols m^{-2} s^{-1} (resulting in an average daily incident light intensity of 636 µmols m^{-2} s^{-1}). The flat panel reactor had a working volume of 1.9 L, light path of 0.02 m, and 0.08 m^{-2} illuminated surface area (Labfors, Infors HT, 2010), reactor's details available at Breuer et al., (2014) [73]. Air flow was set at 1.0 L min^{-1} and air was mixed with CO_2, on demand, to automatically adjust pH at 7.0. Temperature was controlled with an integrated water-jacket at constant 25 ˚C.

The outdoor experiment was carried out with the Original in a 90 L horizontal tubular oriented reactor with a surface area of 4.6 m^{-2}, as described by Benvenuti et al., (2015) [109]. The system was inoculated to reach an initial biomass concentration of 0.4 g L^{-1} in N-free natural seawater (same media composition as in 5.1 section). Nitrogen ($N\text{-}NO_3$) was added after inoculation to achieve the desired concentration. The reactor was sterilized via addition of 5 ppm hypochlorite before starting a run. The 2 outdoors run were performed between August-September 2015 (with online measurements of temperature, light intensity, CO_2 and O_2 gas flow, turbidity and pH).

6.5.3. Daily measurements

For both indoors and outdoors experiments samples were taken ½ hour after sunrise and ½ hour before sunset, which gave us the evolution of biomass and its components due to photosynthetic activity. For the outdoors experiments another extra sample in the middle of the light period, at 14:00, was also taken. For the indoors experiments we wanted to do further investigation on night biomass losses, hence two samples were taken during dark periods, 2 hours and then 5 hours after sunset (which was feasible since at indoors scale it was possible to invert the clock of the reactor, allowing sampling of dark samples during afternoons). For the

outdoors experiments, biomass night respiration was measured with the difference between sunrise – sunset samples.

All samples were analyzed immediately after they were taken. Optical density (OD) of the algal culture was measured in a spectrophotometer (HACH, DR5000) at wavelengths of 680 nm and 750, which were proxies for chlorophyll and turbidity concentrations, respectively. Biomass production in the reactor was measured gravimetrically using GF/C Whatman filters (oven dried at 105°C, 24h). The Quantum Yield (QY) of photosystem II was determined in culture samples using a fluorometer (AquaPen-C AP-C 100, Photon System Instruments, Czech Republic), with the goal to assess the photosynthetic activity of cells throughout cultivation. Absorbance coefficient (α) was calculated using the culture absorbance spectrum, which was determined by a fibre optic spectrometer (AvaSpec-2048, Avantes BV, Apeldoorn, Netherlands; light source: AvaLight-Hal). The measurement (in g m^{-2}), is given by equation 1.

$$\alpha = \frac{\sum_{400}^{700} abs_{\lambda} \frac{\ln(10)}{z}}{300 \cdot c_{DW}} \qquad \textbf{Eq. 1}$$

with z: light path of the precision cell
c_{DW}: dry weight of the sample

Extracellular nitrogen content (N-NO_3, mg L^{-1}) was measured using samples of 1 ml algae suspension. Samples were centrifuged for 5 minutes at 13300 rpm (Micro Star 17R, VWR®) and the supernatant immediately measured with a nutrient analyzer (AQ2, SEAL Analytical Inc., USA) according to the NO_3 method by SEAL-Analytica.

6.5.4. Biomass analyses

The intracellular nitrogen concentration was determined from freeze-dried biomass samples via combustion followed by chromatography (Flash EA 2000 elemental analyser, ThermoFisher Scientific, USA). For analyses of biomass composition (expressed in g g DW^{-1}) freshly harvested samples were centrifuged twice and washed with MilliQ water (3134xg for 10 minutes at 4°C) and followed by freezing at -20°C and freeze-drying for 24 h. Triacylglycerols (TAGs) and polar lipids were extracted from the same samples and quantified using GC/MS column chromatography, as described by Breuer et al. (2013)[77]. Total carbohydrates were analyzed with the phenol-sulfuric acid method developed by Dubois et al., (1956)[90]. Total starch was analyzed with the colorimetric/enzymatic method from the commercial kit from Megazyme (K-STA kit, UK).

6.5.5. Calculations

The following calculations were not used as model input, but they were used to compare the results of experimental data (indoor and outdoor) with each other. Time intervals are indicated in the description of each equation to assist interpretation.

The specific growth rate (Eq. 2) was calculated as the change in biomass concentration (expressed as natural logarithm) as a function of time from inoculation until nitrogen starvation. Where: DW is dry weight of biomass (g L^{-1}), $t_{=0}$ stands for the start of the cultivation, while $t_{N=0}$ stands for the time in which N-NO_3 equals zero.

$$\mu = \frac{\ln(DW_{N=0} - DW_{t_0})}{t_{N=0} - t_0} \quad \textbf{Eq. 2}$$

Biomass productivity (P_{Cx}, Eq. 3) during growth phase was calculated as the change in biomass concentration (g L^{-1}) between inoculation and nitrogen starvation. Where: DW is dry weight of biomass (g L^{-1}), $t_{=0}$ stands for the start of the cultivation, while $t_{N=0}$ stands for the time in which N-NO_3 equals zero.

$$P_{cx} = \frac{DW_{N=0} - DW_{t_0}}{t_{N=0} - t_0} \quad \textbf{Eq. 3}$$

Average night Biomass Loss ($NBL_{,ave}$ in g_{Cx} L^{-1} night) was calculated as the difference of measured biomass (g L^{-1}) before and after each night period, followed by averaging over the nitrogen starvation cultivation period. Average starch night respiration ($SNR_{,ave}$) was calculated in the same way but using the starch concentration instead of biomass concentration.

Average TAG productivity (Eq. 4) was calculated as the change in TAG concentration (g L^{-1}) for the total N-starvation period (period indicated at Tables 6.1 and 6.2). Where: TAG stands for TAG concentration (g L^{-1}), the time frames N=0 indicates the start of the N-starvation period and t=f the end of the N-starvation period (end of cultivations).

$$P_{TAG,avg} = \frac{TAG_f - TAG_{N=0}}{t_f - t_{N=0}} \quad \textbf{Eq. 4}$$

The maximum time average TAG productivity ($P_{TAG,max}$, g L^{-1} d^{-1}) was calculated according to Eq. 4, with the exception that only the period from N-starvation (N=0) to the highest TAG productivity was accounted (Original and S5: day 2 to 4 ; Outdoor: day 3 to 6).

Maximum areal time average ($P_{TAG,max,areal}$, g m^{-2} d^{-1}) was calculated by multiplying the $P_{TAG,max}$ by the illuminated surface area of the reactors (0.08 m^{-2} for indoors and 4.6 m^{-2} for outdoors). For the indoor flat panels the illuminated surface refers to the area of the panel receiving light form one side (no loss is assumed since the reactor is covered to avoid light going out or in). For the outdoors systems we considered the ground area of the tubular, considering that the calculated light is measured as total amount of photons impinging on the surface (the space between tubes was neglected, as was calculated by Benvenuti et al. (2015) and de Vree et al. (2015) [109,116].

Yearly areal TAG productivity ($P_{TAG,yearly,areal,}$ g m^{-2} y^{-1}) was calculated by multiplying $P_{TAG,max}$ by the total amount of production days for each simulated locations: 150 days for Oslo/Wageningen and 300 for Rio/Cádiz.

Yearly average areal daily productivity ($PTAG_{,ave,daily,\ areal}$, g m^{-2} d^{-1}) was calculated dividing the $P_{TAG,yearly,areal}$ for each location by the amount of days per year (365), hence normalizing the productivities.

Biomass and TAG yields on light (g mol^{-1}) were calculated by division of the respective productivities (Eq. 2 and 3) by the corresponding total amount of light impinging on the reactor surface (indicated in Tables 6.1 and 6.2).

6.5.6. Data analyses

The sample standard deviation (SD) was calculated between the biological replicates for every estimated parameter. The estimated SDs were used to show the data variability between biological replicates for productivities and kinetic parameters (Table 6.4). The standard deviations were also used to estimate the 95% confidence intervals (with a two-tailed T-distribution) for every experimentally estimated parameter used to run model simulations (Supplementary materials, Table S6.7.1). These calculations were carried out with Microsoft Excel 2010.

The confidence intervals (as stated above) were used to evaluate goodness of fit between experimentally measured values and simulated values. As a result, the dot plots between experimentally measured values and simulated values show the upper and lower confidence intervals. This analysis was carried out at MATLAB R2015a (© 2016 The MathWorks, Inc.).

6.5.7. Outdoor climate data

Four different locations were chosen to simulate the potential of both *C. littorale* Original and S5, i.e. Wageningen (the Netherlands), Oslo (Norway), Rio de Janeiro (Brazil) and Cádiz (Spain). These locations were chosen to simulate the response of *C. littorale* to different day lengths and light intensities. Locations at higher latitudes, Oslo and Wageningen, cannot sustain year-round phototrophic microalgae production. Hence, for Oslo and Wageningen cultivation periods from April to September were considered. The yearly average light intensity and day length for each location were estimated and are presented in Table 6.2 and Figure 6.4.

The solar radiation data was derived from the HelioClim radiation Databases of SoDa (www.soda-is.com), which estimate total solar irradiance and irradiation values at ground level from Meteosat Second Generation (MSG) satellite images [117]. Data from light on a horizontal plane (global radiation), day length and different measurement intervals (5 min, hourly, weekly and monthly) were included. The conversion from Irradiance (W/m²) to PAR (µmol/m²/s) was calculated manually according to McCree, 1981[118] (factor of 2.3).

Cultivation periods from April to September were assumed for Wageningen and Oslo, because this was the period with the highest light intensity, assumed to sustain biomass productivity. For Rio and Cádiz all year round cultivations were assumed. Cultivations were assumed to be done in a flat panel photobioreactor, similar to the one described in the methods (6.5.2). The input parameters day length, and light intensity were derived from the average of all months during this period. The model is loaded with the light intensity (I; µmol m^2 s^{-1}) and the day length for each location. Hence, to estimate daily total irradiance (photon flux density, PFD; mol m^{-2} d^{-1}), the following equation was used (Equation 5). Where 3600 is the factor to convert the light intensity (I) from seconds to days, and 1000000 is the factor to convert the values from µmol to mol.

$$PFD = I * 3600/1000000 \quad \textbf{Eq. 5}$$

6.6. Supplementary materials

6.6.1. Experimentally estimated parameters

The model parameters and their values for each of the experimental set-ups is show in Table S6.1, which also indicates how were each parameter estimated. All parameter values were derived from the measured experimental data according to Breuer et al. (2015) [99]. A brief explanation for estimating or fitting each parameters is presented in this document.

Initial concentrations of TAG, STA, CHO, N in the reactor (g L^{-1}) were experimentally estimated, and also the fractions of functional biomass of these components (g g^{-1} DW) XCHO, XSTAX, XCHOX, and X (Table S6.7.1). Cellular nitrogen values were calculated based on the measured Q content (as described in materials and methods) at the time point of inoculation and onset of nitrogen depletion. Q_{max} represents the value at the highest biomass specific absorption cross section which is related to the maximum cellular nitrogen content. Q_{min} equals the minimum nitrogen content and Q_{deg} is taken from the time point of the highest starch concentration throughout the cultivation period (after which STA is converted to TAG).

Table S6.7.1: Overview of experimentally derived input parameters for the model simulations of Original, S5 (both indoor) and outdoors (with Original). The units are as applied in the model; confidence intervals are indicated with ± for each value. The last column at the right indicates where from and how were the parameters estimated.

Experimentally derived parameters						
Parameter	**Unit**	**Description**	**Original (indoor)**	**S5 (indoor)**	**Original (Outdoors)**	**Calculated from**
Qmax	$\frac{\text{g N}}{\text{g DW}}$	cellular nitrogen content at maximum absorption cross section	0.0747 ± 0.015	0.0673 ± 0.018	0.0593 ± 0.008	Biomass analyses (5.4.; methods)
Qmin	$\frac{\text{g N}}{\text{g DW}}$	minimum cellular nitrogen content	0.0334 ± 0.015	0.0202 ± 0.013	0.0339 ± 0.014	Biomass analyses (5.4.; methods)
Qdeg	$\frac{\text{g N}}{\text{g DW}}$	conc. of cellular N below which starch is converted to TAG	0.0334 ± 0.072	0.019 ± 0.006	0.0339 ± 0.001	Biomass analyses (5.4.; methods)
rSTATAGmax	$\frac{\text{g TAG}}{\text{g DW} \cdot \text{s}}$	maximum interconversion rate of starch to TAG	1.77E-06 ±9.66E-07	2.20E-06 ±8.85E-07	6.485E-07 ±4.79E-08	Eq. 4
rTAGXmax	$\frac{\text{g TAG}}{\text{g DW} \cdot \text{s}}$	maximum conversion rate of triacylglycerides to functional biomass	2.03E-07 ±1.79E-08	1.14E-07 ±2.09E-08	9.673E-07 ±3.07E-08	Eq. 2
rSTAXmax	$\frac{\text{g TAG}}{\text{g DW} \cdot \text{s}}$	maximum conversion rate of starch to functional biomass	8.05E-07 ±5.83E-08	3.42E-07 ±6.98E-08	8.012E-07 ±4.57E-08	Eq. 3

qphmaxrep		maximum photosynthetic rate at nitrogen replete conditions	9.11E-06 ±1.36E-06	9.99E-06 ±1.01E-06	7.675E-06 ±1.25E-06	Eq. 1
XCHO	$\frac{\text{g CHO}}{\text{g DW}}$	carbohydrate fraction other than starch in biomass after nitrogen depletion	0.1402 ±0.062	0.1394 ±0.459	0.280 ±0.326	Biomass analyses (5.4.; methods)
XSTAX	$\frac{\text{g STA}}{\text{g DW}}$	Fraction of starch in functional biomass	0.2463 ±0.097	0.1684 ±0.067	0.1995 ±0.085	Biomass analyses (5.4.; methods)
XCHOX	$\frac{\text{g CHO}}{\text{g DW}}$	Fraction of carbohydrates other than starch in functional biomass	0.1004 ±0.032	0.0897 ±0.166	0.2197 ±0.159	Biomass analyses (5.4.; methods)
arep	$\frac{\text{m}^2}{\text{g}}$	maximum absorption cross section under replete conditions	0.0877 ±0.008	0.0819 ±0.009	0.1012 ±0.009	Biomass analyses (5.3.; methods)
X	$\frac{\text{g}}{\text{m}^3}$	initial concentration of functional biomass	459.97 ±19.66	484.32 ±17.612	433.6 ±16.754	Biomass analyses (5.4.; methods)
TAG	$\frac{\text{g}}{\text{m}^3}$	initial concentration of triacylglyceride	1.6 ±0.36	18.1 ±2.49	2.81 ±0.05	Biomass analyses (5.4.; methods)
STA	$\frac{\text{g}}{\text{m}^3}$	initial concentration of starch	132.4 ±5.63	172.1 ±23.93	68.29 ±3.43	Biomass analyses (5.4.; methods)
CHO	$\frac{\text{g}}{\text{m}^3}$	initial concentration of carbohydrates other than starch	78.6 ±34.24	120.5 ±125.21	130.3 ±29.57	Biomass analyses (5.4.; methods)
N	$\frac{\text{g (N in NO3}}{\text{m}^3}$	initial amount of dissolved nitrate	124.1 ±2.08	126.16 ±3.04	114.4 ±1.99	Biomass analyses (5.3.; methods)
pA	/	coefficient A for photon partitioning	0.0004 ±0.002	0.0014 ±0.004	0.0236 ±0.016	Eq. 6
pB	/	coefficient B for photon partitioning	2.2053 ±1.004	1.7000 ±1.031	1.0802 ±0.903	Eq. 6

The maximum photosynthetic rate at nitrogen replete conditions is composed by the division of the maximal growth rate (during N-repletion) over the yield of biomass on photons (yXph).

$$q_{ph,max,rep} = \frac{\mu_{max}}{yXph} = \frac{\ln(cx_{t2} - cx_{t1})}{(t_2 - t_1) \cdot yXph} \quad \text{(Eq. 2)}$$

The maximum conversion rates $r_{TAG/X,max}$ and $r_{STA/X,max}$ expresses the highest degradation from starch and TAG to functional biomass, respectively.

$$r_{TAG/\,X,max} = \frac{XTAG_{t1} - XTAG_{t2}}{t_2 - t_1} \quad \text{(Eq. 3)}$$

$$r_{STA/\,X,max} = \frac{XSTA_{t1} - XSTA_{t2}}{t_2 - t_1} \quad \text{(Eq. 4)}$$

The maximum conversion rate from starch to TAG is directly derived from experimental data and only possible under nitrogen deplete conditions and Q lower than Q_{deg}.

$$r_{STA/\,TAG,max} = \frac{XSTA_{t1} - XSTA_{t2}}{t_2 - t_1} \quad \text{(Eq. 5)}$$

The partition coefficient f_{TAG} is defined as the ratio of the amount of photons used for the production of TAG to the amount of photons used for the production of TAG and STA. For the parameter estimation, the amount of generated STA (ΔSTA) is transformed to the amount of TAG, that could have been produced instead, using the yields of STA and TAG on photons (ySTAph and yTAGph).

$$f_{TAG} = \frac{\text{photons for TAG synthesis}}{\text{photons for starch synthesis}} = \frac{\Delta TAG}{\Delta TAG + \frac{\Delta STA \cdot yTAGph}{ySTAph}} \quad \text{(Eq. 6)}$$

The proportion between TAG and starch synthesis is specific for each scenario and defined through the estimated parameters pA and pB. Through the correlation of the partition coefficient f_{TAG} to Q (cellular nitrogen content) it becomes a function of time. It describes the carbon partitioning towards STA and TAG, which biological mechanisms is not fully understood.

$$f_{TAG} = \min\begin{Bmatrix} pA \cdot Q^{-pB} \\ 1 \end{Bmatrix} \quad \text{(Eq. 7)}$$

The parameter a_{rep} defines the maximum absorption cross section of nitrogen replete biomass. This factor is dependent on the species and state of photo-acclimation of the algae [119]. Calculation explained by Equation 1, material and methods (Section 6.5).

6.6.2. Fitted parameters

The maintenance requirements (m_s) for both the Original (in- and outdoor cultivation) and S5 was estimated in Matlab by fitting the model dependent on the biomass concentration and evaluation of the resulting square errors (maximal R-square), using the experimental data from indoor experiments from both Original and S5.

Table S6.7.2: Fitted parameters maintenance (ms) and energy split to replace the respired starch at night (fpart). Parameters were fitted to run the model simulations of Original, S5 (both indoor) and outdoors (with Original). The last column at the right indicates where from and how were the parameters estimated.

Fitted parameters						
Parameter	**Unit**	**Description**	**Original (indoor)**	**S5 (indoor)**	**Original (Outdoors)**	**Calculated from**

ms	$\frac{\text{mol photon}}{\text{g DW} \cdot \frac{Q}{Q_{max}} \cdot}$	maintenance requirement per amount of reproducing biomass and time	1.80E-06	8.80E-07	6.25E-07	Eq. 7
fpart	/	partition coefficient for replacing STA after nights in functional biomass	0.03	0.03	0.03	Eq. 8

$$R^2 = 1 - \frac{SSE}{SST} = 1 - \sum_t \left(\frac{c_x(t) - \text{model}c_x(t)}{c_x(t) - cx_{avg}} \right)^2 \quad \text{(Eq. 8)}$$

Maintenance (ms) was calculated for each experiment individually due to the differing cultivation modes and conditions.

The parameter f_{part} splits the energy towards the replacement of (during night) degraded starch. It was estimated by a statistical parameter estimation, similar to maintenance (ms).

At the time point where all starch in functional biomass is restored, the available energy is partitioned normally again and f_{part} is set to zero (Eq. 12).

$$f_{part} = \begin{cases} f_{part} & \text{if degSTA} < 0 \\ 0 & \text{if degSTA} = 0 \end{cases} \quad \text{(Eq. 9)}$$

6.6.3. Fixed parameters

Table S6.7.3: Fixed parameters set the duration of the cultivation, duration of each day and light period, also the depth of the reactor and the light intensity. These parameters were initially set to run the model simulations of Original, S5 (both indoor) and outdoors (with Original). The last column at the right indicates where from and how were the parameters estimated.

Constant parameters					
Parameter	Unit	Description	Wildtype	S5	Outdoors
cd	s	duration of cultivation (h * s)	240.5*3600	240*3600	264*3600
dds	s	duration of one day	24*3600	24*3600	24*3600
dlds	s	duration of light per day	16*3600	16*3600	**measured**
z	m	light path of the reactor	0.02	0.02	0.02
I_0	$\frac{\mu mol}{m^2 \cdot s}$	Incident light intensity	954.9	954.9	**On-line measured**

6.6.4. Theoretical yields

All used theoretical yields are present at Table S6.7.4. The values for the maximum photosynthetic yields (yXph, yCHOph, ySTAph and yTAGph) for green algae are taken from another research in which they were experimentally derived by experiments with *Chlamydomonas reinhardtii* [120]. Due to the adaption of the model to day/night- cycles (and therefore night respiration) a set of conversion yields (yXTAG, yXSTA, yATPph, yATPSTA) was established based on metabolic pathway data [99].

Table S6.7.4: Theoretical maximum photosynthetic yields and conversion yields used in the model estimations (as derived from Kliphuis et al., 2012[120]).

Parameter	Unit	Value	Description
yXph	$\frac{\text{g X}}{\text{mol photon}}$	1.62	yield of functional biomass on photons when grown on NO3-
yCHOph	$\frac{\text{g CHO}}{\text{mol photon}}$	3.24	yield of other carbohydrates than starch on photons
ySTAph	$\frac{\text{g STA}}{\text{mol photon}}$	3.24	yield of Starch on photons
yTAGph	$\frac{\text{g TAG}}{\text{mol photon}}$	1.33	yield of triacylglycerides on photons
yTAGSTA	$\frac{\text{g TAG}}{\text{g STA}}$	0.39	yield of triacylglycerides on starch
yXCHO	$\frac{\text{g X}}{\text{g CHO}}$	0.644	conversion yield of functional biomass on other carbohydrates
yXSTA	$\frac{\text{g X}}{\text{g STA}}$	0.644	conversion yield of functional biomass on starch
yXTAG	$\frac{\text{g X}}{\text{g TAG}}$	1.404	conversion yield of functional biomass on triacylglycerides
yATPSTA	$\frac{\text{mol ATP}}{\text{g STA}}$	0.149	yield of ATP on starch
yATPTAG	$\frac{\text{mol ATP}}{\text{g TAG}}$	0.325	yield of ATP on TAG
yATPph	$\frac{\text{mol ATP}}{\text{mol photons}}$	0.375	yield of ATP on photons

6.6.5. Model equations (how the model works)

6.6.5.1. Calculations required to convert simulated and outdoor irradiances to light intensities (as a block light)

For the adaption to outdoor light conditions, day/night cycles were implemented. For the indoor experiments the sinus-shaped light curve is provided by LED-lamps controlled by an external software (IRIS). Equation 1 (Eq 9) describes how was the daily sinus function distribution of light intensity, from sunrise to sunset. The resolution of Eq 9 gives the total light irradiance in a day (the integration of a day sinus), expressed as µmol m^{-2} s^{-1}. Equation 10 converts the total daily irradiance to light intensity (I), which is used as a constant model input for the indoor experiments.

$$\int_0^{16} 1500\ \sin\left(\frac{2\pi}{2*16}x\right)\,dx = 15278.8 \qquad \text{(Eq. 9)}$$

Block-light for a light duration of 16 h:

$$\frac{15278.8}{16} = 954.93 \frac{\mu mol}{m^2 s} \quad \text{(Eq. 10)}$$

For the simulations on the outdoor experiment a change in light intensities was introduced. The actual light intensities (µmol m^{-2} s^{-1}) for each cultivation day was measured on-line *in loco*. Outdoor total daily light intensity was converted to light intensity (µmol m^{-2} s^{-1}) using Equation 10.

For the simulations of performance under different locations local measurements of Oslo, Wageningen, Rio de Janeiro and Cádiz were retrieved from an on-line data base (as described at section 5.7 form materials and methods). The actual light intensities (µmol m^{-2} s^{-1}) for each location was measured per day, and the average light intensity for the whole production year was calculated. The total daily light intensity was converted to light intensity (µmol m^{-2} s^{-1}) using Equation 10.

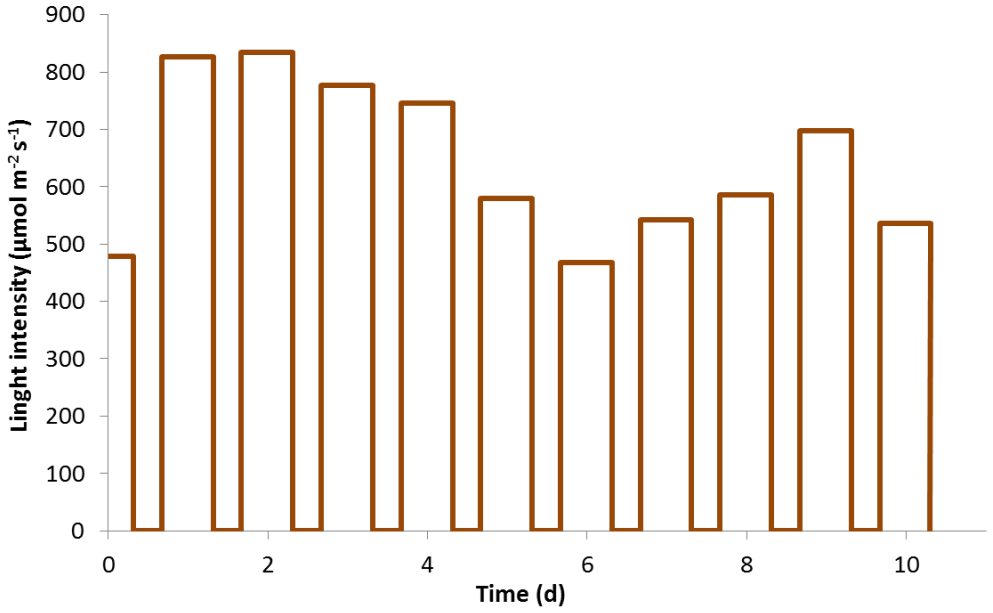

Figure S6.7.1: Daily measured PDF converted to a block light intensity for outdoor data, as used as input for outdoor model simulations.

6.6.6. Equations implemented in the model of Breuer et al. (2015)[99] to introduce day:night cycles

Equation 11 introduces a light change during the cultivation day by using a step function. The light intensity (I_0) is only applied during the daylight hours per day (dlds), leaving a dark period for the rest of the day (intensity (I)=0). Further parameters are: t (cultivation time), nd (number of day), dds (duration of day).

$$I(t) = \begin{cases} I_0 & \text{if } (t - nd \cdot dds) < dlds \\ 0 & \text{if } (t - nd \cdot dds) \geq dlds \end{cases} \quad \text{(Eq. 121)}$$

In addition to the regulation of the time point for light irradiance in Eq. 11, a function for the light distribution within the reactor was implemented in Eq. 12. The light scenario within the reactor incorporates the constant light intensity (I_0) and the attenuation model of Lambert-Beer (whereas the attenuation coefficient (a) equals the absorption cross section (a)). any additional light scattering effects were neglected.

$$I(z) = I_0 \cdot e^{-a \cdot c_x \cdot z} \quad \text{(Eq. 12)}$$

with z: light path
c_x: total biomass concentration

Metabolic principles that are accountable for the partitioning of available energy are under a strong influence of the progress of nitrogen depletion. Through the cellular nitrogen content (Q) those effects can be surrogated in a simplified way. Since the composition of functional biomass is not constant anymore due to dark respiration, a new equation for the cellular nitrogen content (Q) was defined (Eq. 13):

$$Q = Q_{max} \cdot \frac{X - degSTA}{c_x} \quad \text{(Eq. 13)}$$

The quantum yield (QY, Eq. 14) expresses the available fraction of absorbed photons that is not dissipated as heat. As the cellular nitrogen content may exceed Q_{max} due to starch degradation during nights, the quantum yield (QY) is overestimated during nights. Hence, a correction of the quantum yield (QY) is subsequently necessary with the previous equation. Therefore Equation 14 assures a maximum QY of 1, avoiding the utilization of more energy than available.

$$QY = \min \begin{Bmatrix} \left(1 - \frac{Q_{min}}{Q}\right) \cdot \left(1 - \frac{Q_{min}}{Q_{max}}\right)^{-1} \\ 1 \end{Bmatrix} \quad \text{(Eq. 14)}$$

The available energy is partitioned to the *de novo* synthesis of biomass constituents with respect to differing yields for TAG, STA, CHO and reproducing biomass estimated, which have been analyzed through flux balance analyzes.

6.6.7. How the model integrates all previous parameters to estimate growth and productivities

Each of the following equations (Eq. 15 – 20) independently describe the specific production rates for biomass constituents during the light period based on the average biomass specific photosynthetic rate ($q_{ph,avg}$). All specific production rates depend on the available energy from photosynthesis.

Eq. 15 shows the specific production rate of reproducing biomass and is extended (from the continuous light functions) with the correction of starch degradation during night, leaving the same composition before and after the night.

$$qX = \overbrace{\begin{cases} yXph \cdot \left(q_{ph,avg} - \frac{m_s \cdot Q}{Q_{max}}\right) \cdot (1 - f_{part}) + r_{TAG/X} \cdot yXTAG + STAinXdeg & \text{if } N > 0 \text{ and} q_{ph,avg} > \frac{m_s \cdot Q}{Q_{max}} \\ STAinXdeg & \text{if } N = 0 \text{ and } q_{ph,avg} > \frac{m_s \cdot Q}{Q_{max}} \end{cases}}^{qX1} \quad (Eq.15)$$

$$\text{with } STAinXdeg = ySTAph \cdot \left(q_{ph,avg} - \frac{m_s \cdot Q}{Q_{max}}\right) \cdot f_{part}$$

The fraction f_{part} adjusts the available energy during the day due to the replacement of starch in the functional biomass after night respiration. Also included is the conversion of TAG to functional biomass ($r_{TAG/X} \cdot yXTAG$). No functional biomass can be produced when the dissolved nitrogen concentration is zero.

The remaining production rates (Eq. 16: carbohydrates, Eq. 17: starch, Eq. 18: TAGs) correspond to the original model, with the exception of a correction of degraded starch in the total carbohydrates (Eq. 16).

Under nitrogen depletion firstly the general carbohydrate (other than starch) levels are kept constant. Expressed through the multiplication of available energy and the production yield of CHO on photons (yCHOph). As the carbohydrate levels in functional biomass are attempted to kept stable, CHO is only produced in case of a lower value of xCHO than XCHO.

$$qCHO = \begin{cases} \left(\left(q_{ph,avg} - \frac{m_s \cdot Q}{Q_{max}}\right) \cdot (1 - f_{part}) - \frac{qX1}{yXph}\right) \cdot yCHOph & \text{if } xCHO \leq XCHO \\ 0 & \text{if } xCHO > XCHO \end{cases} \quad (Eq. 16)$$

$$\text{with } xCHO = \frac{XCHOX \cdot (X - degSTA) + CHO}{c_x}$$

The residual energy after CHO synthesis is partitioned between TAG and starch. For both cases the available energy for synthesis is constructed out of the specific photosynthetic energy (corrected for maintenance energy), the leftover energy after replacing CHO into functional biomass after nights and the energy already consumed for X and CHO synthesis.

The proportion between TAG and starch synthesis is specific for each scenario and defined through f_{TAG}, which is the energy portion used for TAG synthesis and primarily depending on the cellular nitrogen content. Respectively, ($1\text{-}f_{TAG}$) is the surplus energy going into starch production. In addition to the particular yields on photons, the conversion from starch to TAG (only below Qdeg, Eq. 13) is included. Finally the conversion rates of TAG and STA into functional biomass complete the functions.

$$qTAG = \left\{ \begin{array}{r} \left(\left(q_{ph,avg} - \frac{m_s \cdot Q}{Q_{max}} \right) \cdot \left(1 - f_{part}\right) - \frac{qX1}{yXph} - \frac{qCHO}{yCHOph} \right) \cdot f_{TAG} \cdot yTAGph \\ + r_{STA/TAG} \cdot yTAGSTA - r_{TAG/X} \end{array} \right\} \quad \text{(Eq. 17)}$$

$$qSTA = \left\{ \begin{array}{r} \left(\left(q_{ph,avg} - \frac{m_s \cdot Q}{Q_{max}} \right) \cdot \left(1 - f_{part}\right) - \frac{qX1}{yXph} - \frac{qCHO}{yCHOph} \right) \cdot (1 - f_{TAG}) \cdot ySTAph \\ - r_{STA/TAG} - r_{STA/X} \end{array} \right\} \quad \text{(Eq. 18)}$$

The specific nitrogen consumption rate had to be redefined as the night biomass loss (occurring under day/night cycles) could increase the dissolved nitrogen concentration. Eq. 21 implements the replacement of starch into functional biomass (STAinXdeg), hence avoiding thereby a rising dissolved nitrogen level.

$$qN = \left\{ \begin{array}{ll} -(qX - STAinXdeg) \cdot Q_{max} & \text{if } qX \geq 0 \\ r_{TAG/X} \cdot yXTAG & \text{if } qX < 0 \end{array} \right\} \quad \text{(Eq. 19)}$$

With the shift to a cultivation with day/night cycles, metabolic mechanisms during the dark phase had to be considered. No photosynthetic energy is available (removed energy supply and ms), thus no synthesis of biomass constituents takes place. Rather would the dark respiration cause night biomass loss and degrade energy storing components (starch) to cover the maintenance requirements. Equations 20 and 21 are restricted to the dark phase (through $q_{ph,avg}$), while during light period Eq. 15 and 18 apply.

The maintenance energy during night is preferably cover by accumulated starch (STA), if there is none available, starch will be degraded out of the functional biomass (STAinXdeg). The rate of reproducing biomass in the night (Eq. 20) is therefore implemented by the conversion factor of starch to functional biomass (rSTA/X).

$$qX = \left\{ \begin{array}{ll} r_{STA/X} \cdot yXSTA + r_{TAG/X} \cdot yXTAG & \text{if } STA > 0 \text{ and } q_{ph,avg} < \frac{m_s \cdot Q}{Q_{max}} \\ r_{TAG/X} \cdot yXTAG + STAinXdeg & \text{if } STA = 0 \text{ and } q_{ph,avg} < \frac{m_s \cdot Q}{Q_{max}} \end{array} \right\} \quad \text{(Eq. 20)}$$

$$\text{with } STAinXdeg = -\frac{m_s \cdot Q}{Q_{max}} \cdot \frac{yATPph}{yATPSTA}$$

Equation 21 uses a decrease of the biomass specific production rate of starch ($r_{STA/X}$) for starch degradation (covering ms).

$$qSTA = \left\{ \begin{array}{ll} -r_{STA/TAG} - r_{STA/X} - \frac{m_s \cdot Q}{Q_{max}} \cdot \frac{yATPph}{yATPSTA} & \text{if } STA > 0 \text{ and } q_{ph,avg} < \frac{m_s \cdot Q}{Q_{max}} \\ 0 & \text{if } STA = 0 \text{ and } q_{ph,avg} < \frac{m_s \cdot Q}{Q_{max}} \end{array} \right\} \quad \text{(Eq. 131)}$$

6.6.8. Confidence intervals

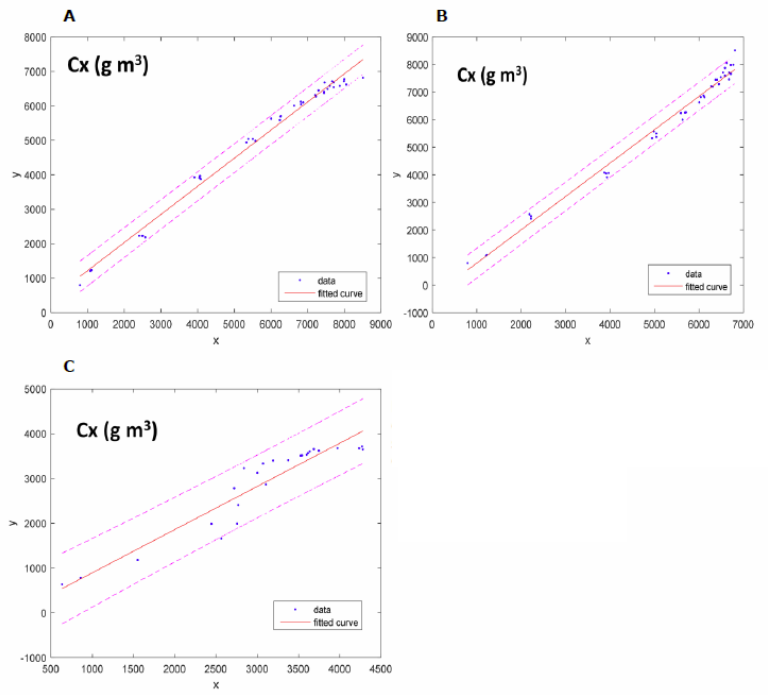

Figure S6.7.2: 95% confidence intervals of total biomass concentration (Cx, (g/m³)) for experimental data (x-axis) and the corresponding simulation (y-axis) for Original (A), S5 (B) and outdoor experiments with Original (C).

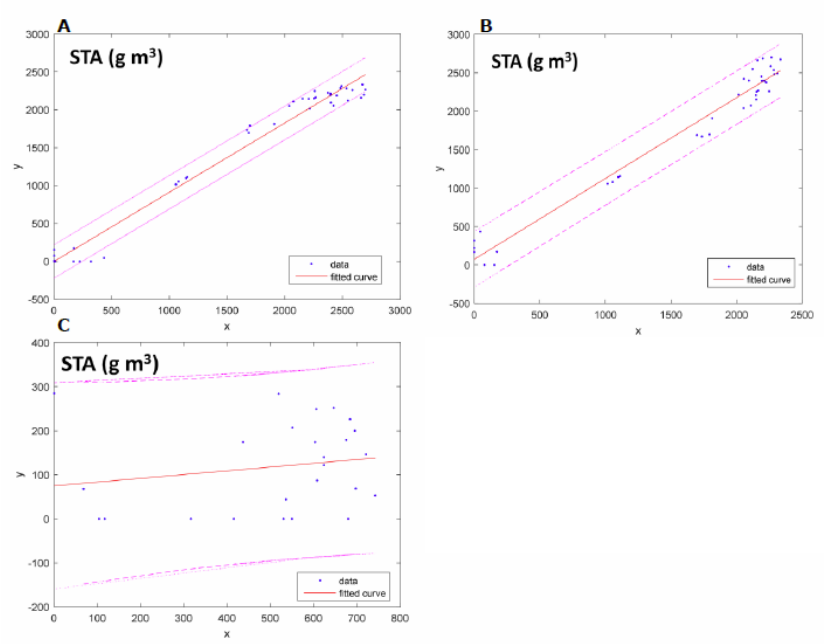

Figure S6.7.3: 95% confidence intervals of total biomass concentration (STA, (g/m³)) for experimental data (x-axis) and the corresponding simulation (y-axis) for Original (A), S5 (B) and outdoor experiments with Original (C).

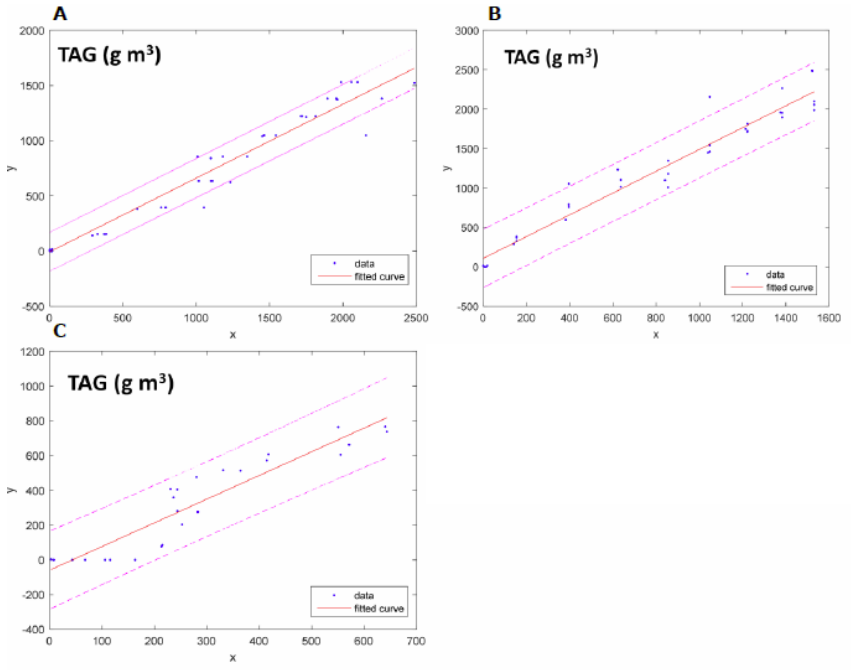

Figure S6.7.4: 95% confidence intervals of total biomass concentration (TAG, (g/m³)) for experimental data (x-axis) and the corresponding simulation (y-axis) for Original (A), S5 (B) and outdoor experiments with Original (C).

General Discussion

ABSTRACT: Microalgae are photosynthetic microorganisms that have potential to replace commodities, such as in food, feed and fuels. Despite extensive research in the last decades, microalgae are still only economically feasible for high value markets (such as omega-3 fatty-acids), and also as feed for aquaculture. We suggest to borrow the concept of plant domestication to develop improved industrial microalgae strains. Two approaches can be successfully used to domesticate microalgae without using genetic manipulation: adaptive laboratory evolution (ALE) and fluorescence assisted cell sorting (FACS). ALE takes advantage of the natural adaptability of microorganism to different environments to select new cell populations. FACS, on the other hand, offers the possibility to actually select cells with specific phenotypes. This discussion demonstrates that both methods are effective to select industrial microalgae cells and presents our view on how ALE and FACS could further improve microalgae strains. New technological advances are being made in the field of cell sorting and the new trends point towards higher precision and more possibilities for microalgae industry. Selecting microalgae cells suitable to industrial applications can exploit nature and achieve cost-competitive microalgae products.

Key-words: microalgae, adaptive laboratory evolution (ALE), Fluorescence assisted cell sorting (FACS), strain improvement, microalgae industry

7.1. Domesticating microalgae for industry

Microalgae are photosynthetic microorganisms that have been gathering attention in the last decades due to their potential to replace commodities, such as in food, feed and fuels [1]. Production costs are still high, reason why microalgae are still only economically feasible for high value markets (such as omega-3 fatty-acids), and also as feed for aquaculture [121]. Microalgae technology has been focusing on growth and product formation via process optimization with a limited number of strains [121]. Behind this lies the idea that a marriage between process engineering and biology would bring microalgae for commodities into reality [12]. Such marriage never took place [2], but countless knowledge has been accumulated on reactor design [116,122], reactor operation and on microalgae cell biology [74,123–126].

We suggest to use this knowledge to **domesticate microalgae** (Figure 7.1), borrowing the concept from agriculture. Microalgae industry is in its infancy when compared with agriculture, that has been exploring the natural potential of plant crops since primordial societies. The principle and workflow of plant domestication can be applied to microalgae, as shown by figure 7.1. Two approaches can be used to select microalgae cells with industrial potential: adaptive laboratory evolution (ALE) and fluorescence assisted cell sorting (FACS). Both approaches are feasible possibilities to domesticate microalgae strains and both have the advantage of not using genetic manipulation (although it could be combined).

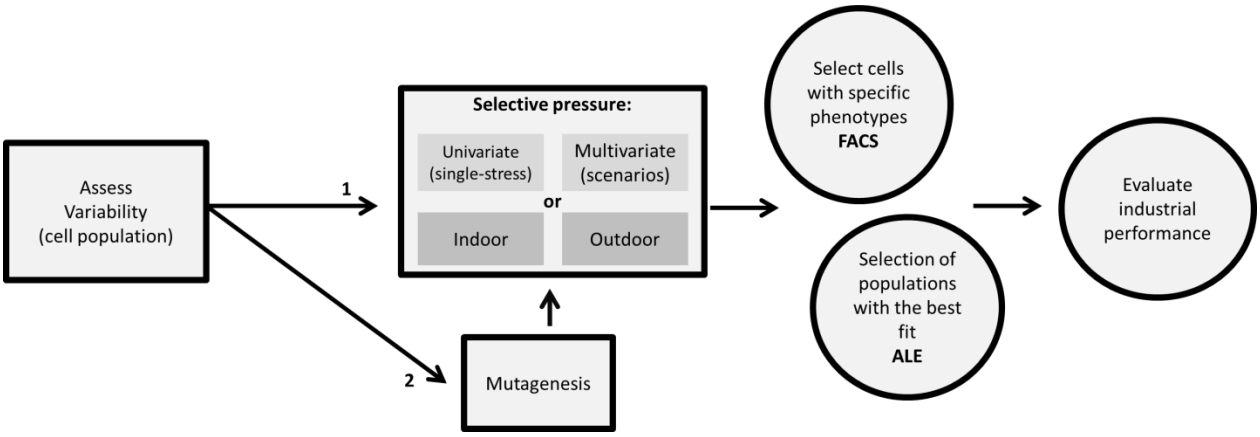

Figure 7.1: Microalgae domestication, based on natural selection and inspired by agriculture. Once the phenotype is decided, a selective pressure should be applied to the population (arrow 1). The pressure can be univariate (one stress-factor) or multivariate (combining different variables to produce specific scenarios). We can select cells with specific phenotypes (FACS) or we can select a part of the population which is more fit under the selection pressure applied (ALE). Finally, the industrial potential should be tested *in loco* or under simulated outdoor conditions. Domestication can be done with or without increasing mutation rates with mutagenesis (arrow 2).

7.2. Adaptive laboratory evolution (ALE)

The natural ability to adapt to different environments is a feature of microorganisms that can be exploited. ALE is an experimental approach that uses specific environmental factors as selection pressure, which can select cells with best fit to the desired conditions. ALE is inspired by natural

selection and can be used to improve growth rates, to improve yields and to adapt microalgae to different environments. ALE is usually done with isolated strains, as a tool to improve strains with known potential. But ecology-based experiments brought the possibility to use multiple species/strains [127], taking advantage of interspecific competition to select strains that better fit among a mixed population [127–131]. ALE can be done at lab-scale or under outdoor fluctuating conditions to select cells more fit for industrial production [127,128,131,132].

Microalgae have been shown to evolve under repeated conditions in periods of 3 to 17 months (40 to 600 generations) [11,17,133]. Similarly, bacteria and yeast have been evolved (with or without mutagenesis) in periods as short as 13 and as long as 1000 generations [13]. Surprisingly, the speed of laboratory evolution is not determined by the microorganism growth rate or whether it has a prokaryotic or eukaryotic cellular organization [11,13,17,133]. This observation shows that the strength of the selection pressure is the most relevant factor when pushing laboratory evolution. ALE was used to evaluate the effect of light on both biomass and pigments formation of *Chlorella vulgaris* and *Dunaliella salina* [11,16]. The results indicated that microalgae can respond to abiotic stress in relatively short period of time (45 to 80 days). It was also successfully used to evolve CO_2-tolerant strains of *Chlorella sp*., without assessing the stability of the improved phenotype [17]. A complete story is shown in the successful evolution of salt-tolerant *Chlamydomonas reinhardtii* strains [133]. In this example the authors demonstrated that after 17 months of repeated cultivation in increased salt concentrations there was solid evidence of genetic evolution.

ALE can be used to domesticate microalgae under specific industrial conditions. With figure 7.2 we present our view on how to use ALE to improve microalgae. Our approach can be used in 3 steps or each step can be used alone. STEP 1: We assume that before step 1 choices have been made: what, where and how you are going to produce. These questions will determine the nature of the screening (step 1) and if it is better to work with previously isolated strains or with environmental samples of phytoplankton. Alternatively the domestication process can start already at step 2, if a working strain is already chosen. The screening will result in the best strain to be used outdoor. STEP 2: The best strain can be further improved towards one specific characteristic, usually enhanced product or biomass yields. The improved strain should then be tested under production conditions to assess stability and can go straight outdoors. STEP 3 is a "fine-tuning" improvement, that will depend on the outdoor performance of the strain. One example could be to increase pH or temperature to reduce contamination risk. Finally, we recommend the ALE experiments to be carried out in the lab, to have controlled conditions and to decrease the chance on expensive culture crashes. ALE is an efficient approach to domesticate microalgae, but depending on experimental set-up and goal can take time and resources. But the benefits might pay-off, because ALE can select strains with a natural advantage under industrial environments.

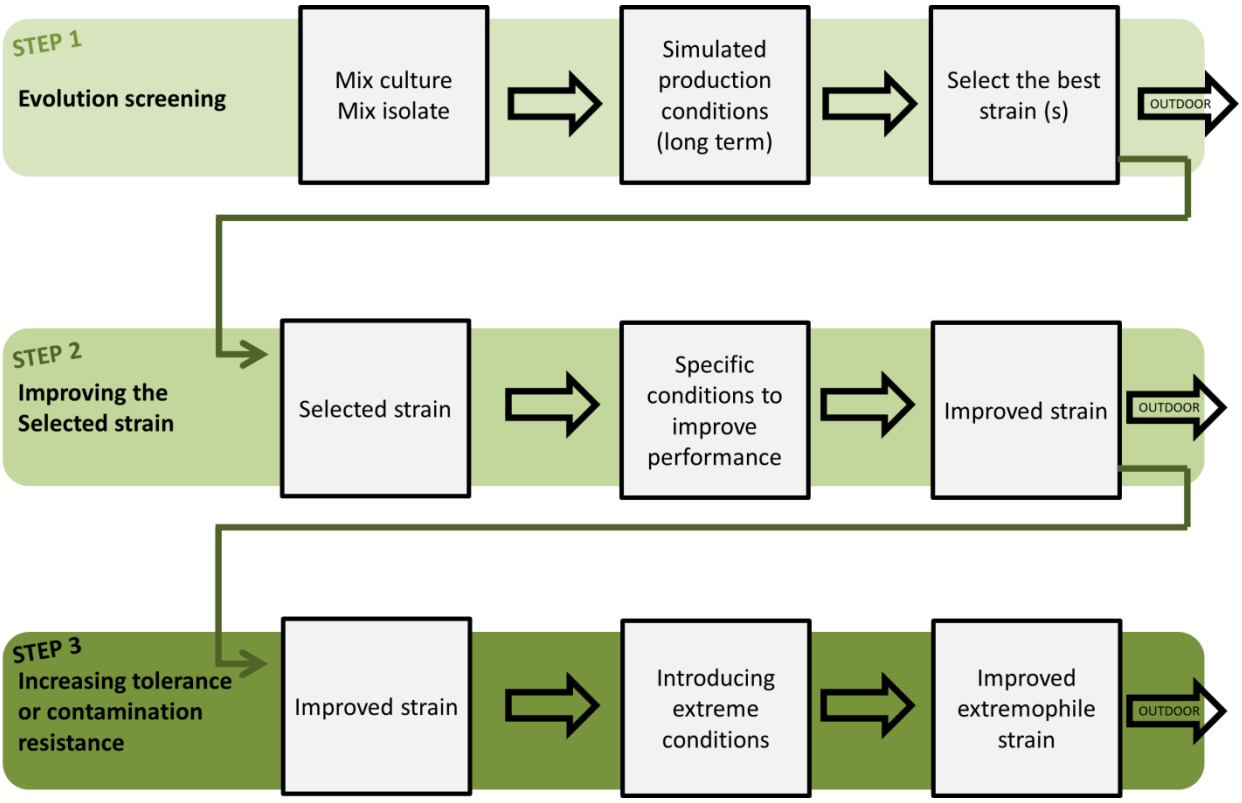

Figure 7.2: how can we use ALE to improve microalgae industrial potential. Our approach goes from the screening all the way to the factory. STEP 1: screening to select the best industrial profile. **STEP 2**: improving the working strain (e.g. more product or higher growth). **STEP 3**: fine-tuning, additional characteristics are added to further improve the working strain. The arrows marking OUTDOOR show a way out of the workflow with direct application at outdoor conditions.

7.3. Fluorescence assisted cell sorting (FACS)

FACS changes the selection target from sub-populations to cells, leading to a more specific domestication [134]. Flow cytometry is a single-cell measurement, normally assisted with fluorescence dyes or natural pigments. Fluorescence assisted cell sorting (FACS) brought the possibility to select cells based on their phenotypes [135]. Sub-populations might be phenotypically heterogeneous or might hide less competent cells inside them [136] and single-cell sorting can guarantee a more homogeneous phenotype. Previous publications show a combination of cell sorting and mutagenesis to select cells with higher lipid content [9,14,23]. In none of the publications, however, productivity values were reported. Furthermore, all these studies were done in small volumes and under continuous light conditions, making it unlikely to approach industrial performance. We suggest improved strains to be tested under simulated production conditions after a period of storage (as done in Chapter 5). This will answer if the improved phenotype is stable and if the strain has potential to be used outdoor.

FACS can take the principle of artificial selection one step further. A good example is the research from Doan and Obbard [10] who selected a cell population of *Nannochloropsis* sp. with increased lipid content. They observed sorted populations were made of cells that produced more lipids than the parental cell line (Figure 7.3A). The work of Cabanelas et al. (Chapter 5, this thesis) selected a cell population of *Chlorococcum littorale* with doubled TAG productivity, using a similar approach. The sorted populations were composed of high-lipid producing cells only, and not by cells that produced more lipids than the parental line (Figure 7.3B). This increased population was tested under simulated summer conditions after 1.5 year storage, meaning that the trait was stable and suitable to outdoor conditions. These results are remarkable and in the following paragraphs we present how to get even better cells for industry.

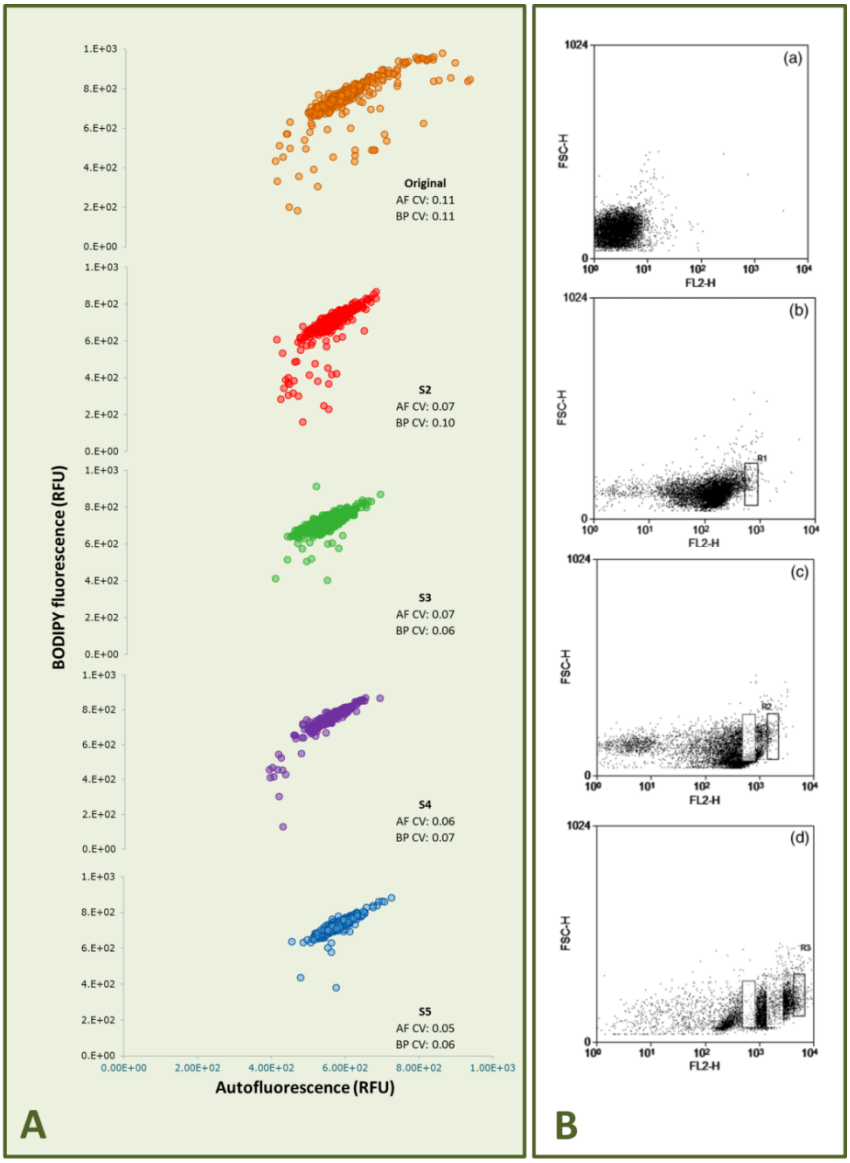

Figure 7.3: Examples of applications of FACS to improve lipid content of microalgae. A: Graphs and caption from Chapter 5 (this thesis). Sorted populations show a progressive increase in lipid productivity due to an increase in the proportion of lipid-rich cells within the populations. Scatter plots represent the relation between autofluorescence (AF, x-axis) and lipid fluorescence (BP, y-axis). On all scatter-plots the coefficient of variation (CV) of both AF and BP are depicted. **B: Graphs and caption from Doan & Obbard** [10]. Two-dimensional dot plots of strain 47 for three rounds of sorting, (a) unstained parent cells (control), (b) first round, (c) second round and (d) third round. Selected regions of R1, R2 and R3 were gated for cell sorting.

We suggest microalgae industry to mimic FACS applications from other types of cells. Flow cytometry and cell sorting are even more robust now, with faster and more reliable sorting options and increments in fluorescent channels available [137]. The limitation for microalgae lies in

the staining procedures, which usually compromise cell viability, since a fixation step or a partial cell disruption is required [138,139]. In Table 7.1 we show a list of possibilities to measure cell characteristics without killing them. The markers from Table 7.1 can be used to customize cell lines according to different industrial demands.

Table 7.1: List of applications of FACS to evaluate intracellular content of different compounds and cell physiology. This table represents a review of fluorescence staining with potential to keep cell viability.

Analysis	Probe	Ex	Em	Strains (used with positive results)	Reference
Cell size	None (Forward light scattering , FSC)	-	-	*Chlamydomonas reinhardtii* *Chlorococcum littorale*	140,141
Pigments	Autofluorescence				142
	Phycocyanin	488	650		
	Chlorophylls	430-665	640-660		
	Carotenoids	480	670		
	Phycoerythrin	570	560		
Cellulose content	Calcofluor white	347	450	*Crypthecodinium cohnii*	143
Protein content	FITC (fluorescein-5-isothiocyanete)	494	518	*Chlorella kessleri*	144
Nucleic acids	DAPI (4´,6-diamidino-2-henylindole hydrochloride)	358	461		
Polyphosphate (intracellular granules)	DAPI	405	490 456	*Saccharomyces fragilis* *Scenedesmus vacuolatus*	145 146
Viability markers	CTC (5-cyano-2,3-ditolyl tetrazolium Chloride) – membrane potential	450	630	*Scenedesmus vacuolatus*	147
	CFSE (5-,6-carboxyfluorescein diacetate succinimidyl ester) - esterase activity	488	519	*Chlorella vulgaris*	138
	Rhodamine 123 – mitochondira membrane polarization	507	529	*Scenedesmus vacuolatus*	147
Neutral lipids	$BODIPY_{505/515}$	505	515	*Chlamydomonas sp.* *Nannochloropsis gaditana* *Tetraselmis subcordiformis* *Chlamydomonas reinhardtii* *Chlorococcum littorale* *Chlorella vulgaris* *Dunaliella primolecta*	15,21,52,59,148–150

				Chaetoceros calcitrans	
	$BODIPY_{493/503}$	493	503	*Auxenochlorella protothecoides* *Chlorella vulgaris* *Scenedesmus dimorphus* *Scenedesmus obliquus* *Nannochloropsis gaditana* *Phaeodactylum tricornutum* *Chlamydomonas reinhardtii*	24,58,78,133,151
Polar lipids	Nile red (NR)[a]	450 560	528-628	*Chlorella saccharophila* *Dunaliella* *Phaeodactylum tricornutum* *Chlorococcum littorale* *Chlamydomonas* *Nannochloropsis sp.* *Chlorococcum sp.* *Tetraselmis suecica*	9,10,14,15,63,85,68,151–155

[a] Nile red can stain both polar and non-polar lipids.

7.4. Upcoming trends and recommendations

Label-free cell sorting can solve the limitation when using fluorophores with microalgae cells. The use of fluorophores is the limitation of FACS, because staining protocols might cause cell damage or cell death. Raman microspectroscopy offers a solution as a laser light scattering provides rapid and label-free determination of single-cell chemical composition. Raman activated cell sorting (RACS) has recently been developed [57], and validated to *Chlamydomonas reinhardtii* [156,157]. The fact that RACS is label-free represents a huge breakthrough in the field of microalgae cell sorting. The limitation is that RACS is not commercially available yet.

We cannot measure photosynthetic capacity with FACS. Erickson and Jimenez [85] have developed a new system to measure single-cell quantum yield (QY) of photosystem II (PSII), estimating photosynthetic capacity at single-cell level. They have shown that after nitrogen starvation *Phaeodactylum tricornutum* cells show a Gaussian distribution of QY. This indicates that there were cells within the population with potentially higher photosynthetic efficiency under nitrogen starvation in comparison with the population median [85]. This system is, however, not capable of sorting and is not commercially available.

If the strain has industrial value it should be preserved, preferably forever. The core of our argument is that microalgae can evolve, not only in nature but also under controlled conditions. The same logic applies to improved strains. It is impossible to answer until when an improved strain is to show a stable phenotype. We need to confirm that there is a genetic background to explain why the improved strain is better than the wildtype. Hence, we claim that parties working on strain improvement should have optimized cryopreservation protocols [158,159].

7.5. Conclusions

While agriculture began with domestication of crops, microalgae industry has focus on cultivation systems and biomass processing technology. We propose to borrow the concept of plant domestication to select industrial microalgae cells. Two approaches can be successfully used and were presented in this discussion: adaptive laboratory evolution (ALE) and fluorescence assisted cell sorting (FACS). ALE takes advantage of the natural adaptability of microorganism to different environments to select new cell populations. FACS, on the other hand, offers the possibility to actually select cells with specific phenotypes. We presented our view on how to select cells fit to outdoor conditions. New technological advances are being made in the field of cell sorting and the new trends point towards higher precision and more possibilities for microalgae industry. Selecting microalgae cells suitable to industrial applications can exploit nature and achieve cost-competitive microalgae products.

References

1. Wijffels, R. H. & & Barbosa, M. J. An outlook on microalgal biofuels. *Science (80-.).* **329,** 796–799 (2010).
2. Tredici, M. R. Photobiology of microalgae mass cultures: understanding the tools for the next green revolution. *Biofuels* **1,** 143–162 (2010).
3. Norsker, N. H., Barbosa, M. J., Vermue, M. H. & Wijffels, R. H. Microalgal production--a close look at the economics. *Biotechnol Adv* **29,** 24–27 (2011).
4. Draaisma, R. B. *et al.* Food commodities from microalgae. *Curr. Opin. Biotechnol.* **24,** 169–177 (2013).
5. Lam, M. K. & Lee, K. T. Microalgae biofuels: A critical review of issues, problems and the way forward. *Biotechnol. Adv.* **30,** 673–690 (2012).
6. Chisti, Y. Biodiesel from microalgae. *Biotechnol Adv* **25,** 294–306 (2007).
7. Apt, K. E. & Behrens, P. W. Commercial developments in microalgal biotechnology. *J. Phycol.* **35,** 215–226 (1999).
8. Münkel, R., Schmid-Staiger, U., Werner, A. & Hirth, T. Optimization of outdoor cultivation in flat panel airlift reactors for lipid production by Chlorella vulgaris. *Biotechnol. Bioeng.* **110,** 2882–93 (2013).
9. Terashima, M., Freeman, E. S., Jinkerson, R. E. & Jonikas, M. C. A fluorescence-activated cell sorting-based strategy for rapid isolation of high-lipid Chlamydomonas mutants. *Plant J.* **81,** 147–159 (2015).
10. Yen Doan, T.-T. & Obbard, J. P. Enhanced lipid production in Nannochloropsis sp. using fluorescence-activated cell sorting. *GCB Bioenergy* **3,** 264–270 (2011).
11. Fu, W. *et al.* Maximizing biomass productivity and cell density of Chlorella vulgaris by using light-emitting diode-based photobioreactor. *J. Biotechnol.* **161,** 242–249 (2012).
12. de Jaeger, L. *et al.* Superior triacylglycerol (TAG) accumulation in starchless mutants of Scenedesmus obliquus: (I) mutant generation and characterization. *Biotechnol. Biofuels* **7,** 69 (2014).
13. Portnoy, V. a., Bezdan, D. & Zengler, K. Adaptive laboratory evolution-harnessing the power of biology for metabolic engineering. *Curr. Opin. Biotechnol.* **22,** 590–594 (2011).
14. Doan, T. T. Y. & Obbard, J. P. Enhanced intracellular lipid in Nannochloropsis sp. via random mutagenesis and flow cytometric cell sorting. *Algal Res.* **1,** 17–21 (2012).
15. Cabanelas, I. T. D., van der Zwart, M., Kleinegris, D. M. M., Barbosa, M. J. & Wijffels, R. H. Rapid method to screen and sort lipid accumulating microalgae. *Bioresour. Technol.* **184,** 47–52 (2015).
16. Fu, W. *et al.* Enhancement of carotenoid biosynthesis in the green microalga Dunaliella salina with light-emitting diodes and adaptive laboratory evolution. *Appl. Microbiol. Biotechnol.* **97,** 2395–2403 (2013).
17. Li, D., Wang, L., Zhao, Q., Wei, W. & Sun, Y. Improving high carbon dioxide tolerance and carbon dioxide fixation capability of Chlorella sp. by adaptive laboratory evolution. *Bioresour. Technol.* **185,** 269–275 (2015).
18. Yu, S., Zhao, Q., Miao, X. & Shi, J. Enhancement of lipid production in low-starch mutants Chlamydomonas reinhardtii by adaptive laboratory evolution. *Bioresour. Technol.* **147,** 499–507 (2013).
19. Katsuragi, T. & Tani, Y. Screening for microorganisms with specific characteristics by flow

cytometry and single-cell sorting. *J. Biosci. Bioeng.* **89,** 217–222 (2000).
20. Sekar, R. *et al.* Flow Sorting of Marine Bacterioplankton after Fluorescence In Situ Hybridization Flow Sorting of Marine Bacterioplankton after Fluorescence In Situ Hybridization. *Appl. Environ. Microbiol.* **70,** 6210–6219 (2004).
21. Velmurugan, N. *et al.* Systematically programmed adaptive evolution reveals potential role of carbon and nitrogen pathways during lipid accumulation in Chlamydomonas reinhardtii. *Biotechnol. Biofuels* **7,** 117 (2014).
22. Lim, D. K. Y., Schuhmann, H., Sharma, K. & Schenk, P. M. Isolation of High-Lipid Tetraselmis suecica Strains Following Repeated UV-C Mutagenesis, FACS, and High-Throughput Growth Selection. *Bioenergy Res.* **8,** 750–759 (2015).
23. Beacham, T. A., Macia, V. M., Rooks, P., White, D. A. & Ali, S. T. Altered lipid accumulation in Nannochloropsis salina CCAP849/3 following EMS and UV induced mutagenesis. *Biotechnol. Reports* **7,** 87–94 (2015).
24. Elliott, L. G. *et al.* Establishment of a bioenergy-focused microalgal culture collection. *Algal Res.* **1,** 102–113 (2012).
25. Rawat, I., Ranjith Kumar, R., Mutanda, T. & Bux, F. Biodiesel from microalgae: A critical evaluation from laboratory to large scale production. *Appl. Energy* **103,** 444–467 (2013).
26. Ali Bahadar, M. B. K. Progress in energy from microalgae: A review. *Renew. Sustain. Energy Rev.* **27,** 128–148 (2013).
27. Ter Veld, F. Beyond the fossil fuel era: On the feasibility of sustainable electricity generation using biogas from microalgae. *Energy and Fuels* **26,** 3882–3890 (2012).
28. Pienkos, P. T. & Darzins, A. The promise and challenges of microalgal-derived biofuels. *Biofuels, Bioprod. Biorefining* **3,** 431–440 (2009).
29. Klok, a. J., Lamers, P. P., Martens, D. E., Draaisma, R. B. & Wijffels, R. H. Edible oils from microalgae: insights in TAG accumulation. *Trends Biotechnol.* **32,** 521–528 (2014).
30. Jobling, M. & Bendiksen, E. a. Dietary lipids and temperature interact to influence tissue fatty acid compositions of Atlantic salmon, Salmo salar L., parr. *Aquac. Res.* **34,** 1423–1441 (2003).
31. Saha, S. K. *et al.* Effect of various stress-regulatory factors on biomass and lipid production in microalga Haematococcus pluvialis. *Bioresour. Technol.* **128,** 118–124 (2013).
32. Combe, C. *et al.* Long-term adaptive response to high-frequency light signals in the unicellular photosynthetic eukaryote Dunaliella salina. *Biotechnol. Bioeng.* **112,** n/a–n/a (2015).
33. Feng, P., Deng, Z., Hu, Z. & Fan, L. Lipid accumulation and growth of Chlorella zofingiensis in flat plate photobioreactors outdoors. *Bioresour. Technol.* **102,** 10577–84 (2011).
34. Zemke, P. E., Wood, B. D. & Dye, D. J. Considerations for the maximum production rates of triacylglycerol from microalgae. *Biomass and Bioenergy* **34,** 145–151 (2010).
35. Griffiths, M. J., Hille, R. P. & Harrison, S. T. L. Lipid productivity, settling potential and fatty acid profile of 11 microalgal species grown under nitrogen replete and limited conditions. *J. Appl. Phycol.* **24,** 989–1001 (2012).
36. Wang, X. *et al.* Two-stage photoautotrophic cultivation to improve carbohydrate production in Chlamydomonas reinhardtii. *Biomass and Bioenergy* **74,** 280–287 (2015).
37. Benvenuti, G. *et al.* Selecting microalgae with high lipid productivity and photosynthetic

activity under nitrogen starvation. *J. Appl. Phycol.* **27,** 1425–1431 (2015).
38. Q. Hu M. Kawachi, I. Iwasaki, S. Miyachi, N. K. Ultrahigh-cell-density culture of a marine green alga Chlorococcum littorale in a flat-plate photobioreactor. *Appl Microbiol Biotechnol* **49,** 655–662 (1998).
39. Chihara, M., Nakayama, T., Inouye, I. & Kodama, M. Chlorococcum littorale, a New Marine Green Coccoid Alga (Chlorococcales, Chlorophyceae). *Arch. für Protistenkd.* **144,** 227–235 (1994).
40. Ota, M. *et al.* Fatty acid production from a highly CO2 tolerant alga, Chlorocuccum littorale, in the presence of inorganic carbon and nitrate. *Bioresour Technol* **100,** 5237–5242 (2009).
41. Breuer, G., Lamers, P. P., Martens, D. E., Draaisma, R. B. & Wijffels, R. H. Effect of light intensity, pH, and temperature on triacylglycerol (TAG) accumulation induced by nitrogen starvation in Scenedesmus obliquus. *Bioresour Technol* **143,** 1–9 (2013).
42. Han, F. *et al.* Enhanced lipid productivity of Chlorella pyrenoidosa through the culture strategy of semi-continuous cultivation with nitrogen limitation and pH control by CO2. *Bioresour. Technol.* **136,** 418–424 (2013).
43. Mandalam, R. K. & Palsson, B. Ø. Elemental balancing of biomass and medium composition enhances growth capacity in high-density Chlorella vulgaris cultures. *Biotechnol. Bioeng.* **59,** 605–611 (1998).
44. Adams, C., Godfrey, V., Wahlen, B., Seefeldt, L. & Bugbee, B. Understanding precision nitrogen stress to optimize the growth and lipid content tradeoff in oleaginous green microalgae. *Bioresour. Technol.* **131,** 188–194 (2013).
45. Klok, A. J. *et al.* A model for customising biomass composition in continuous microalgae production. *Bioresour. Technol.* **146,** 89–100 (2013).
46. Mulders, K. J. M., Lamers, P. P., Wijffels, R. H. & Martens, D. E. Dynamics of biomass composition and growth during recovery of nitrogen-starved Chromochloris zofingiensis. *Appl. Microbiol. Biotechnol.* **99,** 1873–1884 (2014).
47. Benvenuti, G; Bosma, R; Ji, F; Lamers, PP; Barbosa, MJ; Wijffels, R. Batch and semi-continuous microalgal TAG production in lab-scale and outdoor photobioreactors. *J. Appl. Phycol.* (2016). doi:10.1007/s10811-016-0897-1
48. Ota, M., Takenaka, M., Sato, Y., Lee Smith, R. & Inomata, H. Effects of light intensity and temperature on photoautotrophic growth of a green microalga, Chlorococcum littorale. *Biotechnol. Reports* **7,** 24–29 (2015).
49. Chisti, Y. Biodiesel from microalgae beats bioethanol. *Trends Biotechnol.* **26,** 126–131 (2008).
50. Pragya, N., Pandey, K. K. & Sahoo, P. K. A review on harvesting, oil extraction and biofuels production technologies from microalgae. *Renew. Sustain. Energy Rev.* **24,** 159–171 (2013).
51. Brennan, L., Blanco Fernandez, A., Mostaert, A. S. & Owende, P. Enhancement of BODIPY505/515 lipid fluorescence method for applications in biofuel-directed microalgae production. *J Microbiol Methods* **90,** 137–143 (2012).
52. Cooper, M. S., Hardin, W. R., Petersen, T. W. & Cattolico, R. A. Visualizing 'green oil' in live algal cells. *J Biosci Bioeng* **109,** 198–201 (2010).
53. Chen, W., Zhang, C., Song, L., Sommerfeld, M. & Hu, Q. A high throughput Nile red

method for quantitative measurement of neutral lipids in microalgae. *J Microbiol Methods* **77,** 41–47 (2009).
54. Chen, Z., Gong, Y., Fang, X. & Hu, H. Scenedesmus sp. NJ-1 isolated from Antarctica: a suitable renewable lipid source for biodiesel production. *World J Microbiol Biotechnol* **28,** 3219–3225 (2012).
55. Montero, M. F., Aristizábal, M. & García Reina, G. Isolation of high-lipid content strains of the marine microalga Tetraselmis suecica for biodiesel production by flow cytometry and single-cell sorting. *J. Appl. Phycol.* **23,** 1053–1057 (2010).
56. Laurens, L. M. L. & Wolfrum, E. J. Feasibility of Spectroscopic Characterization of Algal Lipids: Chemometric Correlation of NIR and FTIR Spectra with Exogenous Lipids in Algal Biomass. *BioEnergy Res.* **4,** 22–35 (2010).
57. Zhang, Q. *et al.* Towards high-throughput microfluidic Raman-activated cell sorting. *Analyst* **140,** 6163–6174 (2015).
58. De la Hoz Siegler, H., Ayidzoe, W., Ben-Zvi, A., Burrell, R. E. & McCaffrey, W. C. Improving the reliability of fluorescence-based neutral lipid content measurements in microalgal cultures. *Algal Res.* **1,** 176–184 (2012).
59. Govender, T., Ramanna, L., Rawat, I. & Bux, F. BODIPY staining, an alternative to the Nile Red fluorescence method for the evaluation of intracellular lipids in microalgae. *Bioresour Technol* **114,** 507–511 (2012).
60. Ota Y.; Watanabe, H.; Watanabe, M.; Sato, S.; Smith Jr., R.L.; Inomata, I., M. . K. Effect of Inorganic Carbon on Photoautotrophic Growth of Microalga Chlorococcum littorale. **25,** 492–498 (2009).
61. Gminski, R. *et al.* Genotoxic effects of three selected black toner powders and their dimethyl sulfoxide extracts in cultured human epithelial A549 lung cells in vitro. *Env. Mol Mutagen* **52,** 296–309 (2011).
62. Griffiths, M. J., Garcin, C., van Hille, R. P. & Harrison, S. T. L. Interference by pigment in the estimation of microalgal biomass concentration by optical density. *J. Microbiol. Methods* **85,** 119–123 (2011).
63. Pick, U. & Rachutin-Zalogin, T. Kinetic anomalies in the interactions of Nile red with microalgae. *J Microbiol Methods* **88,** 189–196 (2012).
64. Breuer, G., Lamers, P. P., Martens, D. E., Draaisma, R. B. & Wijffels, R. H. The impact of nitrogen starvation on the dynamics of triacylglycerol accumulation in nine microalgae strains. *Bioresour Technol* **124,** 217–226 (2012).
65. De la Hoz Siegler, H., McCaffrey, W. C., Burrell, R. E. & Ben-Zvi, a. Optimization of microalgal productivity using an adaptive, non-linear model based strategy. *Bioresour. Technol.* **104,** 537–546 (2012).
66. Xu, D. *et al.* Detection and quantitation of lipid in the microalga Tetraselmis subcordiformis (Wille) Butcher with BODIPY 505/515 staining. *Bioresour Technol* **127,** 386–390 (2013).
67. Pereira, H. *et al.* Isolation and Fatty Acid Profile of Selected Microalgae Strains from the Red Sea for Biofuel Production. *Energies* **6,** 2773–2783 (2013).
68. Velmurugan, N. *et al.* Evaluation of intracellular lipid bodies in Chlamydomonas reinhardtii strains by flow cytometry. *Bioresour Technol* **138,** 30–37 (2013).
69. Chisti, Y. & Yan, J. Energy from algae: Current status and future trends. *Appl. Energy* **88,**

3277–3279 (2011).
70. Chisti, Y. Biodiesel from microalgae beats bioethanol. *Trends Biotechnol* **26,** 126–131 (2008).
71. Mata, T. M., Martins, a a & Caetano, N. S. Microalgae for biodiesel production and other applications: A review. *Renew. Sustain. Energy Rev.* **14,** 217–232 (2010).
72. La, H. J. *et al.* Effective screening of Scenedesmus sp. from environmental microalgae communities using optimal sonication conditions predicted by statistical parameters of fluorescence-activated cell sorting. *Bioresour Technol* **114,** 478–483 (2012).
73. Breuer, G. *et al.* Superior triacylglycerol (TAG) accumulation in starchless mutants of Scenedesmus obliquus: (II) evaluation of TAG yield and productivity in controlled photobioreactors. *Biotechnol. Biofuels* **7,** 70 (2014).
74. Bišová, K. & Zachleder, V. Cell-cycle regulation in green algae dividing by multiple fission. *J. Exp. Bot.* **65,** 2585–2602 (2014).
75. Matsumura, K., Yagi, T., Hattori, A., Soloviev, M. & Yasuda, K. Using single cell cultivation system for on-chip monitoring of the interdivision timer in Chlamydomonas reinhardtii cell cycle. *J. Nanobiotechnology* **8,** 23 (2010).
76. Umen, J. G. & Goodenough, U. W. Control of cell division by a retinoblastoma protein homolog in Chlamydomonas. *Genes Dev.* **15,** 1652–1661 (2001).
77. Breuer, G. *et al.* Analysis of Fatty Acid Content and Composition in Microalgae. *J. Vis. Exp.* **80,** e50628 (2013).
78. Benito, V., Goñi-de-Cerio, F. & Brettes, P. BODIPY vital staining as a tool for flow cytometric monitoring of intracellular lipid accumulation in Nannochloropsis gaditana. *J. Appl. Phycol.* 233–241 (2014). doi:10.1007/s10811-014-0310-x
79. Ladner, D. A., Vardon, D. R. & Clark, M. M. Effects of shear on microfiltration and ultrafiltration fouling by marine bloom-forming algae. *J. Memb. Sci.* **356,** 33–43 (2010).
80. Praveenkumar, R., Shameera, K., Mahalakshmi, G., Akbarsha, M. A. & Thajuddin, N. Influence of nutrient deprivations on lipid accumulation in a dominant indigenous microalga Chlorella sp., BUM11008: Evaluation for biodiesel production. *Biomass and Bioenergy* **37,** 60–66 (2012).
81. Ho, S. H., Chen, C. Y. & Chang, J. S. Effect of light intensity and nitrogen starvation on CO 2 fixation and lipid/carbohydrate production of an indigenous microalga Scenedesmus obliquus CNW-N. *Bioresour. Technol.* **113,** 244–252 (2012).
82. Van Vooren, G. *et al.* Investigation of fatty acids accumulation in Nannochloropsis oculata for biodiesel application. *Bioresour. Technol.* **124,** 421–432 (2012).
83. Yuelu Jiang Antonietta Quigg, T. Y. Photosynthetic performance, lipid production and biomass composition in response to nitrogen limitation in marine microalgae. *Plant Physiol. Biochem.* **54,** 70–77 (2012).
84. John A. Berges David C. Mauzerall, Paul G. Falkowski, D. O. C. Differential Effects of Nitrogen Limitation on Photosynthetic Efficiency of Photosystems I and II in Microalgae. *Plant Physiol.* **110,** 689–696 (1996).
85. Erickson, R. a & Jimenez, R. Microfluidic cytometer for high-throughput measurement of photosynthetic characteristics and lipid accumulation in individual algal cells. *Lab Chip* **13,** 2893–901 (2013).
86. Liam Brennan Anika S. Mostaert, Philip Owende, A. B. F. Enhancement of BODIPY

505/515 lipid fluorescence method for applications in biofuel-directed microalgae production. *Journal of Microbiological Methods* **90,** 137–143 (2012).
87. Griffiths, M. J. & Harrison, S. T. L. Lipid productivity as a key characteristic for choosing algal species for biodiesel production. *J. Appl. Phycol.* **21,** 493–507 (2009).
88. Klok, A. J., Martens, D. E., Wijffels, R. H. & Lamers, P. P. Simultaneous growth and neutral lipid accumulation in microalgae. *Bioresour. Technol.* **134,** 233–243 (2013).
89. Bonente, G., Pippa, S., Castellano, S., Bassi, R. & Ballottari, M. Acclimation of Chlamydomonas reinhardtii to different growth irradiances. *J. Biol. Chem.* **287,** 5833–5847 (2012).
90. Dubois, M., Gilles, K. A., Hamilton, J. K., Rebers, P. A. & Smith, F. Colorimetric method for determination of sugars and related substances. *Anal. Chem.* **28,** 350–356 (1956).
91. Bradford, M. M. A rapid and sensitive method for the quantitation of microgram quantities of protein utilizing the principle of protein-dye binding. *Anal. Biochem.* **72,** 248–254 (1976).
92. Grobbelaar, J. U., Nedbal, L. & Tichý, V. Influence of high frequency light/dark fluctuations on photosynthetic characteristics of microalgae photoacclimated to different light intensities and implications for mass algal cultivation. *J. Appl. Phycol.* **8,** 335–343 (1996).
93. Benvenuti, G. *et al.* Microalgal TAG production strategies: why batch beats repeated-batch. *Biotechnol. Biofuels* **9,** 64 (2016).
94. Van Vooren, G. *et al.* Investigation of fatty acids accumulation in Nannochloropsis oculata for biodiesel application. *Bioresour. Technol.* **124,** 421–32 (2012).
95. Davis, R., Aden, A. & Pienkos, P. T. Techno-economic analysis of autotrophic microalgae for fuel production. *Appl. Energy* **88,** 3524–3531 (2011).
96. Csögör, Z., Herrenbauer, M., Perner, I., Schmidt, K. & Posten, C. Design of a photo-bioreactor for modelling purposes. *Chem. Eng. Process. Process Intensif.* **38,** 517–523 (1999).
97. Bernard, O. Hurdles and challenges for modelling and control of microalgae for CO 2 mitigation and biofuel production. *J. Process Control* **21,** 1378–1389 (2011).
98. Slegers, P. M., van Beveren, P. J. M., Wijffels, R. H., van Straten, G. & van Boxtel, A. J. B. Scenario analysis of large scale algae production in tubular photobioreactors. *Appl. Energy* **105,** 395–406 (2013).
99. Breuer, G., Lamers, P. P., Janssen, M., Wijffels, R. H. & Martens, D. E. Opportunities to improve the areal oil productivity of microalgae. *Bioresour. Technol.* **186,** 294–302 (2015).
100. Gombert, A. K. & Nielsen, J. Mathematical modelling of metabolism. *Curr. Opin. Biotechnol.* **11,** 180–186 (2000).
101. Baquerisse, D., Nouals, S., Isambert, A., dos Santos, P. F. & Durand, G. Modelling of a continuous pilot photobioreactor for microalgae production. *Prog. Ind. Microbiol.* **35,** 335–342 (1999).
102. Slegers, P. M., Lösing, M. B., Wijffels, R. H., van Straten, G. & van Boxtel, A. J. B. Scenario evaluation of open pond microalgae production. *Algal Res.* **2,** 358–368 (2013).
103. Pruvost, J., Van Vooren, G., Cogne, G. & Legrand, J. Investigation of biomass and lipids production with Neochloris oleoabundans in photobioreactor. *Bioresour. Technol.* **100,**

5988–5995 (2009).
104. Fábregas, J., Maseda, A., Domínguez, A., Ferreira, M. & Otero, A. Changes in the cell composition of the marine microalga, Nannochloropsis gaditana, during a light:dark cycle. *Biotechnol. Lett.* **24,** 1699–1703 (2002).
105. Torzillo, G., Sacchi, a., Materassi, R. & Richmond, a. Effect of temperature on yield and night biomass loss in Spirulina platensis grown outdoors in tubular photobioreactors. *J. Appl. Phycol.* **3,** 103–109 (1991).
106. Johnson, X. & Alric, J. Central carbon metabolism and electron transport in chlamydomonas reinhardtii: Metabolic constraints for carbon partitioning between oil and starch. *Eukaryot. Cell* **12,** 776–793 (2013).
107. Nascimento, I. A. *et al.* Screening Microalgae Strains for Biodiesel Production: Lipid Productivity and Estimation of Fuel Quality Based on Fatty Acids Profiles as Selective Criteria. *Bioenergy Res.* **6,** 1–13 (2013).
108. Rodolfi, L. *et al.* Microalgae for oil: Strain selection, induction of lipid synthesis and outdoor mass cultivation in a low-cost photobioreactor. *Biotechnol. Bioeng.* **102,** 100–112 (2009).
109. Benvenuti, G. *et al.* Microalgal triacylglycerides production in outdoor batch-operated tubular PBRs. *Biotechnol. Biofuels* **8,** 100 (2015).
110. Bondioli, P. *et al.* Oil production by the marine microalgae Nannochloropsis sp. F&M-M24 and Tetraselmis suecica F&M-M33. *Bioresour. Technol.* **114,** 567–572 (2012).
111. Rodolfi, L. *et al.* Microalgae for oil: strain selection, induction of lipid synthesis and outdoor mass cultivation in a low-cost photobioreactor. *Biotechnol. Bioeng.* **102,** 100–12 (2009).
112. San Pedro, A., González-López, C. V., Acién, F. G. & Molina-Grima, E. Marine microalgae selection and culture conditions optimization for biodiesel production. *Bioresour. Technol.* **134,** 353–361 (2013).
113. Tredici, M. R. & Zlttelli, G. C. Efficiency of sunlight utilization: Tubular versus flat photobioreactors. *Biotechnol. Bioeng.* **57,** 187–197 (1998).
114. Norihide Kurano, S. M. Selection of Microalgal Growth Model for Describing Specific Growth Rate-Light Response Using Extended Information Criterion. *J. Biosci. Bioeng.* **100,** 403–408 (2005).
115. Qiang, H., Zarmi, Y. & Richmond, A. Combined effects of light intensity, light-path and culture density on output rate of Spirulina platensis (Cyanobacteria). *Eur. J. Phycol.* **33,** 165–171 (1998).
116. de Vree, J. H., Bosma, R., Janssen, M., Barbosa, M. J. & Wijffels, R. H. Comparison of four outdoor pilot-scale photobioreactors. *Biotechnol. Biofuels* **8,** 215 (2015).
117. Rigollier, C., Lefèvre, M. & Wald, L. The method Heliosat-2 for deriving shortwave solar radiation from satellite images. *Sol. Energy* **77,** 159–169 (2004).
118. McCree, K. J. in *Physiological Plant Ecology* 41–55 (Springer Berlin, 1981). doi:10.1007/978-3-642-68090-8_3
119. MacIntyre, H. L., Kana, T. M., Anning, T. & Geider, R. J. Photoacclimation of photosynthesis irradiance response curves and photosynthetic pigments in microalgae and cyanobacteria. *J. Phycol.* **38,** 17–38 (2002).

120. Kliphuis, A. M. J. *et al.* Metabolic modeling of Chlamydomonas reinhardtii: Energy requirements for photoautotrophic growth and maintenance. *J. Appl. Phycol.* **24,** 253–266 (2012).
121. Spolaore, P., Joannis-Cassan, C., Duran, E. & Isambert, A. Commercial applications of microalgae. *J. Biosci. Bioeng.* **101,** 87–96 (2006).
122. Pulz, O. & Scheibenbogen, K. Photobioreactors : Design and Performance with Respect to Light Energy Input. *Adv. Biochem. Eng. Biotechnol.* **59,** 123–152 (1998).
123. Fang, S. C., De Los Reyes, C. & Umen, J. G. Cell size checkpoint control by the retinoblastoma tumor suppressor pathway. *PLoS Genet.* **2,** 1565–1579 (2006).
124. Hlavova, M., Turoczy, Z. & Bisova, K. Improving microalgae for biotechnology - From genetics to synthetic biology. *Biotechnol. Adv.* **33,** 1194–1203 (2015).
125. Strasser, B. J. *et al.* Comparison of light induced and cell cycle dependent changes in the photosynthetic apparatus: A uorescence induction study on the green alga Scenedesmus obliquus. *Photosynth. Res.* 217–227 (1999).
126. de Winter, L., Klok, A. J., Cuaresma Franco, M., Barbosa, M. J. & Wijffels, R. H. The synchronized cell cycle of Neochloris oleoabundans and its influence on biomass composition under constant light conditions. *Algal Res.* **2,** 313–320 (2013).
127. Mooij, P. R., Stouten, G. R., Loosdrecht, M. C. M. Van & Kleerebezem, R. Ecology-based selective environments as solution to contamination in microalgal cultivation. *Curr. Opin. Biotechnol.* **33,** 46–51 (2015).
128. Peter R. Mooij, Gerben R. Stouten, Jelmer Tamis, M. C. M. van L. and R. K. Survival of the fattest. *energy environemntal Sci.* **6,** 3404–3406 (2013).
129. Kawecki, T. J. *et al.* Experimental evolution. *Trends Ecol. Evol.* **27,** 547–560 (2012).
130. Gangl, D. *et al.* Biotechnological exploitation of microalgae. *J. Exp. Bot.* **66,** 6975–6990 (2015).
131. Bull, J. J. & Collins, S. Algae for biofuel: Will the evolution of weeds limit the enterprise? *Evolution (N. Y).* **66,** 2983–2987 (2012).
132. Cazzaniga, S. *et al.* Domestication of the green alga Chlorella sorokiniana: reduction of antenna size improves light-use efficiency in a photobioreactor. *Biotechnol. Biofuels* **7,** 157 (2014).
133. Perrineau, M. M. *et al.* Evolution of salt tolerance in a laboratory reared population of Chlamydomonas reinhardtii. *Environ. Microbiol.* **16,** 1755–1766 (2014).
134. Collier, J. L. Flow cytometry and the single cell in phycology. *J. Phycol.* **36,** 628–644 (2000).
135. Hazel M. Davey, D. B. K. Flow Cytometry and Cell Sorting of Heterogeneous Microbial Populations: the Importance of Single-Cell Analyses. *Microbiological Reviews* **60,** 641–696 (1996).
136. Bonente, G. *et al.* Mutagenesis and phenotypic selection as a strategy toward domestication of Chlamydomonas reinhardtii strains for improved performance in photobioreactors. *Photosynth. Res.* **108,** 107–120 (2011).
137. Chapman, G. V. Instrumentation for flow cytometry. *J. Immunol. Methods* **243,** 3–12 (2000).
138. Rioboo, C., O'Connor, J. E., Prado, R., Herrero, C. & Cid, Á. Cell proliferation alterations in Chlorella cells under stress conditions. *Aquat. Toxicol.* **94,** 229–237 (2009).

139. Muller, S. & Nebe-Von-Caron, G. Functional single-cell analyses: Flow cytometry and cell sorting of microbial populations and communities. *FEMS Microbiol. Rev.* **34,** 554–587 (2010).
140. Cabanelas, I. T. D., Fernandes, C., Kleinegris, D. M. M., Wijffels, R. H. & Barbosa, M. J. Cell diameter doesn't affect lipid productivity of Chlorococcum littorale. *Algal Res.* (2015). doi:10.1016/j.algal.2016.02.002
141. Seed, C. E., Larma, I. & Tomkins, J. L. Cell size selection in Chlamydomonas reinhardtii gametes using fluorescence activated cell sorting. *Algal Res.* **16,** 93–101 (2016).
142. Hyka, P., Lickova, S., Přibyl, P., Melzoch, K. & Kovar, K. Flow cytometry for the development of biotechnological processes with microalgae. *Biotechnol. Adv.* **31,** 2–16 (2013).
143. Kwok, A. & Wong, J. Cellulose Synthesis Is Coupled to Cell Cycle Progression at G 1 in the Dinoflagellate Crypthecodinium cohnii. *Plant Physiol.* **131,** 1681–1691 (2003).
144. Hutter, K.-J. & Eipel, H. E. Flow cytometric determinations of cellular substances in algae, bacteria, moulds and yeasts. *Antonie Van Leeuwenhoek* **44,** 269–282 (1978).
145. Vítová, M., Hendrychová, J., Cepák, V. & Zachleder, V. Visualization of DNA-containing structures in various species of Chlorophyta, Rhodophyta and Cyanophyta using SYBR Green I dye. *Folia Microbiol. (Praha).* **50,** 333–340 (2005).
146. Tijssen, JPF; Beekes, HW and van Steveninck, J. Localization of polyphosphates in Saccharomyces fragilis, as revealed by 4',6-diamidino-2-phenylindole fluorescence. *Yeast* **721,** 394–398 (1982).
147. Adler, N. I. E. A., Ansen, M. E. S. C. & Ltenburger, R. O. L. F. A. Flow Cytometry As a Tool To Study Phytotoxic Modes of Action. **26,** 297–306 (2007).
148. Dong Xu Feng Li, Xiao Fan, Xiaowen Zhang, Naihao Ye, Shanli Moua, Chengwei Liang, Demao Li, Z. G. Detection and quantitation of lipid in the microalga Tetraselmis subcordiformis (Wille) Butcher with BODIPY 505/515 staining. *Bioresour. Technol.* **127,** 386–390 (2013).
149. Mou, Shanli; Xu, Dong; Ye, Naihao;Zhang, X. & Liang, Chengwei; Liang, Qiang; Zheng, Zhou; Zhuang, Zhimeng; Miao, J. Rapid estimation of lipid content in an Antarctic ice alga (Chlamydomonas sp.) using the lipophilic fluorescent dye BODIPY505/515. *J. Appl. Phycol.* **24,** 1169–1176 (2011).
150. Song-Lin Niu Pascal Retailleau, Jack Harrowfield, Raymond Ziessel, G. U. New insights into the solubilization of Bodipy dyes. *Tetrahedron Lett.* **50,** 3840–3844 (2009).
151. Horst, I. *et al.* Treatment of Phaeodactylum tricornutum cells with papain facilitates lipid extraction. *J. Biotechnol.* **162,** 40–49 (2012).
152. Harwati, T. U., Willke, T. & Vorlop, K. D. Characterization of the lipid accumulation in a tropical freshwater microalgae Chlorococcum sp. *Bioresour. Technol.* **121,** 54–60 (2012).
153. Isleten-Hosoglu, M., Gultepe, I. & Elibol, M. Optimization of carbon and nitrogen sources for biomass and lipid production by Chlorella saccharophila under heterotrophic conditions and development of Nile red fluorescence based method for quantification of its neutral lipid content. *Biochem. Eng. J.* **61,** 11–19 (2012).
154. Popovich, C. a. *et al.* Neochloris oleoabundans grown in enriched natural seawater for biodiesel feedstock: Evaluation of its growth and biochemical composition. *Bioresour. Technol.* **114,** 287–293 (2012).

155. Songcui Wu Aiyou Huang, Li Huan, Linwen He, Apeng Lin, Jianfeng Niu, Guangce Wang, B. Z. Detection of intracellular neutral lipid content in the marine microalgae Prorocentrum micans and Phaeodactylum tricornutum using Nile red and BODIPY 505/515. *J Appl Phycol* (2013).
156. Wang, T. *et al.* Quantitative dynamics of triacylglycerol accumulation in microalgae populations at single-cell resolution revealed by Raman microspectroscopy. *Biotechnol. Biofuels* **7,** 58 (2014).
157. Ji, Y. *et al.* Raman spectroscopy provides a rapid, non-invasive method for quantitation of starch in live, unicellular microalgae. *Biotechnol. J.* **9,** 1512–1518 (2014).
158. Hubálek, Z. Protectants used in the cryopreservation of microorganisms. *Cryobiology* **46,** 205–229 (2003).
159. Taylor, R. & Fletcher, R. L. Cryopreservation of eukaryotic algae - A review of methodologies. *J. Appl. Phycol.* **10,** 481–501 (1998).

Summary
Samenvatting
Resumen
Resumo

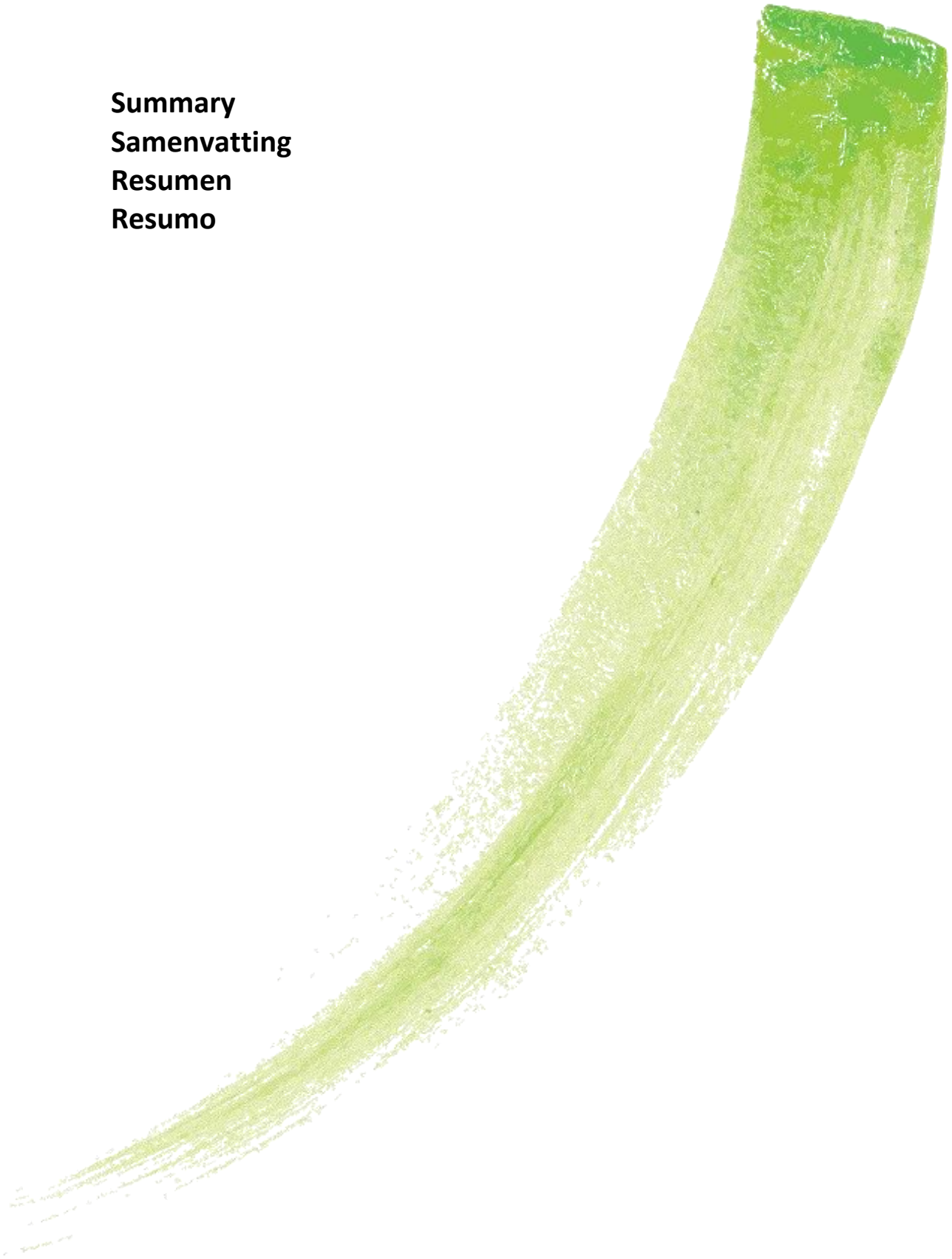

Summary

In **chapter 1** we introduce microalgae, photosynthetic microorganisms with potential to replace commodities (such as food, feed, chemicals and fuels). Production costs are still high, reason why microalgae are still only economically feasible for niche markets. We suggest to borrow the concept of plant domestication to select industrial microalgae cells. Two approaches can be successfully used to domesticate microalgae: adaptive laboratory evolution (ALE) and fluorescence assisted cell sorting (FACS). ALE takes advantage of the natural adaptability of microorganisms to different environments, while FACS actually select cells with specific phenotypes. This thesis aimed to select cells of *Chlorococcum littorale* with improved phenotypes, assuming that these cells could establish new populations with increased industrial performance.

In **Chapter 2** we wanted to know what happened during time to biomass and lipid productivities of *Chlorococcum littorale* repeatedly subjected to N-starvation. We tested 2 different cycles of N-starvation, short (6 days) and long (12 days). Short cycles didn't affect lipid productivity, highlighting the potential of *C. littorale* to be produced in semi-continuous cultivation. Repeated cycles of N-starvation could have caused adaptations of the strain. Hence, we also discussed the implications of using repeated N-starvation for adaptive laboratory evolution (ALE) experiments. **Chapter 3** introduces a method to detect and to select microalgae cells with increased lipid content. Here we optimized a method to rapidly screen and sort lipid rich cells of *C. littorale* using FACS. The method requires only the fluorescence dye $Bodipy_{505/515}$ dissolved in ethanol, which is added directly to the diluted microalgae culture. The method was designed to maintain cellular viability so the cells could be used to produce new inoculum. In **chapter 4** we evaluated a question that emerged while deciding which criteria to use to sort lipid-rich cells: does cellular size affects lipid productivity of *C. littorale*? We hypothesized that cells with different diameters have different division rates, which could affect lipid productivity. Therefore, we assessed the influence of cell diameter, as a sorting parameter, on both biomass and lipid productivity of *Chlorococcum littorale* (comparing populations before and after sorting, based on different diameters). Results showed that the size of vegetative cells doesn't affect the lipid productivity of *C. littorale*. In **chapter 5** we present a strategy to sort cells of *C. littorale* with increased TAG productivity using the method developed at chapter 3. Our strategy consisted of sorting cells with a high lipid/cell content after a period of N-starvation. The sorted populations were used to start another round of N-starvation followed again by sorting, which was done in 5 subsequent rounds. Both the original and the sorted population with the highest lipid productivity (namely, S5) were compared under simulated Dutch summer conditions. The results confirmed our data from experiments done under continuous light: S5 showed a double TAG productivity. Our results showed also that the selected phenotype was stable (1.5 year after sorting) and with potential to be used under industrial conditions. In **chapter 6** we extrapolated our results (indoor and outdoor) to other climate conditions. We first validated, for *C. littorale*, a previously developed model that describes the carbon partitioning of microalgae under N-starvation (i.e. which components are photosynthetically produced by the cells in the absence of nitrogen). Next, we ran simulations changing the light

conditions to four different locations worldwide (the Netherlands, Norway, Brazil and Spain) to estimate both biomass and TAG productivities. Results indicated that biomass yields were reduced at locations with higher light intensities (Brazil/Spain) when compared with locations with lower light intensities (Norway/Netherlands). This might be due to photoinhibition, which is a common effect of high light intensities on microalgae. TAG yields, on the other hand, were not affected by the locations. The choice of location should not be based on light intensity, but on how stable irradiation is, since only Brazil/Spain could sustain year-round microalgae phototrophic production. **Chapter 7** is the general discussion of the thesis, demonstrating that both ALE and FACS are effective approaches to select industrial microalgae cells. We also present our view on how ALE and FACS could further improve microalgae strains for industry.

All things considered, this thesis filled gaps from previous research on how to select microalgae cells with confirmed increased performance under simulated outdoors conditions. We believe that the knowledge from this thesis can be used to select industrial microalgae cells.

Samenvatting

In **hoofdstuk 1** introduceren we microalgen, fotosynthetische micro-organismen met de potentie om grondstoffen te vervangen (zoals voedsel, veevoer, chemicaliën en brandstoffen). De productiekosten zijn nog steeds hoog, daarom is de productie economisch alleen nog maar haalbaar voor nichemarkten. Wij stellen voor om het concept van plantenveredeling te lenen om industriële microalgen cellen te selecteren. Twee benaderingen kunnen met succes worden gebruikt om microalgen te veredelen: *adaptive laboratory evolution* (ALE) en *fluorescence assisted cell sorting* (FACS). ALE maakt gebruik van het natuurlijke aanpassingsvermogen van microorganismen aan verschillende omgevingen, terwijl FACS cellen met specifieke fenotypes selecteert. Dit proefschrift is gericht op het selecteren van *Chlorococcum littorale* cellen met verbeterde fenotypes, in de veronderstelling dat deze cellen nieuwe bevolkingsgroepen met een verhoogde industriële prestaties kunnen vormen.

In **Hoofdstuk 2** wilden we weten wat er gebeurde in de tijd met biomassa en lipide productiviteiten van *Chlorococcum littorale* die herhaaldelijk onderworpen zijn aan N-uithongering (d.w.z. zonder stikstof in het groeimedium). We testten 2 verschillende cycli van N-uithongering, kort (6 dagen) en lang (12 dagen). Korte cycli hadden geen invloed op de lipide productiviteit, dit geeft de potentie aan om *C. littorale* in semi-continue teelt te produceren. Herhaalde cycli van N-uithongering kunnen aanpassingen van de stam veroorzaken. Vandaar dat we ook de gevolgen van het gebruik van herhaalde N-uithongering voor ALE experimenten bespraken. **Hoofdstuk 3** introduceert een methode voor het opsporen en selecteren van microalgen cellen met een verhoogde vetgehalte. We optimaliseerden een methode waarmee we snel lipide rijke cellen van *C. littorale* met behulp van FACS kunnen screenen en sorteren. De werkwijze vereist alleen de fluorescente kleurstof Bodipy505/515 opgelost in ethanol, die aan de verdunde microalgen cultuur wordt toegevoegd. De methode is ontworpen om cellulaire levensvatbaarheid te behouden, zodat de cellen kunnen worden gebruikt als nieuwe entstof. In **hoofdstuk 4** onderzochten we een vraag die naar voren kwam, tijdens het nemen van de beslissing welke criteria te gebruiken om lipide-rijke cellen te sorteren: beïnvloedt cellulaire grootte de lipide productiviteit van *C. littorale*? Onze hypothese was dat cellen met verschillende diameters een verschillende delingsnelheid hebben, die van invloed kunnen zijn op de lipide productiviteit. Daarom onderzochten we de invloed van de celdiameter als sorteringsparameter, op zowel biomassa als lipide productiviteit van *Chlorococcum littorale* (door populaties voor en na sortering te vergelijken, op basis van verschillende diameters). De resultaten toonden aan dat de grootte van vegetatieve cellen de lipide productiviteit van *C. littorale* niet beïnvloedt. In **hoofdstuk 5** presenteren we een strategie om cellen van *C. littorale* met een verhoogde triacylglycerol (TAG) productiviteit te sorteren volgens de methode ontwikkeld in hoofdstuk 3. Onze strategie bestond uit het sorteren van cellen met een hoge lipide per cel inhoud na een periode van N-uithongering. De gesorteerde populaties werden gebruikt om een nieuwe ronde van N-uithongering te starten, gevolgd door sortering, die werd uitgevoerd in 5 opeenvolgende ronden. Zowel de oorspronkelijke als de gesorteerde populatie met de hoogste lipide productiviteit (namelijk S5) werden vergeleken onder gesimuleerde Nederlandse zomerse weersomstandigheden. De resultaten bevestigden onze data uit

experimenten die waren uitgevoerd onder continu licht: S5 vertoonde een dubbele TAG productiviteit. Onze resultaten toonden ook aan dat het geselecteerde fenotype stabiel was (1,5 jaar na sortering) en met potentie om onder industriële omstandigheden te gebruiken. In **hoofdstuk 6** hebben we onze resultaten (binnen en buiten) geëxtrapoleerd naar andere klimatologische omstandigheden. We hebben eerst gevalideerd voor *C. littorale* een eerder ontwikkeld model dat de koolstof partitionering van microalgen onder stikstof-uithongering beschrijft (d.w.z. welke componenten fotosynthetisch geproduceerd worden door de cellen in afwezigheid van stikstof). Vervolgens we simuleerden het veranderen van de lichtomstandigheden naar vier verschillende locaties (Nederland, Noorwegen, Brazilië en Spanje), om zowel de biomassa als de TAG productiviteiten te schatten. De resultaten gaven aan dat de opbrengsten van biomassa werden gereduceerd op locaties met hogere lichtintensiteiten (Brazilië/Spanje) in vergelijking met locaties met een lagere lichtintensiteit (Noorwegen/Nederland). Dit zou het gevolg kunnen zijn van fotinhibitie, wat een algemeen effect van hoge lichtintensiteiten op microalgen is. Daarentegen werden de TAG opbrengsten niet beïnvloed door de locaties. De keuze van de locatie mag niet worden gebaseerd op de lichtintensiteit, maar op hoe stabiel de bestraling is, omdat alleen in Brazilië/Spanje microalgen het hele jaar fototrofe productie in stand kunnen houden. **Hoofdstuk 7** is de algemene discussie van het proefschrift, waaruit blijkt dat zowel ALE en FACS effectieve methodes zijn om industriële microalgen cellen te selecteren. We presenteren ook onze visie hoe ALE en FACS microalgen stammen voor de industrie verder kunnen verbeteren.

Alles bij elkaar genomen, dit proefschrift vulde lacunes in eerder onderzoek hoe microalgen cellen te selecteren met bevestigde verbeterde prestatie onder gesimuleerde buiten omstandigheden. Wij zijn van mening dat de kennis uit dit proefschrift kan worden gebruikt om industriële microalgen cellen te selecteren.

Resumen

En el **capítulo 1** se introducen las microalgas, microorganismos fotosintéticos con potencial para reemplazar los productos básicos (tales como alimentos, piensos, productos químicos y combustibles). Los costes de producción siguen siendo elevados, por lo que las microalgas son, hoy en día, económicamente factibles únicamente en nichos de mercado. Sugerimos el tomar prestado el concepto de domesticación de plantas para nuestra aplicación, seleccionando así las células industriales de microalgas. Dos enfoques pueden ser utilizados con éxito para domesticar microalgas: evolución adaptativa en laboratorio (ALE) y la Selección celular assistida por fluorescencia (FACS). El enfoque ALE aprovecha la capacidad de adaptación natural de los microorganismos a diferentes ambientes, mientras que FACS en realidad selecciona células con fenotipos específicos. Esta tesis tuvo como objetivo seleccionar células de *Chlorococcum littorale* con fenotipos mejorados, en el supuesto de que estas células podrían establecer nuevas poblaciones con un mayor rendimiento industrial.

En el **capítulo 2** queríamos saber lo que le ocurría con el tiempo a las productividades de biomasa y lípidos de *C. littorale* sometida repetidamente a inanición celular de nitrógeno (N-inanición). Hemos probado 2 ciclos diferentes de N-inanición: cortos (6 días) y largos (12 días). Los ciclos cortos no afectaron la productividad lipídica, destacando el potencial de *C. littorale* a ser producido en cultivo semicontínuo. Ciclos repetidos de N-inanición podrían causar adaptaciones de la cepa, por tanto, también discutimos las implicaciones del uso repetido de N-inanición en los experimentos ALE. El **capítulo 3** presenta un método para detectar y seleccionar aquellas células de microalgas con un contenido de lípidos aumentado. Aquí hemos optimizado un método para la detección y clasificación rápida de células de *C. littorale* ricas en lípidos mediante FACS. El método requiere únicamente el colorante de fluorescencia Bodipy505 / 515 disuelto en etanol, que se añade directamente al cultivo de microalgas diluido. El método fue diseñado para mantener la viabilidad celular por lo que las células podrían ser utilizadas para producir nuevo inóculo. En el **capítulo 4** se evaluó una pregunta que surgió al decidir qué criterios utilizar para clasificar las células ricas en lípidos: ¿Afecta el tamaño celular a la productividad de lípidos de *C. littorale*? Nuestra hipótesis era que las células con distinto diámetro tienen diferentes tasas de división, lo que podría afectar a la productividad de lípidos. Por lo tanto, se evaluó la influencia del diámetro de las células, como parámetro de clasificación, tanto en la productividad de biomasa como en la lipídica de *Chlorococcum littorale* (comparando las poblaciones antes y después de la clasificación, sobre la base de diferentes diámetros). Los resultados mostraron que el tamaño de las células vegetativas no afecta a la productividad de lípidos de *C. littorale*. En el **capítulo 5** se presenta una estrategia para clasificar aquellas células de *C. littorale* con un aumento en la productividad de triacilglicéridos (TAGs) utilizando el método desarrollado en el capítulo 3. Nuestra estrategia consistió en clasificar las células con un alto contenido de lípidos por célula, después de un período de N-inanición. Las poblaciones clasificadas se utilizaron para iniciar una nueva ronda de N-inanición seguida posteriormente por una nueva clasificación, lo cual se hizo durante 5 rondas. Tanto la población original como aquella población clasificada con la mayor productividad de lípidos (es decir, tras la quinta ronda: S5) se compararon bajo condiciones simuladas del verano holandés.

Los resultados confirmaron nuestros datos de los experimentos realizados bajo luz continua: S5 mostró una productividad de TAG duplicada. Nuestros resultados mostraron también que además el fenotipo seleccionado se mantuvo estable (1,5 año después de la clasificación) y con potencial para ser utilizado en condiciones industriales. En el **capítulo 6** se extrapolaron los resultados (de cultivo en interior y en exterior) a otras condiciones climáticas. En primer lugar, se validó para *C. littorale* un modelo desarrollado previamente que describe la partición de carbono de microalgas bajo N-inanición (es decir, qué componentes son fotosintéticamente producidos por las células en ausencia de nitrógeno). A continuación, simulamos las condiciones de luz de cuatro lugares diferentes (los Países Bajos, Noruega, Brasil y España) para estimar las productividades de biomasa y de TAGs. Los resultados indicaron que los rendimientos de biomasa se redujeron en lugares con altas intensidades de luz (Brasil / España), en comparación con aquellos con bajas intensidades de luz (Noruega / Países Bajos). Esto podría ser debido a la fotoinhibición, efecto común debido a altas intensidades de luz en microalgas. Los rendimientos de TAG, por otra parte, no se vieron afectados por la localización. La elección del lugar no debe basarse en la intensidad de la luz, sino en la estabilidad de la irradiación, ya que sólo Brasil / España podrían sostener una producción fototrófica de microalgas durante todo el año. El **capítulo 7** es la discusión general de la tesis, que demuestra que tanto ALE como FACS son métodos eficaces para seleccionar células de microalgas industriales. También presentamos nuestra opinión sobre cómo ALE y FACS podrían mejorar aún más las cepas de microalgas para la industria.

En resumen, esta tesis subsana carencias de investigaciones anteriores en la selección de células de microalgas con un mayor rendimiento confirmado en condiciones simuladas de exterior. Creemos que el conocimiento de esta tesis se puede utilizar para seleccionar células de microalgas industriales.

Resumo

No **capítulo 1** apresentamos as microalgas, microorganismos fotossintéticos com potencial para substituir *commodities* (tais como alimentos, rações animais, produtos químicos e combustíveis). Os custos de produção são ainda elevados, razão pela qual microalgas ainda são apenas economicamente viável em certos nichos de mercado. Sugerimos pedir emprestado o conceito de domesticação de plantas para selecionar células industriais de microalgas. Duas abordagens podem ser usadas com sucesso para domesticar microalgas: adaptive laboratory evolution (ALE – evolução adaptativa em laboratório) e fluorescence assisted cell sorting (FACS – seleção de células assistida por fluorescência). ALE tira vantagem da capacidade natural de adaptação de microrganismos a ambientes diferentes, enquanto que FACS seleciona de fato células com fenótipos específicos. Esta tese teve como objetivo selecionar células de *Chlorococcum littorale* com fenótipos melhorados, presumindo que essas células poderiam estabelecer novas populações com maior desempenho industrial.

No **Capítulo 2** quisemos saber o que aconteceu com as produtividades (biomassa e lípidos) de *Chlorococcum littorale* repetidamente submetida a deprivação de nitrogênio (N-deprivação). Testamos 2 ciclos diferentes de N-deprivação, curtos (6 dias) e longos (12 dias). Ciclos curtos não afetetaram a produtividade de lipídios, destacando o potencial de *C. littorale* de ser produzida em cultivos semi-contínuos. Os ciclos repetidos de N-deprivação poderiam, em teoría, causar adaptações na estirpe. Por isso, também discutimos as implicações do uso de ciclos repetidos de N-deprivação para experimentos ALE. O c**apítulo 3** apresenta um método para detectar e selecionar células de microalgas com teor de lípidos aumentado. Aqui nós otimizamos um método para rastrear e selecionar rapidamente células de *C. littorale* ricas em lípidos utilizando FACS. O método requer apenas o corante de fluorescência Bodipy505/515 dissolvido em etanol, o qual é adicionado diretamente à cultura diluída de microalgas. O método foi concebido para manter a viabilidade celular e poder ser utilizado para produzir um novo inóculo. No **capítulo 4**, avaliamos uma questão que surgiu quando decidíamos quais critérios utilizar para selecionar as células ricas em lípidos: o tamanho celular afeta a produtividade lipídica de *C. littorale*? Trabalhamos com a hipótese de que células com diâmetros diferentes têm taxas diferentes de divisão, o que poderia afetar a produtividade de lípidos. Portanto, avaliamos a influência do diâmetro das células, como um parâmetro de seleção (*sorting*), sobre as produtividades em biomassa e em lípidos de *Chlorococcum littorale* (comparando populações antes e após a seleção, com base em diferentes diâmetros). Os resultados mostraram que o tamanho das células vegetativas não afeta a produtividade lipídica de *C. littorale*. No **capítulo 5** apresentamos uma estratégia para selecionar (*sorting*) células de *C. littorale* com produtividade de lípidos aumentada, utilizando o método desenvolvido no capítulo 3. A nossa estratégia consistiu em selecionar células com um elevado conteúdo de lípidos por célula depois de um período de N-deprivação. As populações selecionadas foram usadas para iniciar uma nova rodada de N-deprivação seguido novamente por outra rodada de seleção, o que foi feito em 5 rodadas subsequentes. Tanto a população original e a população classificada com a mais alta produtividade de lipídios (ou seja, S5, após 5 rodadas de seleção) foram comparadas em condições laboratoriais controladas (simulando o verão holandês). Os

resultados confirmaram os nossos dados de experimentos feitos sob luz contínua: S5 mostrou uma produtividade de lípidos duplicada. Nossos resultados mostraram também que o fenótipo selecionado é estável (1,5 ano após a seleção) e com potencial para ser usado em condições industriais. No **capítulo 6** extrapolamos os nossos resultados (em escala de laboratório e escala piloto/*outdoors*) a outras condições climáticas. Primeiramente validamos, para *C. littorale*, um modelo previamente desenvolvido que descreve a partição de carbono de microalgas sob N-deprivação (isto é, quais são os componentes fotossinteticamente produzidos pelas células na ausência de nitrogênio). Em seguida, fizemos simulações mudando as condições de luz a quatro locais diferentes (Países Baixos, Noruega, Brasil e Espanha) para estimar as produtividades de biomassa e de lípidos. Os resultados indicaram que a produção de biomassa foi reduzida em locais com maior intensidade luminosa (Brasil/Espanha), quando comparada com localidades com intensidades luminosas mais baixas (Noruega/Holanda). Isso pode ser devido a fotoinibição, que é um efeito comum de alta intensidade de luz sobre microalgas. Contudo, os rendimentos de lípidos (i.e., lípidos/fótons), não foram afetados pelas localidades. A escolha do local não deve basear-se na intensidade luminosa, mas em o quão estável é a irradiação, uma vez que só o Brasil/Espanha poderiam sustentar produção fototrófica de microalgas durante todo o ano. O **capítulo 7** é a discussão geral da tese, demonstrando que tanto ALE e FACS são abordagens eficazes para selecionar células industriais de microalgas. Também apresentamos nosso ponto de vista sobre como ALE e FACS poderiam melhorar ainda mais estirpes de microalgas para a indústria.

Em resumo, esta tese preencheu lacunas de pesquisas anteriores para selecionar células de microalgas com confirmado maior desempenho em escala de produção. Acreditamos que o conhecimento desta tese pode ser utilizado para selecionar células industriais de microalgas.

Acknowledgments
Dankwoord
Agradecimientos
Agradecimentos

Here we are, at the final and most exciting words of this thesis.

First, to René. Bedankt dat jij mij geaccepteerd hebt. Het was een fantastische ervaring om bij BPE te promoveren en het was ook fantastisch om jou als promotor te hebben. Je zegt niet veel, maar als jij iets zegt had jij (bijna) altijd gelijk. Bedankt voor de vrijheid om mijn eigen gedachten verder te ontwikkelen en om me te ervaren dat er wetenschappers zijn die niet autoritair zijn en die ook kunnen luisteren. Tenslotte wil ik je bedanken voor jouw vertrouwen in mij. Ik zal mijn ervaring hier nooit vergeten en ik hoop dat we meer samen kunnen werken in de toekomst.

Maria. Que prazer enorme foi chegar ao AlgaePARC por primeira vez e receber um “bom dia”e dois beijinhos teus. Muito obrigado por nunca ter esquecido do Iago e sempre lembrar a todos que, apesar de ter sido o último a chegar ao Projeto, eu era sim parte da equipe (disso nunca me esquecerei). Nossas reuniões foram sempre frutíferas mas nunca deixaram de ser um pouco “gezellig”. Aprendi muito contigo nestes quatro anos e espero ter oportunidades de aprender mais no futuro. Obrigado por tudo, de coração.

The Algae Parc team, what a special group of people and what a special location. It was a real pleasure to bike every day to Nergena and to spend my days (and evenings) there. To Rouke, Maria B., Maria C., Dorinde, Jesus, Snezana, Rick, Fred, Mathijs, Giulia, Jeroen, Marta F., Gibran, Marta Paiva, all the interns and guests colleagues that we received in the last 4 years, my gratitude. My special thanks to Rouke, who always took care of everything and to Fred, who is always willing to help everyone and to rescue us from last minutes crashes. I also want to say thank you to the Nergena team, especially to Rinnie.

To my dear colleagues at BPE, it was a pleasure to share a bit of these last 4 years with you all. I was never so present at BPE, but I always felt part of the group whenever I needed to use one of the machines or when I joined one of the many group drinks and social activities. My big hug to Ward, Youri, Kiira, Camilo, Catalina, Edgar, Ilse, Rafael, João, Anne, Lenny, Marjon, Lenneke, Rupali. Also many thanks to the technicians who always helped me at BPE: Wendy, Sebastiaan and Fred.

An especial thanks to Miranda and Marina, who always took good care of me. Meisjes, hartstikke bedankt voor jullie hulp en gezelligheid tijdens de koffie en feestjes. Jullie zijn de ziel van de groep en ik kan mij de afdeling niet zonder jullie voorstellen.

A especial thank You to Pauline B., who was always available for a cigarette brake and to open my mind with non-algae related subjects, it never mattered if it was French cuisine or GMO bacteria.

Gracías también a Rafael por tu compañerismo y amistad. Gracias por nuestras largas conversaciones. Chegaste quase na fase final desta tese, mas de tão rápido que entraste para o grupo tenho a impressão de que estás conosco há anos. Gracia.

A meu *brother* João. Que alegria era (é) encontrar-me contigo, onde quer que fosse: no BPE, na piscina pela manhã, a caminho de casa (o João a correr) ou num bar. Somos tão diferentes, mas compartilhamos a Liberdade como princípio maior. Muito obrigado por todas as viagens que fizemos juntos a trabalho e pelas lembranças que compartilhei contigo. Meu abraço enorme para ti.

To Ellen. We hebben bijna gedurende 2 jaar samengewerkt. Het was geen dagelijkse samenwerking maar we hadden best regelmattig overleg. Het modelleren had ik zonder jouw hulp nooit op tijd klaar gekregen. Bedankt voor het gezelschap, de gezellige korte gesprekken met een kopje koffie en jouw steun.

To the students who worked with me: you were never my students and you never worked for me. All of you were special and taught me something. Thanks for your help during my PhD: Mathijs, Carolina, Daniel, Kira, Daan and Hanna.

Mathijs, jij was de eerste student in mijn project. Het was bijzonder om mijn PhD met zo'n geïnteresseerde student te beginnen. Het was nog meer bijzonder om jou als collega te hebben. Ik ben blij dat jij nu jouw PhD zal starten: heel veel succes. Jij zal een briljante carrière krijgen, dat weet ik zeker.

Minha querida Carolina. Que meses tranquilos foram aqueles em que fizeste tua tese conosco (tranquilos para mim). Executaste a pergunta mais interessante de nosso projeto, uma pena que o tamanho não importa! Mas o que ficou de importante em minha vida foram aqueles meses contigo. Continuamos em contato, sempre desejando ao outro muita felicidade. És mais uma amiga que tenho pelos lados de Lisboa. Beijinhos!

My dear and brave Hanna. During the last year of my PhD I got you as a gift and without you I could never have finished this thesis the way I did, at the same deadline and with the same mental health. Your 4 months here were smooth and we made a great team together. Our quick 1 hour skype talks were always fruitfull, and went always on something else than algae. What a challenge you took, and I was very proud of what you accomplished at the end. My eternal thank you to you.

A mi gran amigo Jesus. Mi alegro mucho en tener lo aqui a mi lado como mi paraninfo. Que alegre coincidencia fué llegar a Wageningen y encontrar me otra vez contigo, sentado en la oficina al lado. Gracías por ser mi amigo "normal", creo que eres el único que tengo. En España si dice que el mundo es un pañuelo, pues yo espero que sigamos asi, tu y yo, nos encontrando en las esquinas.

Ao Leo, que é a única pessoa além de meus co-autores que de fato (ou facto) leu parte desta tese. Nos conhecemos por casualidade, mas nem ao trocar de países, coisa que fizemos os dois, esquecemos um do outro. Tua amizade é muito especial para mim. É com muita alegria que o tenho a meu lado como paraninfo, afinal *if you want something well done, call a German*.

My Wageningen family: Jeroen, Giulia, Snezy, Alessandra, Vasco, Henrique, João y Yodit. My blood family is not present here today, but it is equally important to have you all seated in the front row, as the family I made during the last 4 years.

Troelstraweg 21, to think about my phd without remembering of you is not possible. I arrived in Wageningen and was taken to this very special place, which always brought very special people to spend a few months or years. Thanks to Vasco, Marta M., Valerie, Birthe, Laura, Nana, Stephanie, Andrea, Alessandra, Thomas, George, Natalia and Yodit

Christos, You were the first face I have seen here. Without a warning you came to pick me up at Ede-wageningen. My first impression from the city and the University came from your words during those first 20 minutes. It was even more special to find out that I would take over your room (with the special colors) and because we became friends. Sharing Troelstraweg, the Heineken giant bottle and the wooden tulips with you and Giulia will always be in my memory. I wish both of you a lifetime of happiness and fun.

Vasco. O Christos pode ter sido o primeiro rosto que vi em Wageningen, mas foste o primeiro cidadão de Wageningen que conheci, ainda que à distância. Disseste que a casa era um lugar especial, o que pude comprovar ser verdade logo que cheguei. Comprovei ser tu também a razão de uma casa tão especial. Obrigado por ter compartilhado toda tua experiência (e o Buda) comigo e por termos vivididó aquele tão especial primeiro ano de meu PhD.

Henrique, aquele que me deu boas vindas a Wageningen e que boas vindas! O Vasco foi-se a Portugal mas continuamos amigos, e podíamos juntos “chorar”a falta que ele nos fazia. Muito obrigado pelo apoio durante o PhD, foram sempre úteis as palavras de um homem mais velho. Obrigado pelo presente que é a tua familia, bedankt voor Karin e o Arthur.

Laura. Viveste 6 meses conmigo en Wageningen. Que invierno más aburido hubiera sido si no fuera por tu compañia todas las tardes/noches. Por las botellas de Bordeux, por el international club que nunca hemos ido (reconosco la deuda), por todas las veces que cenamos juntos y por todos los postales. Te hecho de menos, siempre.

Stephanie, que idioma hablamos? Aunque no estubiera siempre en casa, fuiste la compañera de casa perfecta. Gracías por los concejos y por tu apoyo durante mi PhD. Mucha suerte en Malasya que lo sepas que nunca mi olvidaré de ti.

Ale! You came to live with me for 9 months, and you never left my live ever since. Thanks for everything and never forget that you are my family. In many of the stressfull moments of this thesis I was able to arrive home to hear *Ciao Ovetto*! This, and much more, I will never forget.

Yodit, no te escribiré en francés, que me falta todavía este idioma. Maar we kunnen wel elkaar begrijpen toch? I can’t imagine 2 people being happier living together (and not being married) than the two of us. He compartido un montón de cosas buenas contigo y los recuerdos los

guardo en mi corazón. Gracías por mantener el Buda siempre contento, por todas las cenas juntos y por las largas conversaciones en el comedor del Troelstraweg 21. Te quero muito bem e guardarei saudades imensas.

Snezana, mijn Mama. Jij bent de meest geweldige en sterke persoon die ik ooit ontmoet heb. Bedankt dat jij er bent en bij ons staat. Bedankt voor alle sigaretten en de koffiepauzes. Tijdens mijn drukste momenten was jij altijd beschikbaar om mij te helpen. Met jouw glimlach was altijd alles automatisch een stukje beter, heel vaak met een stukje taart er bij. Ik zal je nooit vergeten.

Gosse, ik ging elk week naar jou toe om mijn Nederlands te verbeteren. Bedankt daarvoor. Na een jaar gingen we verder met praten en heb ik jou en jouw familie beter leren kennen. Door jou kan ik mijn werk in het Nederlands uitleggen. Bedankt voor de microbiologie mini-colleges (ik had het nodig). Bedankt ook aan Hanneke, voor de gezeligheid tijdens mijn gesprekken met Gosse en de uitnodigingen om mee te eten.

Minha familia no Brasil. Meus grandes abraços, beijos e carinho. Vocês sempre me enviaram teu apoio e teu amor. A meus pais que sempre deram a Liberdade para que eu fizesse aquilo que desse na cabeça, minha eterna gratidão, admiração e amor. Por todas a vezes que conversamos via skype, as muitas vezes. Tenho a alegria de dizer que sou amigo de meus pais, e esta tese, meus amigos, é também de vocês dois.

À minha irmã Marta, pelo amor incondicional e por ter-me feito tio. À minha sobrinha Maria, que me da uma amostra do que é a paternidade. Meu amor e gratidão.

A meus queridos amigos e irmãos, sempre presentes em minha vida. À Lorena por tudo aquilo que vivemos juntos e que se reflete na minha vida aqui, sempre em meus pensamentos. Ao Jairo, por tudo aquilo que vivemos juntos. Tua amizade foi um presente que a vida adulta deu e conversar contigo é como voltar ao tempo e, como se o tempo não tivesse passado, voltamos a ser duas crianças.

A suelen, que já acho pouco chamar de amiga ou irmã. Na verdade faltam palavras nos dicionários para descrevê-la. Tu és minha parceira e juntos estamos, seja lá onde estivermos. Participamos cotidianamente da vida um do outro. Trabalhamos em mundos opostos, mas sempre perguntas: como vão as algas? Sinto-me privilegiado em tê-la em minha vida todos estes anos e espero manter este privilégio em anos por vir. Te quiero.

As Professoras e amigas, Lília e Iracema. Duas mulheres e profissionais distintas, mas aprendi muito com ambas. Se cheguei até aqui, foi com ajuda de ambas. Terão sempre todo meu carinho e admiração.

Hier, at the end we find my special thanks. I have met a lot of special people in my life, there are a lot of special people in this last few pages. But the following ones where by my side, from the beginning and all the way to the end.

First my daily partners, my algae siblings: Giulia and Jeroen.

To Giulia, mía dottoressa. The memories I have from Wageningen must include you, from Troelstraweg to AlgaePARC, the axis of our lives. I have you as a sister, and if it was not enough together came Christos (twee halen één betalen). Thanks for all your support during the thesis, all the rides and the help with stubborn reactors and softwares. For sharing our frustrations and for the wonderful weeks in Lisbon. This thesis has a bit of you as well.

To Jeroen, the manager. Wat een lol was het om samen met jou te promoveren! Jij was altijd beschikbaar om te helpen en altijd beschikbaar om samen te drinken (meestal te veel). Dit jaar waren wij beide op het eind van onze thesis en het was heel bijzonder om dit laatste jaar met jou te delen. Ik heb heel veel herinneringen met jou en dit proefschrift heeft ook iets van jou (veel dank voor de uitbreiding van mijn woordenschat). Bedankt voor het zijn van mijn broertje die ik nooit heb gehad. Ik ga jou altijd missen!

Dorinde. You were my supervisor, but to me you were my work partner, en dit proefschrift is evenveel van jou als het van mij is. Jij was de beste begeleider die ik me zou kunnen wensen, jij was niet dagelijks bij mij, maar je hebt mij 100% gesteund en ik voelde mezelf nooit alleen. Onze wekelijkse vergaderingen waren nooit een verplichting, het was een plezier om met jou over ons werk te praten. Ik heb geen spijt van mijn PhD en dat is ook thanks to you. Ik ga jou altijd missen.

To you, the most patient one. Mijn PhD ervaring was geweldig, maar in het begin van mijn PhD heb ik iets ondekt, iets met meer waarde dan alle resultaten van dit proefschrift. Jij bent de perfecte partner voor mij. Samen hebben we iets heel bijzonders gemaakt, bijzonder en rustig, precies wat we willen toch? Lindeboompjes ook bedankt, ik voelde me altijd welkom in jullie familie. Dirry, Evert, Hester, Marieke en Mark, bedankt. Derk Jan, bedankt voor alle momenten dat je op mij moest wachten en voor al je steun. Heel vaak zei je: ga maar Iago, jouw experimenten zijn meer belangrijk dan ik! Sorry, maar dit keer had jij niet helemaal gelijk Derk Jan. Ik geloof in wat we samen hebben opgebouwd en ik hoop dat het heel lang gaat duren. Ik houd van jou.

Iago Teles

About the author

Iago Teles was born in Salvador de Bahia (Brazil) on the 2nd of October of 1986, son of a Brazilian mother and Spanish father. In 2005 he started his university studies to pursue a degree in Biology, concluded in 2009 (Federal University of Bahia, UFBA, Brazil). During his degree he worked with research projects, completing three years of training in research in the Lab of Mutagenesis. In 2009, after graduating, he started working in Lab of Marine Biology & Biotechnology as a research assistant in a project to produce biofuels from microalgae. In 2011, parallel to his work, he started his MSc program in Industrial Biotechnology. In 2011 he went to Puerto Real (Cádiz, Spain) to do an internship in wastewater treatment with microalgae at the CACYTMAR (Centro Andaluz de Ciencia y Tecnología Marinas). He concluded his Master degree in 2012 with distinction. On the 28th of October of 2012 Iago arrived in the Netherlands to start his PhD research in the Group of Bioprocess Engineering (BPE), which resulted into this thesis. Iago has a strong interest in Applied Science, Statistics applied to biological problems and Scientific Writing; areas which he plans to pursue in his future carrier.

List of publications

Nascimento, I.A., Marques, S.S.I., **Cabanelas, I.T.D.**, Pereira, S.A., Druzian, J.I., de Souza, C.O., Vich, D.V., de Carvalho, G.C., Nascimento, M.A., 2013. Screening Microalgae Strains for Biodiesel Production: Lipid Productivity and Estimation of Fuel Quality Based on Fatty Acids Profiles as Selective Criteria. Bioenergy Research 6, 1–13.

Cabanelas, I.T.D., Arbib, Z., Chinalia, F.A., Souza, C.O., Perales, J.A., Almeida, P.F., Druzian, J.I., Nascimento, I.A., 2013. From waste to energy: Microalgae production in wastewater and glycerol. Applied Energy 109, 283–290.

Cabanelas, I.T.D., Ruiz, J., Arbib, Z., Chinalia, F.A., Garrido-Pérez, C., Rogalla, F., Nascimento, I.A., Perales, J.A., 2013. Comparing the use of different domestic wastewaters for coupling microalgal production and nutrient removal. Bioresource Technology 131, 429–436.

Nascimento, I.A., Marques, S.S.I., **Cabanelas, I.T.D.**, de Carvalho, G.C., Nascimento, M.A., de Souza, C.O., Druzian, J.I., Hussain, J., Liao, W., 2014. Microalgae Versus Land Crops as Feedstock for Biodiesel: Productivity, Quality, and Standard Compliance. Bioenergy Research 7 (3), 1002-1013.

Nascimento, I.A., **Cabanelas, I.T.D.**, Santos, J.N. dos, Nascimento, M.A., Sousa, L., Sansone, G., 2015. Biodiesel yields and fuel quality as criteria for algal-feedstock selection: Effects of CO_2-supplementation and nutrient levels in cultures. Algal Research 8, 53–60.

Cabanelas, I.T.D., Marques, S.S.I., de Souza, C.O., Druzian, J.I., Nascimento, I.A., 2015. *Botryococcus*, what to do with it? Effect of nutrient concentration on biorefinery potential. Algal Research 11, 43–49.

Cabanelas, I.T.D., van der Zwart, M., Kleinegris, D.M.M., Barbosa, M.J., Wijffels, R.H., 2015. Rapid method to screen and sort lipid accumulating microalgae. Bioresource Technology 184, 47–52.

Cabanelas, I.T.D., Fernandes, C., Kleinegris, D.M.M., Wijffels, R.H., Barbosa, M.J., 2016. Cell diameter doesn't affect lipid productivity of *Chlorococcum littorale*. Algal Research doi:10.1016/j.algal.2016.02.002

Cabanelas, I.T.D., Kleinegris, D.M.M., Wijffels, R.H., Barbosa, M.J., 2016. Repeated Nitrogen starvation doesn't affect lipid productivity of *Chlorococcum littorale*. Bioresource Technology 219, 576–582.

Cabanelas, I.T.D., Zwart, M.V.D., Kleinegris, D.M., Wijffels, R.H., Barbosa, M.J., 2016. Sorting cells of the microalga *Chlorococcum littorale* with increased triacylglycerol productivity. Biotechnology for Biofuels. doi:10.1186/s13068-016-0595-x.

Cabanelas, I.T.D., Slegers, P. M., Böpple, H., Kleinegris, D.M., Wijffels, R.H., Barbosa, M.J., 2016. Outdoor performance of *Chlorococcum littorale* at different locations. Submitted for publication.

Overview of completed training activities

Discipline specific activities

AlgaePARC Consortium meeting (Wageningen, the Netherlands; 2012, 2013,2014,2015)[1]

Microalgae process design: from cell metabolism to photobioreactors (Wageningen, the Netherlands, 2013)

Masterclass of Biobased Innovation (Wageningen, the Netherlands, 2013)[1]

1st Lisbon International Microalgae Advanced Course (Lisbon, Portugal, 2013)

Advanced Course on Process Design (Wageningen, the Netherlands, 2014)

FlowJo 10 Basics Software Training (Bergisch Gladbach, Germany, 2014)

5th International Conference on Algal Biomass, Biofuels and Bioproducts (San Diego, USA, 2015)[1]

AlgaEurope 2016 (Lisbon, Portugal, 2015)[2]

3rd Young Algeneers Symposium (Valeta, Malta, 2016)[1,2]

General courses

VLAG PhD week (Wageningen, the Netherlands, 2013)

Multivariate analysis (Wageningen, 2013)

Presentation skills (Wageningen, 2013)

PhD scientific writing (Wageningen, 2014)

Techniques for Writing and Presenting a Scientific Paper (Wageningen, 2014)

Optional

Preparation of research proposal (Wageningen, 2013)

Bioprocess Engineering PhD trip – Portugal (Wageningen, 2014)[1,2]

Weekly group meetings (Wageningen, 2013 - 2016)[1]

[1] Oral presentation
[2] Poster presentation

The research presented in this thesis was carried out at the Bioprocess Engineering Group of Wageningen University (Wageningen, the Netherlands). Also, CNPq is acknowledged for the grant 236614/2012-6. This thesis was within the AlgaePARC Research Program, which was financially supported by: Ministry of Economic Affairs, Agriculture and Innovation (the Netherlands), Province of Gelderland (the Netherlands), and the companies: BASF, BioOils, Drie Wilgen Development, DSM, Exxon Mobil, GEA Westfalia Separator, Heliae, Neste, Nijhuis, Paques, Cellulac, Proviron, Roquette, SABIC, Simris Alg, Staatsolie Suriname, Synthetic Genomics, TOTAL and Unilever.

Printed by Digiforce (Vianen, the Netherlands, www.proefschrftmaken.nl).